Department of Geomatics Engineering

Modelling Spatial Dependence in Multivariate Regression Models of Grizzly Bear Health in Alberta, Canada
(URL: http://www.geomatics.ucalgary.ca/graduatetheses)

by

Tracy Timmins

September 2010

SCHULICH
School of Engineering
UNIVERSITY OF CALGARY

UNIVERSITY OF CALGARY

Modelling Spatial Dependence in Multivariate Regression Models of Grizzly Bear Health

in Alberta, Canada

by

Tracy Timmins

A THESIS

SUBMITTED TO THE FACULTY OF GRADUATE STUDIES

IN PARTIAL FULFILMENT OF THE REQUIREMENTS FOR THE

DEGREE OF MASTER OF SCIENCE

DEPARTMENT OF GEOMATICS ENGINEERING

CALGARY, ALBERTA

SEPTEMBER, 2010

Abstract

To ensure the preservation of grizzly bears in Alberta, the effect of environmental change on grizzly bear health must be understood. This thesis investigated the relationship between grizzly bear health and environment using regression models with a focus on modelling spatial dependence. Ordinary least squares (OLS) regression models tend to misestimate the variance of estimated parameters in the presence of spatial dependence. This can lead to faulty inferences.

A variety of spatial neighbourhoods were created to detect spatial dependence in OLS regression models and to develop spatial autoregressive models as an alternative. It was found that significant negative spatial dependence was present in the grizzly bear data and caused the variance of parameters to be overestimated in OLS models. The use of spatial autoregressive models improved the fit of the models and increased the significance of the parameter estimates. Those spatial neighbourhoods that grouped together known grizzly bear population groups were best able to detect spatial dependence.

Acknowledgements

Dedication

I dedicate this thesis to my loving and wonderful parents,

Marita and Ken.

I could not have done this, if it were not for you.

Table of Contents

List of Tables

List of Figures and Illustrations

List of Abbreviations and Symbols

Abbreviation/Symbol	Definition
AIC	Akaike's information criterion
AICc	Akaike's information criterion corrected for small samples.
CanClo	Average canopy closure
CldFst	Percentage closed forest
DecFst	Percentage deciduous forest
Dist_Town	Average distance to towns
Dist_Wat	Average distance to waterbodies and rivers
East	Average degree to which the slope faces east
Elev	Average elevation above sea level
FRI	Foothills Research Institute
Herbs	Percentage herbaceous and shrubby vegetation
KDE	Kernel density estimator
MaxX	x coordinate of the point of maximum use on the utilization surface
MaxY	y coordinate of the point of maximum use on the utilization surface
NN	Nearest neighbours
Northeast	Average degree to which the slope faces northeast.
North	Average degree to which the slope faces north
OLS	Ordinary least squares
OpConFst	Percentage open coniferous forest
OpDecFst	Percentage open deciduous forest
OpFst	Percentage open forest
OpMixFst	Percentage open mixed forest
PerCon	Average percentage conifer
RegAll	Percentage total regenerating area
Regfst	Percentage regenerating forest
SLL100	Transformed straight-line length
Slope	Average slope, where slope is measured as a percentage elevation change over horizontal distance.
Wetfst	Percentage wet forest
WetAll	Percentage total wet forest and wet herbs
Δ_i	Akaike's difference
I	Moran's I
λ	Lamda – the spatial parameter of spatial error models
ρ	Rho – the spatial parameter of spatial lag models
p	Probability value
r	Correlation coefficient
R^2	Multiple coefficient of determination
w	Akaike's weight

Chapter One: Introduction

1.1 Background

If grizzly bears (*Ursus arctos*) are to prosper in the Alberta Rockies and foothills a

thorough understanding of the effects of human activities on grizzly bears must be

acquired. Only then can this multi-use landscape be managed to balance the needs of both

humans and grizzlies. This study hopes to contribute to this goal through an investigation

of the relationship between grizzly bear health and environment, with a particular focus

on modelling spatial dependence to improve the reliability of inferences from regression

models. In the process, interesting behavioural, ecological and environmental processes

may also be identified for further exploration.

The protection of grizzly bears habitat is beneficial for the preservation of a great

diversity of species. Although grizzly bears have the basic physiology common to all

carnivores, they are omnivorous and eat a large volume of vegetative material (Schwartz

et al., 2003). They have often been considered an umbrella species due to their use of

diverse habitat types to meet their dietary needs and large land-space requirements, thus

the protection of grizzly bear habitat ensures that many other species are protected at the

same time (Paquet & Hackman, 1995; Ross, 2002). Also, due to grizzly bear sensitivity

to habitat disturbance and population perturbations, their presence is can indicator of

ecosystem integrity (Ross, 2002; Stenhouse & Munro, 2000).

Grizzly bears originally occupied most of western North America, but were

extirpated from the south-western United States following the arrival and settlement of

Europeans. This dramatic reduction in the grizzly bear range and overall population size

was caused by the transformation of their natural habitat for human purposes and the

deliberate extermination of grizzlies (Brown, 1985; Mattson & Merrill, 2002; McLellan, 1998; Storer & Trevis, 1955). Nevertheless, grizzly bears have been able to survive in areas generally unfavourable to humans, primarily in the remote and mountainous regions of Alaska, Montana (USA) and western Canada. The Rocky Mountains and foothills of Alberta (CA) and Montana now form the eastern and southern fringe of the bears' range (Mattson & Merrill, 2002; McLellan, 1998). The large-scale reduction of grizzly bear range can be seen in Figure 1-1, which shows the post-glacial (approximately 10,000 to 13,000 years ago), historical (pre-European settlement) and current distribution of grizzly bears in North America.
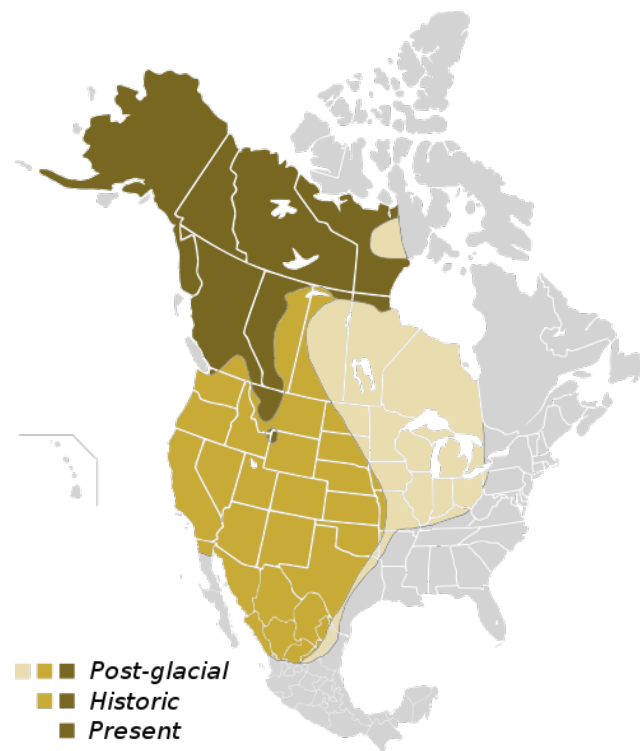
Figure 1-1. Shrinking distribution of the grizzly bear range during post-glacial, historic and present time (Adapted from Schwartz et al., 2003)

In contrast to carnivores such as the cougar and wolf, grizzly bears have a low resilience when confronted with anthropogenic disturbance. This is attributed mainly to the fact that grizzlies require high quality food in spring after den emergence and in fall before hibernation, and have low reproductive and dispersal rates (Weaver, Paquet, & Ruggiero, 1996). Grizzly bear populations have been predicted to continue to decline in Canada due to their inherent sensitivity to human disturbance (Ross, 2002). They are particularly vulnerable at the edge of their range and in the harsh environment of the Arctic (Ross, 2002). For these reasons grizzlies are listed as a species of *Special Concern* according to COSEWIC (Committee on the Status of Endangered Wildlife in Canada) (Government of Canada, 2002; 2009).

The grizzly bear population of Alberta is small and occurs at the edges of the grizzly bear range making these bears particularly vulnerable to local extinction or range contraction (Mace et al., 2008; Proctor et al., 2004; Ross, 2002). The most recent population estimates indicate that as few as 580 grizzly bears remain in the area south of Grand Prairie, excluding most of the national parks (Government of Alberta, 2009). According to the World Conservation Union criteria for red listing taxon, a population with fewer than 2,500 mature individuals can be categorized as endangered. A population can be listed as critically endangered if fewer than 250 mature individuals remain in the wild (IUCN Standards and Petitions Subcommittee, 2010). A mature adult is defined as an individual capable of reproduction and excludes those living in areas of such low density that acquisition of a mate is precluded. Furthermore, the Alberta and BC grizzlies are under increased stress as populations have been fragmented by the Trans-Canada Highway (Highway 1) and Highway 3, which pass through Banff National Park and

Crowsnest Pass respectively. These highways effectively reduce genetic flow between sub-populations (Ross, 2002).   Alberta has also experienced rapid human population growth, with the population doubling in size since the 1970's (Statistics Canada, 2009). This demographic trend has naturally been accompanied by a similar expansion in residential, industrial, agricultural, and recreational areas (Linke et al., 2008; McDermid et al., 2009; McLellan, 1998), which fragment, transform, and reduce the quality of grizzly bear habitats, as well as displace bears and increase human-caused mortalities (Benn & Herrero, 2002; McLellan, 1998). As a result of these threats, the Government of Alberta listed the Alberta grizzly bear population as *Threatened* under the Wildlife Act in 2010 (The Calgary Herald, 2010).

Human disturbance and alteration of the natural environment can cause long-term stress in wildlife (Moberg & Mench, 2000), compromise their resilience, and eventually contribute to their decline (Paquet & Hackman, 1995; Weaver et al., 1996). Also, the reduction in availability of good quality food through habitat fragmentation and transformation can also lead to reduced body size, reproductive rates and ultimately population size (Schwartz et al., 2003, p. 556).

The long-term effect of environmental change on grizzly bear health in Alberta is being studied by the Foothills Research Institute Grizzly Bear Program (FRI). The FRI has a holistic conception of health and considers it to be the level of biological functioning with respect to stress, growth, reproduction, immunity, and movement (Cattet et al., 2007). The study of grizzly bear health is an important component necessary to fulfil the FRI's overarching goal to ensure the long-term survival of grizzlies in Alberta

through the provision of scientific knowledge and planning tools to resource managers

(Stenhouse & Munro, 2000).

Numerous datasets have been collected by the FRI to achieve this goal. These

include various environmental maps produced from satellite imagery, detailed grizzly

bear movement data acquired from GPS collars attached to grizzly bears, and various

serum-based, physical and physiological measurements of individual bears. The GPS

data in particular can be used to identify the home ranges of individual bears.

Natural resources and anthropogenic disturbance within home ranges can be

quantified using environmental maps. Finally, serum-based, physical and physiological

measurements can provide indicators for stress, growth, immunity, and overall health for

individual bears (Cattet et al., 2007). Altogether, these data can be used to develop

models relating grizzly bear health to environmental conditions.

This thesis looks at the development of multivariate regression models relating

grizzly bear health and environment, with a particular focus on the use of spatial data and

dependence in regression modelling. This is discussed further in the problem statement in

section 1.2.

1.2 Problem Statement

Multivariate regression modelling is a commonly used technique to explore the

relationship between a single dependent variable and several explanatory variables. This

technique will be used to examine the relationship between grizzly bear health and

environmental variables. However, the analysis of phenomenon and features distributed

over geographic space can present particular challenges and issues. According to

Griffith (1996):

> "Spatial statistics differs from classical statistics in that the
> observations analyzed are not independent; this single
> assumption violation is the crux of the difference."

The problem of non-independent data presents problems for many conventional

statistical approaches such as ordinary least squares regression modelling. It is likely that

spatial dependence exists in the grizzly bear datasets as is shown in Figure 1-2. The

grizzly bear home ranges (black polygons) within the FRI study area appear highly

clustered and overlapping. It is therefore possible to hypothesize that the environmental

characteristics of these home ranges are spatially autocorrelated. If the environment does

indeed have a significant effect on grizzly bear health, it is further hypothesized that

grizzly bear health should be similar for bears occupying habitats close to one other.
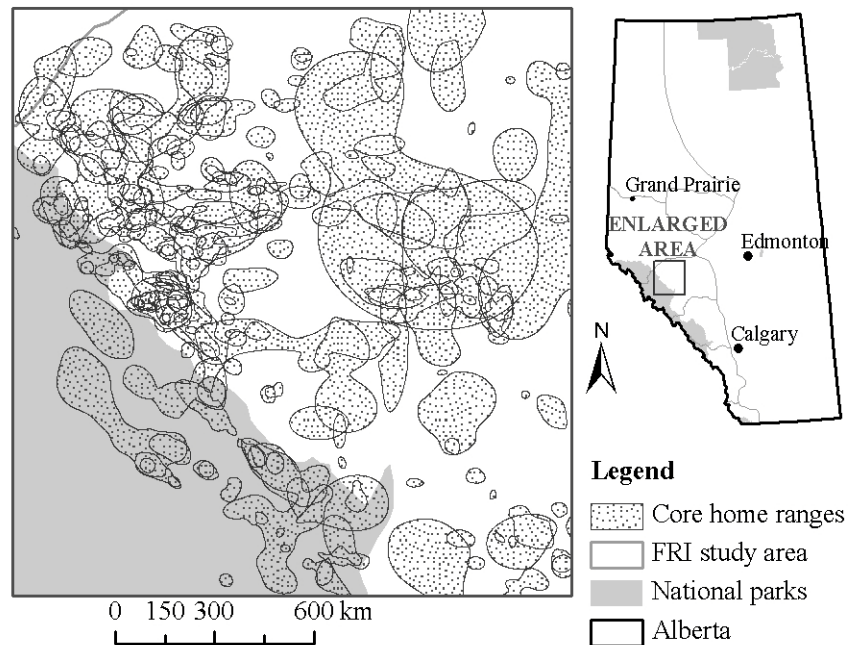
Figure 1-2. Overlapping home ranges

1.2.1 The nature of spatial data

Tobler's First Law of Geography (1970) states that, "Everything is related to everything else, but near things are more related than distant things." The occurrence of similar attribute values at nearby locations is also known as positive spatial dependence (Anselin & Bera, 1998). Negative spatial dependence may also occur in spatial data. This is the occurrence of dissimilar values in locations close to each other (Fortin & Dale, 2005).

Spatial dependence is an inherent characteristic of spatial phenomenon that arises from the continuity of space and the operation of spatial processes (Haining, 2003). Spatial dependence can also be induced in spatial data by the spatial sampling framework (shape, size, and extent of measurement units) chosen to observe reality. This occurs when the spatial sampling framework does not correspond to the scale, extent and/or orientation of underlying processes (Messner & Anselin, 2004).

Consequently, the mean and standard deviation are no longer sufficient summary statistics in a spatially dependent geo-referenced sample, and additional statistics are required to characterise the geographic arrangement of observations, as well as the nature and degree of spatial dependence among them (Griffith, 1996).

Positive spatial dependence effectively reduces the number of independent samples which can cause the variance of parameters calculated from the sample to be underestimated (Anselin & Bera, 1998; Haining, 2003; Schabenberger & Gotway, 2005). Conversely, in the presence of negative spatial dependence, parameter variances can be overestimated (Schabenberger & Gotway, 2005). Significantly, it has been demonstrated in several studies that the variance of regression model coefficients estimated using ordinary least squares (OLS) can be substantially affected by the presence of spatial

dependence in the data, often leading to faulty inferences based on the significance of explanatory variables within the model (Anselin & Bera, 1998; Cliff & Ord, 1981; Cordy & Griffith, 1993; Griffith, 1996; Loftin & Ward, 1983).   This is caused by the violation of the OLS assumption of identically and independently distributed errors (Cliff & Ord, 1981).

To improve the reliability of parameter estimates and inferences, it is necessary to model the nature and degree of spatial dependence among observations. This can be achieved using a spatial weight matrix, wherein each row-column element represents the weight, i.e., covariance, between a pair of observations. These weights are a function of the relationship between observations, and can be determined using a data-driven (empirical), or model-driven (theory/substantive) approach (Anselin, 1990). For example, spatial weights can be a function of the distance between observations or the proportion of shared boundary in the case of aerial units (Anselin, 1984). The formulation of the spatial weight matrix is the most important step in detecting spatial dependence (Odland, 1988).

The spatial weight matrix can be incorporated into multivariate regression models, known as spatial autoregressive models, to improve the variance estimates of explanatory variables (Cliff & Ord, 1981; Haining, 2003). However, the inaccurate specification of the weight matrix, i.e., which observations are spatially dependent and to what degree, can also influence the variance of regression estimates and cause bias in parameter estimates (Stetzer, 1982). Specification of the weight matrix can be problematic as there are many possible ways to define the spatial weights, especially when little substantive knowledge or theory is available to guide selection. For these

reasons Griffith (1996) and Stetzer (1982) recommend that close attention be given to the specification of the spatial weights matrix in quantitative geographic research.

1.3 Research Objectives

Due to the proximity and overlap of grizzly bear home ranges as shown in Figure 1-2, it is hypothesized that spatial dependence exists in the FRI grizzly bear data, specifically the explanatory environmental variables, and possibly the dependent health variable. If the hypothesis is true, the residuals of an OLS regression model of grizzly bear health and environmental variables may be spatially dependent, thus violating a key assumption of identically and independently distributed errors, and thereby biasing the variances of the estimated coefficient parameters. If this is the case, it is necessary to develop spatial autoregressive models which incorporate a spatial weights matrix to improve estimates and inferences drawn from the multivariate regression model. The importance of accurately specifying the spatial weights matrix before developing a spatial autoregressive models has already been outlined in Section 1.2.1. Considering the large number of possible spatial weight matrices that can be defined, and the sensitivity of spatial autoregressive models to the spatial weights matrix, the exploration and testing of a variety of spatial weight matrices is necessary.

1.3.1 Objectives and tasks

The primary objectives of this research are therefore to define a variety of spatial weight matrices, and evaluate these in terms of their ability to characterize spatial dependence

and improve model inferences, as well as their suitability in the context of this study. The specific objectives are to:

1. Test the hypothesis of spatial dependence in the health variable of interest;

2. Explore the relationship between the health variable and the environment through OLS regression models;

3. Test the hypothesis of spatial dependence in the residuals of OLS health-environment regression models;

4. Develop spatial autoregressive models if necessary and evaluate these in comparison to OLS regression models;

5. Evaluate the ability of different spatial weight matrices to capture spatial dependence in the data; and

6. Demonstrate the significance of considering spatial dependence when developing grizzly bear health-environment regression models using spatial data.

The specific tasks that must be conducted to meet these objectives are summarized below:

1. Delineate the grizzly bear home range. The core home range will be used as the unit of analysis for this study.

2. Define various spatial weight matrices for quantifying spatial dependence.

3. Select an appropriate health variable for study.

4. Develop a set of non-spatial health-environment regression models using OLS estimation.

5. Test the residuals of the above OLS models for spatial dependence using the spatial weight matrices developed as part of this thesis.

6. If spatial dependence is found in the residuals, develop spatial autoregressive models and evaluate the effect of different spatial weight matrices on the estimation of parameters and overall fit, particularly in comparison to the OLS regression models.

7. Determine which spatial weight matrices best characterize the spatial dependence which may be present in the data.

1.4 Significance of research

This research hopes to demonstrate that the presence of spatial dependence should be considered when developing regression models relating grizzly bear health to environmental variables in the Alberta Rocky Mountains and foothills. If spatial dependence is not considered inferences about the significance of explanatory variables based on the estimated parameter variances could be mistaken. It is possible that incorrect explanatory variables would be identified as significant for grizzly bear health or vice versa. If the aim is to improve our understanding of which variables affect grizzly bear health so that this multi-use landscape is managed to conserve grizzlies in the long-term, it is essential that important variables are correctly identified.

It is also hoped that appropriate spatial weight matrices will be determined for quantifying spatial dependence in the data so that FRI researchers will have a good basis for selecting spatial weight matrices for further studies.

Finally, if interesting spatial patterns are detected, these could provide the basis of future research into the ecological and environmental spatial processes that may be their cause.

To the best of the author's knowledge modelling spatial dependence in regression models of grizzly bear health has not been conducted as part of any FRI project or any other grizzly bear studies in North America at this stage.

1.5 Organisation of Thesis

This chapter has provided the contextual background of grizzly bear status and conservation in Alberta that is necessary for understanding the significance of this research. The specific research problem of spatial dependence in the FRI data has also been described, and the objectives of this research have been defined.

Chapter two examines two common home range estimation algorithms and their strengths and weaknesses in different contexts.

Chapter three presents a comprehensive treatment of the occurrence of spatial dependence in spatial data. This section describes the formulation of various spatial weights and explains how to proceed in testing spatial data for spatial dependence. Finally, various means of incorporating spatial weight matrices into regression models are presented.

Chapter four details the study area and data used for this study, as well as the research methodology. This section includes home range estimation, spatial neighbourhood development, and the creation of linear and autoregressive models.

Chapter five presents the results and offers a discussion of these. The final conclusions taken from this research and suggestions for future research are provided in Chapter six.

Chapter Two: Grizzly bear home ranges and home range estimation

Chapter two provides essential material for conducting the first step of this research, i.e.

the delineation of grizzly bear home ranges. The delineation of the home range is critical

as it determines what is included and/or excluded for analysis. The aim is to delineate

home ranges that encapsulate those environmental resources and human disturbances

which may have the biggest effect on grizzly bear health.

This chapter will present a brief overview of the biological theory of animal home

ranges and a description of grizzly bear ecology that is relevant to home range size and

shape. Further, it details two of the most commonly used home range estimators today:

the minimum convex polygon and the kernel density estimator.

2.1 Home ranges and territories

Burt's (1943) definition of the home range,

> "[the] area traversed by the individual in its normal
> activities of food gathering, mating, and caring for young.
> Occasional sallies outside the area, perhaps exploratory in
> nature, should not be considered as part of the home
> range,"

has provided the theoretical basis for many home range studies (Powell, 2000).   The

establishment of a home range allows animals to more efficiently exploit their landscape

through increased familiarity with it (McLellan, 1985; Powell, 2000). It is posited that

many animals have cognitive maps of their home range and surrounding areas, such as

the location of features and resources, corridors between resources, escape routes, and

home ranges of conspecifics and other species (Powell, 2000). The boundary of a home

range cannot be clearly defined in space as animals perceive well beyond their actual location through sight, hearing and smell. This total area of perception and awareness could well be considered part of an animal's home range. It is believed that animals however, are generally more concerned about the interior of their home range where they carry out the majority of their life activities (Powell, 2000, p. 69). It is these areas that provide information that may suggest how an animal lives and why it is in that place. Nevertheless, these areas do not always represent the best habitat for animals that may be relegated into less suitable areas as a result of human settlement and transformation of the environment (Schwartz et al., 2003, p. 565).

Although Burt's (1943) definition of the home range is clear and broad enough to be applicable to most animal species, it does not help the biologist quantify the home range, i.e., it is not an operational definition. The scientist cannot view an animal's cognitive map of its home range directly, only the locations where it actually visits. These observations are obtained sequentially such that an idea of the home range is built up only after some period of time has passed. It is important therefore that enough time passes so that the full behaviour of the animal can be observed. However, the cognitive maps of animals may change with changes in the environment, and, the longer an animal is observed the more likely it is that the home range may shift (Powell, 2000).

Home ranges should not be confused with territories. Many species have home ranges but no territory. Territories, which may be a subset of the home range, are specifically defended by fighting, scenting, marking, calling and/or displays (Powell, 2000, p. 70). Territories are usually required if and when there is some limited resource such as food (Powell, 2000, pp. 71 - 74).

The size and shape of home ranges are dependent on specific characteristics of the species, such as movement patterns (Nathan et al., 2008; Turchin, 1998) and foraging strategy (Stephens et al., 2007), as well as environmental context, e.g., topography, food, competitors and predators (Stephens et al., 2007). Movement patterns can be influenced by food, breeding, reproductive status, dominance, security and human disturbance. These factors will determine the pattern and extent of the landscape used by an animal (Burt, 1943).

2.2 Grizzly bear home range characteristics

It is necessary to have an understanding of grizzly bear ecology before choosing a home range estimation technique. This allows the selection of the technique with the most appropriate assumptions that would more likely produce realistic results. Ross (2002) and Schwartz, et al. (2003) summarised the general habitat characteristics of grizzly bears in Canada and North America. Grizzlies are habitat generalists, occurring naturally in a wide variety of habitats from the arctic tundra to boreal and coastal forests, to mountain forests/grassland ecotones. Although they have the digestive physiology of carnivores, they are omnivorous and many eat a diet consisting primarily of vegetation. Due to their dependence on vegetation, habitat associations are strongly seasonal following local phenology. This is particularly prominent in mountainous regions where grizzly bears may move substantially between lower and higher elevations. If food availability is low during hyperphagia in autumn, bears are known to roam widely in search of high-quality food resources to ensure survival through the winter.

The size of home ranges will generally vary with the quantity and quality of food available. A concentration of high quality food resources allows bears to meet their energetic requirements in smaller areas with less movement in search of food (Craighead & Mitchell, 1982). Due to the demand for large volumes of high-quality food, combined with the need to move between seasonally available food sources, grizzlies, in addition to establishing large home ranges, are multimodal, or have multiple centres of activity.

There is a close relationship between food availability, home range size and population density. The less food that is available, the larger home ranges tend to be and the lower the population density (Schwartz, et al., 2003). However, population density itself can influence the home range area of individuals independently from food availability. When population density is decreased from human-caused mortalities, competition for resources is reduced, thus enabling larger home range areas (Nagy & Haroldson, 1990).

The sex and reproductive class of bears also influences home range size (Ross 2002, p 32). Male bears tend to have home ranges several times larger than females, most likely due to their breeding activity and larger energetic requirements. Females with young cubs will have the smallest due to the reduced mobility of cubs and the need to keep them secure (Schwartz, et al. 2003).

Some environments do not provide resources to grizzly bears. Grizzlies will generally avoid these areas, except to traverse between two locations. High elevation areas consisting of rock, snow, and glaciers do not provide food resources or shelter to bears (Munro et al., 2006; Nielsen et al., 2006). Other areas of potential suitable habitat may also be avoided if they are near to areas of human activity (Ross, 2002, p. 25).

Grizzlies are not territorial and their home ranges often overlap (McLellan & Hovey, 2001). The home ranges of adult males may overlap with several females, and related females tend to have overlapping home ranges with each other (Schwartz et al., 2003, p. 566).

2.3 Home range estimation

Schwartz, et al. (2003) note that the use of home range estimation techniques can cause confusion when trying to generalise and compare animal home ranges between studies. Differences among home ranges can arise due to the estimation techniques used rather than actual biological differences. For this reason it is important to understand the effects of and differences between home ranges estimation techniques and their parameters.

Some home range estimators (e.g. minimum convex polygon) generate only a single polygon boundary delineating the home range. However, this assumes a hard edge and an even use of space within the home range. As described in section 2.1, this is unlikely in reality. An alternative approach is to generate a density or utility distribution surface which maps the intensity of use within different areas of the home range (Powell, 2000). Thus, higher density or utility is assigned to areas which have higher concentrations of observations. These are the areas where the animal spends more time, and are useful for identifying habitat use and preference (Seaman & Powell, 1996). This approach assumes that those areas where the animal spends most of its time are of primary importance, which is not always true (Powell, 2000, p. 90). At this stage, this problem is shared by all estimators that generate utility distribution surfaces.

A variety of point and line-based, parametric and nonparametric home range estimation methods exist. However, a recent review by Laver and Kelly (2008) of 141 papers on home range studies, published between 2004 and 2006, found that the majority of these studies employed minimum convex polygon (96), kernel density estimators (84) or both (51). For this reason, the minimum convex polygon (MCP) and kernel density estimation (KDE) will be explained in the following section.

2.4 Minimum Convex Polygon

The minimum convex polygon (MCP) is the simplest home range estimator and is generated by drawing the smallest possible polygon that encloses all observed locations of the animal in such a way as to create a convex polygon (Mohr, 1947). The area of the MCP will increase asymptotically as points are added (Arthur & Schwartz, 1999; Belant & Follmann, 2002).

MCP, however, has several problems which can make it unreliable and/or biased, and these preclude it from comparison with other studies (Laver & Kelly, 2008). Powell (2000) and Laver and Kelly (2008) summarise some criticisms of MCP. MCP is sensitive to number of location estimates/sample size (Bekoff & Mech, 1984) and extremely sensitive to spatial outliers. It often includes areas never used by the animal and does not take into account interior points at all, thereby assuming uniform use throughout the home range. Areas of home ranges can be greatly inflated as shown by Belant and Follman (2002). In their study grizzly bear home range areas estimated by MCP were up to seventeen times larger than areas estimated by fixed kernel estimators using the same data.

2.5 Kernel density estimators

Silverman (1986) provided the methodological basis of KDE approaches, while Worton

(1989) was the first to publicize its use for home range estimation in ecology (Seaman &

Powell, 1996). The kernel density estimator (KDE) is a probabilistic nonparametric

approach to home range estimation. Nonparametric approaches offer the advantage of not

having to make unrealistic assumptions about the use of space by animals. KDE assumes

that an animal has a fixed surface over the landscape which it uses and traverses in a non-

random fashion in some time frame (Calhoun & Casby, 1958). It estimates a utility

surface which can be transformed into a probability density surface. This new probability

surface then provides the probability that an animal is in a particular area of its home

range (Powell, 2000, p. 75). Using this approach, Worton (1995) offers an operational

definition of the home range as "the minimum area in which an animal has some

specified probability" of "being located". In practice this is achieved by selecting a

particular probability density contour derived from the utilization distribution.   A

polygon representing a particular probability contour can be derived by estimating the

probability for each cell (i.e., the volume of the probability distribution function for that

cell) and then selecting the smallest number of cells whose probability (volume under the

density surface) is equal to the probability contour of interest, e.g. 95 %. The most

frequently used probability contour is the 95 %, though this choice is essentially arbitrary

and not supported by biological evidence (Powell, 2000, p. 76).

2.5.1 Calculating the KDE home range

KDE estimates the intensity of utilisation by overlaying a grid on the observation points

and calculating the weighted density of observed locations in a moving window. The

contribution of each observation within the window to the density is a function of

distance between the evaluation point (center of window) and that observation. The

weights are based on a hill-shaped probability distribution function, such as the Gaussian,

Biweight, Epanechnikov or Triangular. The greater the distance between an observation

point and the evaluation point, the less it contributes to the average density computed.

The kernel density estimator can be expressed mathematically as:

$$\hat{f}(x) = \left[\frac{1}{nh^2}\right]\sum_{i=1}^{n} K\left[\frac{(\mathbf{x} - \mathbf{X}_i)}{h}\right] \qquad 2.1$$

where *h* represents the bandwidth or the radius of the moving window (Silverman, 1986).

K is the kernel and gives the shape of the probability function used to weight

observations within the window. $\mathbf{X}$ is the vector of *x* and *y* coordinates of the

observations within the window, and $\mathbf{x}$ is the *x, y* position of the evaluation point

(Seaman and Powell, 1996). The width of the window, or bandwidth *h,* determines the

degree of smoothing (Worton, 1989).

Commonly used probability density functions are the bivariate normal and

Biweight functions. The bivariate normal density kernel is defined as follows (Worton,

1989)

$$K = \frac{1}{2\pi}\exp\left(-\frac{(\mathbf{x} - \mathbf{X}_i)^{'}(\mathbf{x} - \mathbf{X}_i)}{2h^2}\right). \qquad 2.2$$

The Biweight kernel is

$$K_2(\mathbf{x}) = \begin{cases} 3\pi^{-1}(1 - \mathbf{x}'\mathbf{x})^2 & \text{if } \mathbf{x}'\mathbf{x} < 1 \\ 0 & \text{otherwise,} \end{cases}$$

2.3

where $\mathbf{x}'\mathbf{x}$ is the distance between the evaluation point and every observation in the window divided by h (Seaman & Powell, 1996).

It has been shown that the shape of the probability density distribution function has little effect on the final shape and size of the home range (Worton, 1989) provided it is hill-shaped and rounded (Silverman, 1986). The results of KDE have been found to be most affected by the choice of h (Harris et al., 1990; Silverman, 1986).

2.5.2 Estimating the bandwidth, h

The reference bandwidth, h_{ref}, of a set of location observations can be obtained by assuming the location data is normally distributed in x and y, where

$$h_{ref} = sn^{-1/6},$$

$$s = \sqrt{(s_x^2 + s_y^2)/2},$$

2.4

and s_x^2 and s_y^2 are estimates of the variances of the x and y coordinates respectively (Worton, 1989). However, very few home ranges are bivariate normal in reality (Horner & Powell, 1990; Seaman & Powell, 1996). For multimodal home ranges h_{ref} will be upwards biased, causing the utilisation surface to be over-smoothed (Worton, 1995).

Least-squares cross validation (LSCV), described in Silverman (1986, p. 87) and Worton (1989), is another automated method to determine appropriate bandwidth (h_{lscv}) which can be used for multimodal home ranges. Laver and Kelly (2008) found that

LSCV was the most commonly used technique for estimating bandwidth in home range papers published between 2004 and 2006.

LSCV selects h_{lscv} so that it minimizes the difference between the estimated density and the unknown true density (Worton, 1995). The minimum of this function must be found through numerical methods. The LSCV-estimated bandwidth, like h_{ref}, tends to be biased upwards in datasets with smaller sample sizes, although less so (Worton, 1995, p. 797, Seaman and Powell, 1996).

Due to the bias associated with h estimation, KDE may be better suited to describing intensity of use within the home range rather than estimating home range size (Harris et al., 1990; Worton, 1995).

The value of h may be fixed over the entire dataset (fixed kernel), or varied (adaptive kernel) so that areas with a lower density of points will have a higher value of h and those areas with a greater density of points will have a smaller h. When an adaptive kernel is used the local smoothing parameter can be formulated as $h_i = h\lambda_i$, where h is a global or pilot parameter, which can be estimated using the reference, LSCV, or other bandwidth estimation methods (Silverman, 1986, p. 101). It had been assumed that adaptive bandwidths would be better than fixed kernel estimators (Silverman, 1986); however, several studies have shown that the fixed kernel can be at least as good or better than the adaptive (Seaman et al., 1999; Seaman & Powell, 1996). Seaman and Powell (1996) recommend fixed smoothing, and Laver and Kelly (2008) found that the fixed kernel is more commonly used than the adaptive kernel.

2.5.3 Standardizing and scaling data

If a single parameter for bandwidth is chosen, this implies that the points are equally

distributed in both the *x* and *y* directions (Silverman 1986, p. 77). Therefore both

Silverman (1986, p. 77) and Worton (1989) suggest standardising data in *x* and *y* if the

variances are unequal in these two directions. This can be achieved by dividing *x* and *y*

coordinates by the standard deviation of *x* and *y* respectively to obtain unit variances.

After applying the KDE to the transformed data, the results can be rescaled back to their

original *x* and *y* range.

2.5.4 Sample size

KDE, like MCP, is sensitive to the number of observation points. When there are two few

points the KDE home ranges tend to overestimate the home range size since the

smoothing bandwidth tends to be large when selected by methods such as LSCV

(Seaman & Powell, 1996).   The reliability and precision of KDE home ranges increases

as more points are used (Arthur & Schwartz, 1999). According to Arthur and Schwartz

(1999) and Beland and Follmann (2002), 80 points or more are required to ensure that

annual grizzly bear home ranges are accurate (i.e,. ≤ 1 % change per additional point

added) and precise (the coefficient of variation (CV) ≤ 50 %) when using fixed kernel

estimation. The CV in fact tends to be lower for MCP than kernel estimators when the

same data is used, or, in other words, the CV in MCP stabilises before the CV in KDE

home ranges (Belant & Follmann, 2002).

The exact number of points required to achieve a stable home range may vary

between different populations of bears or individual bears, and may be dependent on

environmental conditions. Hence, Laver and Kelly (2008) recommend determining

when home ranges reach an asymptote.

2.5.5 Cores

An advantage of kernel density estimation is that it allows the identification of areas

within the home range that have a greater intensity of use than expected by random use

(Harris et al., 1990; Powell, 2000, p. 91). This is useful as not all areas within the home

range are of equal importance to the animal as resources are usually distributed in patches

across the landscape. Areas which have a greater intensity of use are known by biologists

as cores (Burt, 1943, p. 91; Powell, 2000; Seaman & Powell, 1990). The core can be

extracted from the utilisation distribution surface by choosing a low probability threshold

such as 25 % and selecting the smallest number of cells that sum to that probability.

However, the choice of a probability threshold is essentially arbitrary and even home

ranges with random or even use will have "cores" by this definition (Powell, 2000, p. 92).

Fortunately, Seaman and Powell (1990) introduced an objective method for

selecting a probability contour to delineate the core area. Areas of intensive use occurring

within the home range can be observed by plotting the percentage area of the total home

range area against the equivalent percentage probability of the maximum probability of

use, as illustrated in Figure 2-1. Here, 100% of the home range area is equivalent to 0 %

probability of use and, at 0 % area the percentage probability is 100 %. This is because

the maximum probability of use is associated with the smallest area within the core range

and the probability of use decreases as home range area extends beyond this area.   If the

use of space were random, this plot would be a straight line with a gradient of -1 or – 45˚

(Figure 2-1a). If the plot is concave (Figure 2.1b), it indicates core areas which are

used more than outlying areas and, if the graph is convex (c), there is even (dispersed)

use of the home range. For the concave plot, the inflection point (where the slope

(derivative) is equal to – 1) indicates the probability contour that delineates the core of

the home range.
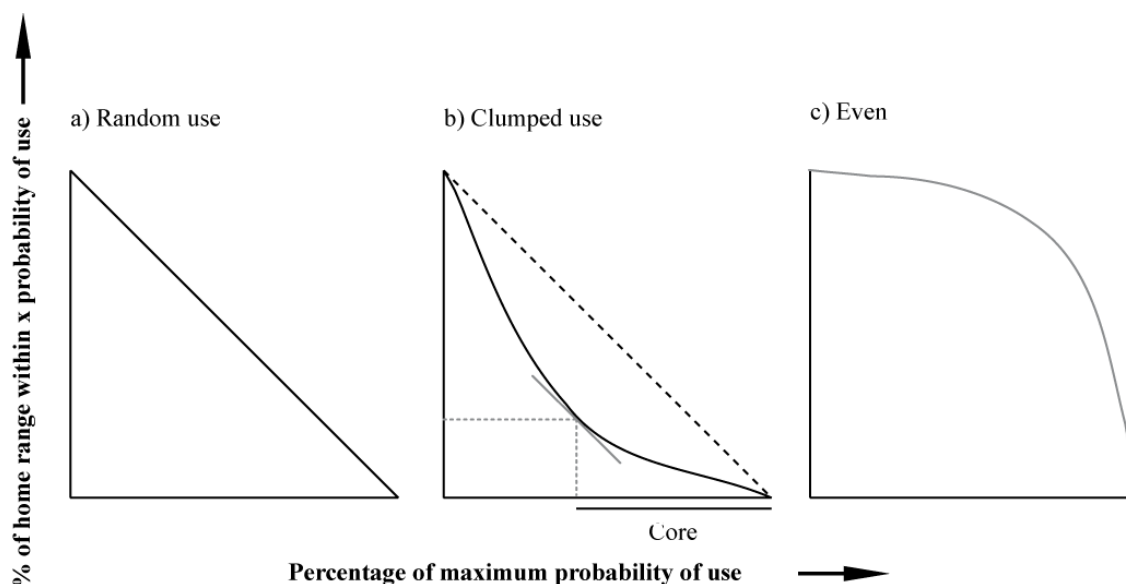
Figure 2-1. Percentage of maximum probability of use. (Adapted from Powell, 2000, p. 93)

2.5.6 Advantages of KDE

Due to the fact that KDE is nonparametric, it can be used to estimate home ranges for a

large variety of multimodal non-normal home ranges if the smoothing parameter is

selected appropriately (Seaman & Powell, 1996). KDE is also unaffected by grid size

and its placement unlike several other estimators such as the harmonic mean estimator

(Silverman, 1986). KDE also allows the identification of core areas from the utilization

distribution surface (Seaman & Powell, 1990).

KDE does have some shortcomings. Like most point-based home range estimators, KDE ignores the sequencing information within position data (White & Garrot, 1990, in Powell, 2000, p. 89). It can also generate islands that look unrealistic, and objective bandwidth estimation is difficult and sensitive to the number of points. Despite these disadvantages, KDE has been one of the most successful home range estimators since its introduction by Worton in 1989 (Laver & Kelly, 2008; Schwartz, et al. 2003; Seaman & Powell, 1996). KDE is recommended by several authors as the best nonparametric home range estimation technique for point data and has been widely implemented (Belant & Follmann, 2002; Powell, 2000; Seaman et al, 1998; Seaman et al., 1999; Steiniger et al., 2010; Worton, 1995, etc.).

2.6 Summary

In summary, this chapter has provided a general background to home range theory and a description of grizzly bear home range characteristics. In addition, two popular home range estimation techniques, the minimum convex polygon and the kernel density estimation, were described in detail. Based on this review the kernel density estimation technique was chosen as the most appropriate home range estimator for grizzly bears. The home range estimation process and choice of parameters is described in detail in section 4.3.1.

Chapter Three: Spatial dependence and modelling

This chapter provides a review of the theory of spatial dependence. Section 3.1 provides an understanding of what spatial dependence is, why it occurs in spatial data, and the challenges this poses; section 3.2 shows how spatial dependence can be modelled through spatial neighbourhood relationships and spatial weight matrices; section 3.3 describes how to quantify spatial dependence and test its significance using the spatial weights defined in the previous section; and finally, section 3.4, demonstrates how structures of spatial dependence can be included into spatial autoregressive models.

This review forms the theoretical basis necessary to carry out several of the tasks outlined in chapter one. These are to:

- Define various spatial weight matrices for quantifying spatial dependence.

- Test the residuals of OLS regression models for spatial dependence using the spatial weight matrices developed as part of this thesis.

- Develop spatial autoregressive models and evaluate the effect of different spatial weight matrices on the estimation of parameters and overall fit, particularly in comparison to the OLS regression models.

- Determine which spatial weight matrices best characterize any spatial dependence present in the data.

3.1 Spatial dependence in spatial data

3.1.1 Spatial data and spatial stationarity

Spatial data can be interpreted as an incomplete sample *of a single realisation* of a stochastic process as defined by

$$\{Z(\mathbf{s}) : \mathbf{s} \in D \subset \mathsf{R}^d\}, \qquad\qquad 3.1$$

where $Z(\mathbf{s})$ is the attribute value of Z at location $\mathbf{s}$, and D is a subset of real numbers with d dimensions consisting of a set of spatial coordinates $\mathbf{s} = [s_1, s_2, \ldots, s_d]$. d usually equals two in spatial data representing the x and y coordinates of the mapping surface. A spatial stochastic process is commonly referred to as a random field. By the Daniell-Kolmogorov theorem a stochastic process can be specified by defining the joint distributions of any finite subset (Sui, 2004).

A stochastic process exhibits strict (or strong) spatial stationarity when the joint probability distributions are the same through any translation of spatial coordinates as shown in the equation below

$$\Pr\{Z(s_1) < z_1, Z(s_2) < z_2, \ldots, Z(s_k) < z_k\} = \Pr\{Z(s_1 + \mathbf{h}) < z_1, Z(s_2 + \mathbf{h}) < z_2, \ldots, Z(s_k + \mathbf{h}) < z_k\}$$

$$3.2$$

for all k and $\mathbf{h}$, where $\mathbf{h}$ is a vector displacement (Cressie, 1993, p. 43; Schabenberger & Gotway, 2005, p. 53). However, this strict condition is usually not able to be met with a spatial dataset, hence a weaker requirement is that the moments of the distribution, rather

than the distribution itself, are invariant under translation (Cliff & Ord, 1981, p. 43; Schabenberger & Gotway, 2005).

Second-order or weak stationarity occurs when the mean and variance is independent of location, but the covariance between two observations is dependent on their relative positions (Schabenberger & Gotway, 2005, p. 142). This can be written formally as follows:

$$E[Z(\mathbf{s})] = \mu, \qquad Var[Z(\mathbf{s})] = \sigma^2,$$

and

$$Cov[Z(\mathbf{s}_i), Z(\mathbf{s}_j)] = C(\mathbf{s}_i - \mathbf{s}_j) = \sigma^2 R(\mathbf{s}_i - \mathbf{s}_j),$$

3.3

where C is a covariance function or covariogram, and R is a correlation function (Cressie, 1993, p. 53). $\mathbf{s}_i - \mathbf{s}_j$, is the vector separation between points and is replaced by $\mathbf{h}$. If $C(\mathbf{h})$ is only a function of the distance, $\|\mathbf{h}\|$, then the covariance is isotropic. In anisotropic processes, the covariance between observations is dependent on direction as well as distance. The covariance and correlation function are formulated as (Schabenberger & Gotway, 2005, pp. 25, 26):

$$C(\mathbf{h}) = E\big[(Z(\mathbf{s}) - E[Z(\mathbf{s})])(Z(\mathbf{s}+\mathbf{h}) - E[Z(\mathbf{s}+\mathbf{h})])\big],$$

3.4

and

$$R(\mathbf{h}) = \frac{C(\mathbf{h})}{\sqrt{Var[Z(\mathbf{s})]Var[Z(\mathbf{s}+\mathbf{h})]}}$$
$$= \frac{C(\mathbf{h})}{\sigma^2}.$$

3.5

$C(\mathbf{0})$ is equal to the variance of $Z(\mathbf{s})$, hence the above equation can also be expressed as

$$R(\mathbf{h}) = \frac{C(\mathbf{h})}{C(\mathbf{0})}.$$
3.6

An important property of a subset of second-order stationary processes is ergodicity, which allows the estimation of the mean and covariances of the set of all possible realisations (Ω) using sample data from a single realisation (ω). If the random field is normally distributed and $\lim_{h\to\infty} C(\mathbf{h}) = 0$, then the field is ergodic (Cressie, 1993, p. 57).

All second-order stationary processes are subsets of intrinsically stationary processes. An intrinsically stationary process has the following properties (Cressie, 1993, pp. 43, 61, 69):

$\mathrm{E}[Z(\mathbf{s})] = \mu,$ for all $\mathbf{s} \in D$, and

$$\mathrm{Var}\big[Z(\mathbf{s}+\mathbf{h}) - Z(\mathbf{s})\big] = 2\gamma(\mathbf{h}).$$
3.7

$\gamma(\mathbf{h})$ is known as the semivariogram. When a stochastic process is second-order stationary, the semivariance can be determined from the covariance function as follows (Haining, 2003, p. 295; Schabenberger & Gotway, 2005, p. 135)

$$\gamma(\mathbf{h}) = C(0) - C(\mathbf{h}).$$
3.8

Although all second-order stationary processes are intrinsically stationary, not all intrinsic processes are second-order stationary. Intrinsic stationarity only requires that the first differences, $Z(\mathbf{s}) - Z(\mathbf{s} + \mathbf{h})$, are second-order stationary. The variance of $Z(\mathbf{s})$ may vary throughout the study region, and the covariance of $Z(\mathbf{s})$ is dependent on position relative to the origin of the coordinate system (Schabenberger & Gotway, 2005,

p. 44). Covariance does not exist as a parameter of the spatial process when it is intrinsically but not second-order stationary (Cressie, 1993, p. 71).

3.1.2 Spatial dependence

Intrinsic and second-order spatial stationarity indicate the interdependence of data among locations, usually exhibited as spatial clustering of similar values in locations close to each other, although clustering of dissimilar vales is also possible. The correlation between points close to each other is referred to as positive spatial autocorrelation or dependence, while negative spatial dependence is the clustering of dissimilar values. This appears as small-scale patchiness and localized trends. It is also possible for spatial dependence to exist in the presence of a global trend, where the mean of the phenomenon of interest varies over the study area (Fortin & Dale, 2005, p. 9). The figure below shows patterns of values which are positively, negatively and randomly (independently) distributed over space.
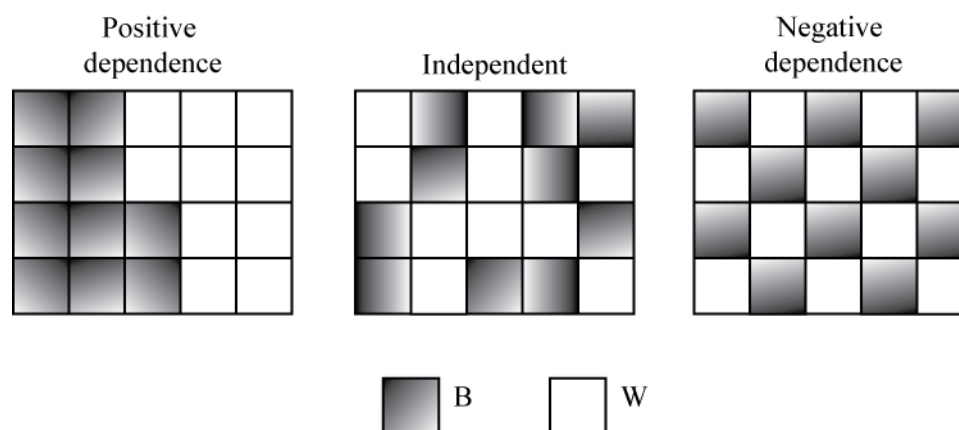
Figure 3-1 Patterns of spatial dependence and independence (Adapted from Haining, 2003, p. 80)

Positive spatial dependence implies that there is redundancy in the information of nearby samples, thereby effectively decreasing the degrees of freedom to less than the actual number of samples (Anselin & Bera, 1998; Haining, 2003, p. 41; Odland, 1988, p. 13). The reduction of independent observations should be taken into account when estimating parameters as the variance of estimates tends to be under-estimated in the presence of positive spatial dependence, while they are over-estimated in the presence of negative spatial dependence (Haining, 2003, p. 273; Schabenberger & Gotway, 2005, p. 31). In addition, maximum likelihood estimation methods are recommended for incorporating spatial dependence structures into regression models (Doreian, 1981; Schabenberger & Gotway, 2005).

3.1.3 Causes of spatial dependence: spatial processes

Spatial dependence occurs in spatial data due to the continuity of space and the operation of spatial processes (Haining, 2003). Generic spatial processes that can give rise to spatial dependence are diffusion (or contagion), exchange and transfer, interaction, dispersal and competition (Fortin & Dale, 2005, p. 21; Haining, 2003).

Diffusion occurs when a phenomenon is spread to an adjacent or connected population or area that previously did not have it. An example is the spread of contagious or infectious diseases by people travelling and coming into contact with unaffected people in adjacent areas.

Exchange and transfer take place when goods are exchanged and transferred from one place to another, e.g. trade between countries or nearby economic centers. The

revenue generated from sales in one area may be spent in another, thus the areas become economically dependent on each other. Economic statistics, such as per capita income, may begin to look similar in these areas.

Interaction occurs when outcomes at one location are influenced by events and circumstances in another place. This is usually precipitated by some movement between locations and/or sharing of information. For example, the price of products will be related in markets that are close enough for those products to be exchanged, or for people from those markets to be able to move between them (Haining, 2003; Odland, 1988).

In the process of dispersal, the population itself spreads physically through space. An example is the wind dispersal of seeds from a tree (Fortin & Dale, 2005; Haining, 2003).

Finally competitive processes may induce negative spatial dependence between adjacent objects (Fortin & Dale, 2005; Haining, 2003). Adjacent plants may compete for resources such as nutrients and light. The plants that are established first are likely to acquire the larger share of resources through extended and developed roots and foliage, thus reducing resources for neighbouring plants. All things being equal, the first plant will be larger and healthier in comparison to adjacent plants.

Spatial dependence may be inherent to the variable of interest, where internal/endogenous spatial processes such as diffusion cause the variable to be correlated with itself, or induced by exogenous factors which are themselves spatially autocorrelated (Fortin & Dale, 2005, p. 7). For example, the patch-like distribution of certain plants can be caused by the patchiness of the underlying soil types which it requires.

3.1.4 Causes of spatial dependence: sampling framework

The spatial patterns that are detected depend upon and are sometimes created by the interaction between the sampling framework, the "actual" spatial patterns on the ground, and the assumptions of the particular spatial autocorrelation statistics used (Fortin & Dale, 2005, p. 112; Messner & Anselin, 2004).

The size and/or spatial lag between units limit the scale of patterns that can be identified (Fortin & Dale, 2005, p. 112; Odland, 1988, p. 27). If the spatial resolution of units, and/or the spatial lags are larger than the scale of the underlying process, the pattern may not be detected at all. For example, in satellite imagery a single value is assigned to a pixel although the area covered by the pixel may be composed of heterogeneous objects. Negative spatial dependence could be detected if the spatial lag is larger than homogenous patches in a heterogeneous landscape (Cliff & Ord, 1981, p. 22). Conversely, if the resolution and spatial lag are smaller than the scale of the process, positive spatial dependence will be observed. Finally, in count and remote sensing data for example, smaller measurement units tend to have a larger variance, and are therefore more likely to contain spurious outliers (Fortin & Dale, 2005, p. 20; Haining, 2003; Messner & Anselin, 2004). Local spatial outliers can in turn lead to false detection of significant spatial autocorrelation because several spatial autocorrelation test statistics, such as Moran's I, rely on deviations from the average, and Geary's c, squares the difference between nearby observations (Fortin & Dale, 2005, p. 125; Messner & Anselin, 2004, p. 130). The definitions and descriptions of these spatial autocorrelation statistics are given in section 3.3.

The shape and orientation of the measurement units may minimize or maximize within-unit variance if they are orientated across or parallel to an environmental gradient respectively (Fortin & Dale, 2005, p. 112; Odland, 1988, p. 27). If the sampling units run across the gradient, the trend would not be detected, while it would be strongly detected if the units were aligned parallel to the gradient. An elongated shape may also cause the appearance of artificial anisotropic patterns (Fortin & Dale, 2005, p. 20). The problems of shape, size and spatial lag can be reduced by selecting random locations for sampling (Fortin & Dale, 2005, p. 20)

The number of sampling units and their spatial configuration can increase or decrease the power of detecting significant spatial patterns (Fortin & Dale, 2005, pp. 112, 142). Fortin and Dale (2005, p. 18) recommend that a minimum of 30 observations are taken to detect spatial dependence when there is a fairly strong signal. Ideally, for reliable detection and estimation of parameters one-hundred observations should be used. Another potential problem of smaller sample sizes is caused by the assumption that the distributions of several spatial autocorrelation test statistics, such as Moran's *I* (see Section 3.3) are asymptotically normal. Small sample sizes (of fewer than 50) may falsely detect spatial autocorrelation if a normal distribution is used for comparison (Odland, 1988, p. 27). However, this can be resolved by using a random distribution to test significance.

A common assumption of several spatial autocorrelation statistics is that the variable of interest is second-order stationary. For example, Moran's *I* is computed using the deviation from the estimated mean. However, if the extent of the study area incorporates heterogeneous areas with differing ecological and environmental conditions

it is likely that the response variable will become non-stationary, thus biasing test

statistics or invalidating inferences (Fortin & Dale, 2005, pp. 11,174). In heterogeneous

study areas where non-stationarity exists, local spatial autocorrelation statistics should be

used rather than global to avoid misleading inferences (Fortin & Dale, 2005, p. 13).

In contrast to large study areas that incorporate diverse regions, a study area may

be too small to detect spatial patterns at all. For example the often arbitrarily or politically

chosen boundary may cut off spatial processes and patterns that extend beyond the study

area.   This can cause bias in the estimation of parameters that describe the

interdependence of locations (such as in spatial autoregressive models), and make

comparison of different weighting functions difficult.

The shape of the study area and number of samples will determine how many

units are affected by boundary issues. It is best to keep the proportion of boundary units

as low as possible as boundary units will have fewer neighbours than observations in the

core of the study area (Fortin & Dale, 2005, p. 22; Odland, 1988, p. 29).

3.2 Exploring and modelling spatial dependence

3.2.1 Semivariograms, covariograms and correlograms

The distance over which spatial dependence occurs between two observations can be

explored using various plots such as the semivariogram, covariogram and correlogram, in

which the semivariance, covariance or correlation are computed at increasing distances of

$||\mathbf{h}||$ and plotted against $||\mathbf{h}||$ (Haining, 2003). If the process is anisotropic these should

also be computed in various directions.

The semivariogram from equation 3.7 can be estimated using the classical semivariogram estimator,

$$\hat{\gamma}(\mathbf{h}) = \frac{\sum_{i=1}^{N(\mathbf{h})}\sum_{i=j}^{N(\mathbf{h})}(Z(\mathbf{s}_i) - Z(\mathbf{s}_j))^2}{2|N(\mathbf{h})|}$$ 3.9

as proposed by Matheron in 1962 (Cressie, 1993, pp. 40, 69). $Z(\mathbf{s}_i)$ and $Z(\mathbf{s}_j)$ are separated by $\mathbf{h}$ and $/N(\mathbf{h})|$ is the number of distinct pairs of sites at a separation of $\mathbf{h}$ from each other. In irregularly spaced data, a tolerance or bandwidth should be specified around $\mathbf{h}$ to ensure that there are enough observation pairs at each value of $\mathbf{h}$ (Cressie, 1993, p. 70). This semivariance estimator is unbiased when $Z(\mathbf{s})$ is intrinsically stationary (Schabenberger & Gotway, 2005, p. 137).

Although in theory the semivariogram should equal zero at the origin, i.e. no variance at $\mathbf{h} = \mathbf{0}$, there is usually a small shift along the y-axis such that as $\mathbf{h} \to \mathbf{0}$ $\gamma(\mathbf{h}) \to c_0 > 0$. c_0 is known as the nugget (Cressie, 1993, p. 59). The nugget is caused by local random effects, often termed microscale variation, and/or measurement error (Fortin & Dale, 2005, p. 134, Cressie, 1993). Figure 3-1 shows the nugget, sill and range.

If $C(\mathbf{h}) \to 0$, as $\|\mathbf{h}\| \to \infty$, i.e. if the process is ergodic, then the semivariogram will approach the variance of $Z(\mathbf{s})$ either asymptotically or at some lag $\|\mathbf{h}\|$ (Cressie, 1993, p. 67). The asymptote itself is known as the sill, c_s (Schabenberger & Gotway, 2005, p. 138) and is equivalent to $C(\mathbf{0})$ or the Var$[Z(\mathbf{s})]$. The **range**, a, is the distance, $\|\mathbf{h}\|$, at which the sill is reached. Observations separated by a distance greater than the range are no longer correlated with each other (Haining, 2003, p. 295).

There are several reasons why the semivariogram may not have a sill. The process, $Z(\mathbf{s})$, may not be stationary, or it is second-order stationary but the largest observed lag size is shorter than the actual range of the process, or the process does not meet the requirements of intrinsic stationarity, i.e. $2\dfrac{\gamma(\mathbf{h})}{\|\mathbf{h}\|^2} \to 0$ as $\|\mathbf{h}\| \to 0$ (Schabenberger & Gotway, 2005, p. 139) .
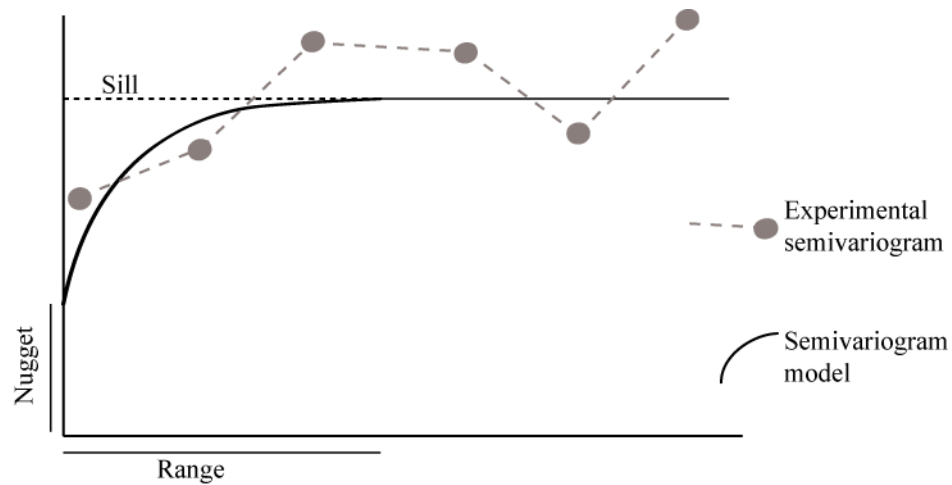
Figure 3-2. Empirical and theoretical semivariogram (Adapted from Fortin & Dale, 2005)

By fitting a model to the empirical semivariogram important properties of spatial dependence can be explored such as the range of spatial interdependence (if the sill is reached), and the rate that covariance decreases with distance.

Common isotropic models are the exponential, Gaussian, and bounded spherical model as shown below (Cressie, 1993, pp. 61, 89).

The *exponential model*:

$$\gamma(\mathbf{h};\boldsymbol{\theta}) = c_0 + c_s\left\{1 - \exp\left(-\frac{\|h\|}{a}\right)\right\};$$

3.10

the *Gaussian model*:

$$\gamma(\mathbf{h};\boldsymbol{\theta}) = c_0 + c_s \left\{1 - \exp\left(-\|\mathbf{h}\|^2 / a^2\right)\right\};$$ 3.11

and the *bounded spherical model*:

$$\gamma(\mathbf{h};\boldsymbol{\theta}) = \begin{cases} c_0 + c_s \left\{ \frac{3}{2}\left(\frac{\|\mathbf{h}\|}{a}\right) - \frac{1}{2}\left(\frac{\|\mathbf{h}\|}{a}\right)^3 \right\}, & 0 < \|\mathbf{h}\| \le a \\ c_0 + c_s, & \|\mathbf{h}\| \ge a; \end{cases}$$ 3.12

where $\boldsymbol{\theta} = (c_0, c_s, a)'$, and $c_0 \ge 0$, $c_s \ge 0$ and $a \ge 0$.

If the spatial process is second-order stationary, then the semivariogram, $\gamma(\mathbf{h})$ can easily be expressed in terms of the covariance function, $C(\mathbf{h})$, using $\gamma(\mathbf{h}) = C(\mathbf{0}) - C(\mathbf{h})$ (Schabenberger & Gotway, 2005, p. 135). The covariogram (the graph of $C(\mathbf{h})$ against $\mathbf{h}$) can as easily be transformed into a correlogram by dividing the covariogram by $C(\mathbf{0})$. The covariance can be estimated from the data using

$$\hat{C}(\mathbf{h}) = \frac{\sum\limits_{i=1}^{N(\mathbf{h})}\sum\limits_{j=1}^{N(\mathbf{h})}\left(Z(\mathbf{s}_i) - \bar{Z}\right)\left(Z(\mathbf{s}_j) - \bar{Z}\right)}{|N(\mathbf{h})|}.$$ 3.13

Cressie (1993, pp. 70 - 73) argues that the semivariogram is preferable to the covariogram for modelling spatial dependence. For one, the semivariogram can be applied to all intrinsically stationary processes, while the covariogram is only defined for second-order stationary processes (Cressie, 1993, p. 71; Schabenberger & Gotway, 2005, p. 136). Although the semivariogram and covariogram are theoretically equivalent in second-order processes, the empirical estimators are not exactly equivalent. Thus when the semivariogram is calculated from the estimated covariance it will be biased, although

this bias decreases as $|N(\mathbf{h})|/n \to 1$ (Cressie, 1993, p. 70; Schabenberger & Gotway, 2005, p. 137). The cause of this bias is shown below where the semivariance is rewritten as

$$\hat{\gamma}(\mathbf{h}) = \frac{\sum_{i=1}^{N(\mathbf{h})}\sum_{i=j}^{N(\mathbf{h})}\left(\left(Z(\mathbf{s}_i) - \overline{Z}\right) - \left(Z(\mathbf{s}_j) + \overline{Z}\right)\right)^2}{2|N(\mathbf{h})|}$$

$$= \sum_{i=1}^{N(\mathbf{h})}\frac{\left(Z(\mathbf{s}_i) - \overline{Z}\right)^2}{|N(\mathbf{h})|} - \hat{C}(\mathbf{h}).$$

3.14

However,

$$\hat{C}(\mathbf{0}) = \frac{\sum_{i=1}^{n}\left(Z(\mathbf{s}_i) - \overline{Z}\right)^2}{n},$$

3.15

hence $\hat{C}(\mathbf{0}) - \hat{C}(\mathbf{h}) \neq \hat{\gamma}(\mathbf{h})$.

Also, while the classical variogram estimator given in equation 3.9 is unbiased for all intrinsically stationary processes, the covariance estimator (3.13) is biased for second-ordinary stationary processes when the mean must be estimated from the data (Schabenberger & Gotway, 2005, p. 137). If there is a linear trend in the data, it is also advantageous to use the semivariogram rather than the covariogram to model the spatial dependency in the residuals. This is because the bias of the semivariogram is smaller than that of the covariogram. See Cressie (1993, p. 71 - 72) for details. The advantages of the semivariogram over the covariogram arise from the fact that the mean does not need to be estimated in the semivariogram (Schabenberger & Gotway, 2005, p. 137).

3.2.2 Spatial neighbourhoods, contiguity and weight matrices

To model spatial dependence it is necessary to define which observations are "close" to each other and the strength of their relationship. Those observations that covary with each other based on their spatial relationship are known as "neighbours". A formal definition of a neighbour is given by (Cressie, 1993, p. 414): a site k is a neighbour of site i if the conditional distribution of $Z(s_i)$, given all other site values, is functionally dependent on $Z(s_k)$, for $k \neq i$. The neighbourhood of site i consists of all those sites that can be defined as neighbours as described above.

Neighbourhood relationships can be represented by a weight matrix, **W,** which has n x n rows and columns, where n equals the number of sample observations. Each matrix element is a measure of the covariance between a pair of observations (Haining, 2003) with non-diagonal elements being greater than or equal to zero *($w_{ij} \geq 0$)*, and diagonal elements, w_{ii} equal to zero, as an observation cannot be a neighbour with itself.

Closeness can be determined in topological or Euclidian space (Fortin & Dale, 2005, p. 113). In topological space, it is the relative position of observations to each other that is important, whereas in Euclidian space, absolute position, distance, and/or direction matters. Weights can be determined by connectivity, contiguity, or as functions of distances, shared borders, interaction factors, theoretical considerations, etc.

The specification of weights can be guided by substantive knowledge and theory, or empirical approaches. For example, if there is data about the flow of people between places, the spread of a contagious disease can be based on substantive knowledge. When theory is not available, weights are chosen by convention or empirical approaches (Stetzer, 1982). The empirical specification of the weight matrix is difficult however, as

there is an "infinity of possible representations", and involves "substantive concerns and technical constraints" (Doreian, 1981). Various methods for specifying the weight matrix are described hereafter.

3.2.3 Spatial dependence as a function of distance

Distance-based contiguity can be defined by a simple binary relationship, where observations within a threshold distance of each other are neighbours, and those further apart are not. A more common assumption following from Tobler's Law of Geography (1970), is that the correlation between observations tends to decrease with increasing distance. This assumption is very likely correct for continuous variables sampled at discrete locations (Kaluzny et al., 1998). Distance neighbours can also be defined for areal units by using a single reference point, such as the centroid, for computing distances and other relationships (Fortin & Dale, 2005, p. 114; Kaluzny, et al., 1998).

Distances can be measured in several other metrics besides Euclidian straight line distances, including route distances, the time or cost taken, perceived distances or networks of relationships (Haining, 2003, pp. 18, 19).

Although there are many possible distance decay functions, a few commonly used functions are given below (Brunsdon et al., 1996; Haining, 2003).

Inverse distance and inverse distance squared respectively:

$$w_{ij} = d_{ij}^{-1} \text{, and} \tag{3.16}$$

$$w_{ij} = d_{ij}^{-2} \text{,} \tag{3.17}$$

where d_{ij} is the distance between observations *i* and *j*.

The exponential distance decay function:

$$w_{ij} = \exp(-d_{ij}^{-1}),$$
<div align="right">3.18</div>

where exp() denotes an exponential function.

The Gaussian decay function:

$$w_{ij} = \exp(-\beta d_{ij}^{2}),$$
<div align="right">3.19</div>

where β is a constant to be determined. The larger β is the more rapidly dependence decreases with distance.

The bi-square decay function:

$$w_{ij} = \left[1 - \left(d_{ij}^{2} / b^{2}\right)\right]^{2}, \quad \text{if } d_{ij} < b,$$
<div align="right">3.20</div>

 where b is a distance threshold beyond which no spatial interaction occurs.

The rate of decay or distance thresholds can be obtained from semivariograms, covariograms or correlograms.

3.2.4 Shared boundaries in areal units

A common method used to specify neighbours for areal units are those based on shared borders. In the case of a regular square tessellation, rook, bishop and queen neighbours can be defined based on Chess moves. Rook neighbours share common boundaries in the four cardinal directions, bishop neighbours along diagonals and queen in all eight directions (Fortin and Dale, 2005). Chess moves can be adapted for irregular units such that rook neighbours share a boundary, bishop neighbours share corners, and queen neighbours share both. Chess neighbours are usually represented in a binary weight matrix.

Other common weighting functions are based on the proportion of shared

border or a combination of shared border and distance (Haining, 2003). A commonly

used function of shared border length is shown below:

$$w_{ij} = l_{ij}/l_i ,$$
3.21

where l_{ij} is the length of the shared boundary over the length of the boundary for i.

A combined distance-boundary function can be specified as follows:

$$w_{ij} = \left(l_{ij}/l_i \right) d_{ij}^{-1} .$$
3.22

Second and higher-order neighbourhoods can also be constructed where neighbours are

connected by 1 or more shared neighbours (Odland, 1988, p. 25).

3.2.5 Connectivity network algorithms

Neighbours can also be defined topologically using connectivity network algorithms.

Fortin & Dale (2005, p. 57) describe a hierarchical set of connectivity networks,

technically known as graphs, that can be used to model spatial neighbourhoods. Each

graph is a subset of a more complex graph which is higher up in the hierarchy. Graphs

are defined by vertices (v_i) which are connected together by lines known as edges. A

sequence of vertexes connected by edges is known as a path, and paths that start and end

on the same vertex without crossing any edges twice are known as cycles. In spatial data,

each observation point, or centroid in the case of areal data, becomes a vertex. Pairs of

observations connected by edges are neighbours, which can be represented in a simple

binary format within the weight matrix.

The simplest graph, with the fewest number of connections, is the mutual nearest neighbour (MNN) graph. In this graph only mutual nearest neighbours are connected by edges.

The MNN graph is a subgraph of the nearest neighbour (NN) graph. In a NN graph, every vertex will be connected to at least one other.

The minimum spanning tree (MST) graph is formed by connecting all non-connected parts of the NN graph by the shortest distances possible. All vertexes are connected to all others through a path, none of which are cyclic.

The MST graph is a subgraph of the relative neighbour (RN) graph (Toussaint, 1980, p. 59). The RN graph is formed by connecting two vertices if the lens of overlap created by two circles centred on each vertex with a radius equal to the distance between the vertices, contains no other vertices. This concept is illustrated in Figure 3-3a where F and G are the two vertices of interest, and r is the radius of the circles centered on F and G. The lens of overlap created by these two circles must contain no other vertices.

The next graph in the hierarchy is the Gabriel Graph (GG), see Figure 3-3b. The GG is formed by connecting any two vertices which lie opposite each other on the circumference of the circle whose diameter equals the distance between them, provided that no other vertices are found within this circle (Gabriel & Sokal, 1969, p. 59).

The most complex graph in the hierarchy is a Delaunay triangulation which incorporates all edges from the GG. A Delaunay triangulation is created by joining any three vertices where the circumcircle defined by those three points contains no other vertex (Hjelle & Daehlen, 2006, p. 56; Okabe, Boots, & Sugihara, 1992, p. 94) as shown in Figure 3-3c.
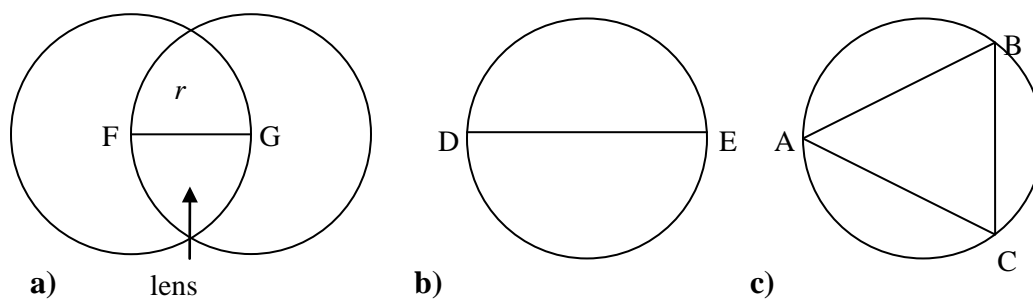
Figure 3-3. a) Relative neighbour graph b) Gabriel Graph c) Delaunay triangulation

A Delaunay triangulation also requires that the minimum interior angle of any pair of adjacent triangles is the maximum possible (Hjelle & Daehlen, 2006, pp. 49, 56). This will be explained using Figure 3-4. Consider the four vertexes, A, B, C and D in the figure. There are two possible triangulations that can be created between ABCD shown in a) and b). It can be seen in b) that the smallest angle of the six interior angles (a_{min}') is larger than the smallest angle (a_{min}) in a). For this reason the triangulation in b) is the Delaunay triangulation.
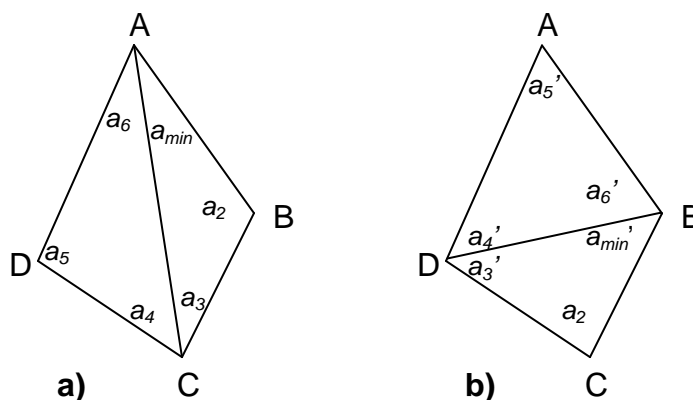
Figure 3-4. The maximum minimum requirement of Delaunay triangulation

Each graph in the network hierarchy of graphs is a subgraph of a more complex connectivity network, thus the number of edges or connections increases for each graph

higher up in the hierarchy. Different network structures should be used to test for

spatial dependence as it is typically not known *a priori* which structures may best capture

spatial dependence, if at all.

In the following section two important statistics are provided to test for spatial

dependence. These statistics rely on the specification of the weights matrix.

3.3 Quantifying and testing for spatial dependence

Following the specification of a weight matrix, it is possible to test for spatial

autocorrelation amongst neighbouring observations. There are many possible statistics to

measure and test spatial autocorrelation; however, this section will review the following

popular and well-understood statistics, Moran's *I* (Moran, 1950) and Geary's *c* (Geary,

1954). The Gestis-Ord *G* is a useful alternative test and can be reviewed in Getis and Ord

(1992).

3.3.1 Measures of global spatial autocorrelation

Moran's *I* provides a measure of the average covariance between each unit, *i*, and its

neighbours, *j*, as shown in equation 3.23,

$$I = \frac{n}{[\mathbf{W}]} \frac{\sum_{i=1}^{n}\sum_{j=1}^{n} w_{ij}\left(Z(\mathbf{s}_i)-\overline{Z}\right)\left(Z(\mathbf{s}_j)-\overline{Z}\right)}{\sqrt{\sum_{i=1}^{n}\left(Z(\mathbf{s}_i)-\overline{Z}\right)^2}}, i \neq j, \qquad 3.23$$

where $\overline{Z}$ is the mean value of $Z(\mathbf{s})$, *n* is the number of observations, w_{ij} is the weight of

the contribution of the pair at locations $\mathbf{s}_i$ and $\mathbf{s}_j$, and [**W**] is the sum of all elements in the

weight matrix. The weights can be derived from neighbourhood functions as described in section 3.2.

When $I > \mathrm{E}[I]$, which is slightly less than zero (the value of $\mathrm{E}[I]$ is shown in equation 3.24), it indicates positive spatial dependence, and negative spatial dependence when $\mathrm{I} < \mathrm{E}[\mathrm{I}]$ (Fortin and Dale 2005, p. 124). Assuming the null hypothesis of n random and independent observations drawn from a population of any distribution, the expected value of I is given in equation 3.24 (the proof is given in (Cliff & Ord, 1981, pp. 42 - 45)

$$\mathrm{E}(I) = -\frac{1}{n-1}.$$ 3.24

Although the estimated value of I will normally lie between -1 and 1, I is not restricted to this range. The extreme values of I are given by the eigenvalues of the following matrix (Griffith & Layne, 1999, p. 25):

$$[\mathbf{I} - \mathbf{Z}(\mathbf{s})(\mathbf{Z}(\mathbf{s})'\mathbf{Z}(\mathbf{s}))^{-1}\mathbf{Z}(\mathbf{s})']\mathbf{W}[\mathbf{I} - \mathbf{Z}(\mathbf{s})(\mathbf{Z}(\mathbf{s})'\mathbf{Z}(\mathbf{s}))^{-1}\mathbf{Z}(\mathbf{s})'].$$ 3.25

Moran's I can fall outside of its normal range when there are too few pairs of sampling points, or there is an irregular pattern of weights and extreme values are heavily weighted (Cliff & Ord, 1981, p. 21, Fortin & Dale, 2005, p.124).

While the expected value of I is the same for any underlying probability distribution of $Z(\mathbf{s})$, the variance will differ for different distributions. The variance of I under the normality assumption is given by Cliff and Ord (1981, p. 44). If the distribution of $Z(\mathbf{s})$ is unknown, a randomisation procedure (R) (explained later in this section) can be used to estimate the expected variance of I under the null hypothesis of no spatial autocorrelation. The randomisation procedure provides an unbiased estimate of the variance such that $\mathrm{Var}[I] = \mathrm{Var}_R[I]$ for any distribution (Cliff & Ord, 1981, pp. 45 - 46).

Geary's c (equation 3.26) is similar to Moran's I, but does not use the mean value of $Z(\mathbf{s})$ to estimate autocorrelation. Rather, it is based on the squared difference between neighbouring observations i and j,

$$c = \frac{n-1}{[2\mathbf{W}]} \frac{\sum_{i=1}^{n}\sum_{j}^{n} w_{ij}\left(Z(\mathbf{s}_i) - Z(\mathbf{s}_j)\right)^2}{\sqrt{\sum_{i=1}^{n}\left(Z(\mathbf{s}_i) - Z(\mathbf{s}_j)\right)^2}}, i \neq j.$$ 3.26

Geary's c ranges from 0 to 2, where $0 \leq c < 1$ indicates positive autocorrelation, and $1 < c \leq 2$, negative (Fortin & Dale, 2005). Assuming a normal distribution, $E[c] = 1$, indicates no spatial autocorrelation, (Schabenberger & Gotway, 2005, p. 22).

Cliff and Ord (1981, pp. 47 - 49) show that both Geary's c and Moran's I, are asymptotically normally distributed under the null hypothesis of zero spatial autocorrelation when $Z(\mathbf{s})$ is normal. Geary's c is useful for confirming Moran's I, which is the more powerful test statistic (Griffith & Layne, 1999, p. 15).

Both Moran's I and Geary's c are based on the assumption of spatial stationarity, i.e. constant mean and variance (Haining, 2003, p. 244; Messner & Anselin, 2004, p. 22; Schabenberger & Gotway, 2005). Since the estimation of Moran's I is based on the deviation from the mean, outliers, a skewed distribution or the presence of a trend in the data can bias the estimate. Similarly, the value of c may also be biased by outliers or a skewed distribution, due to squaring the differences between nearby observations (Fortin & Dale, 2005, p. 125).

The significance of both Moran's I and Geary's c can be tested using various methods, including the normality assumption, randomisation procedure, exact and Saddlepoint approximation tests.

Normality assumption

The normality assumption assumes that the spatial autocorrelation statistic, M, is normal if the distribution of $Z(\mathbf{s})$ is normal (e.g. Moran's I and Geary's c). Using this assumption, the mean and variance of M can be derived under the null hypothesis such that $\text{Cov}[Z(\mathbf{s}_i), Z(\mathbf{s}_j)] = 0, \ i \neq j$ (Schabenberger & Gotway, 2005, p. 16). The spatial autocorrelation statistic can then be tested as a standardized normalized deviate:

$$z = \frac{M - \text{E}[M]}{\text{var}[M]^{1/2}}, \qquad\qquad 3.27$$

where $\text{E}[M]$ is the expected value of the spatial autocorrelation statistic, and $\text{var}[M]$ is the operationalized variance (Cliff & Ord, 1973, pp. 13 - 15, 29 - 33; Schabenberger & Gotway, 2005).

Randomisation procedure

A randomisation procedure can be used when the population distribution of $Z(\mathbf{s})$ is unknown. If the null hypothesis of no spatial clustering of values, $Z(\mathbf{s}_1), \ldots, Z(\mathbf{s}_n)$, is true, then the observation values are randomly distributed among the spatial locations, or in other words, each permutation of the spatial allocation of values is equally likely (Cliff & Ord, 1981, p. 45; Schabenberger & Gotway, 2005). Hence, if there are n sites, there are n! possible ways that the values of $Z(\mathbf{s})$ may be arranged. By re-assigning observed values to locations so that all possible arrangements are made, and computing the spatial autocorrelation for each of these arrangements, it is possible to determine the null distribution (expected value and variance) of the autocorrelation statistic. The observed spatial autocorrelation statistic can then be compared to the empirical distribution to determine its probability (Schabenberger & Gotway, 2005).

Exact test

The exact test is used when the exact reference distribution of the spatial

autocorrelation statistic is known (Tiefesldorf, 2002). For example, when testing

normally distributed residuals, the exact distribution of Moran's *I* can be computed using

numerical integration (Tiefesldorf, 2002).

Saddlepoint approximation test

The Saddlepoint approximation generates an approximate reference distribution

that optimises the fit of the approximation (Tiefesldorf, 2002). The Saddlepoint

approximation is more reliable in the face of unusual spatial weights matrices, unknown

reference distributions and strong underlying spatial dependence which tend to skew the

reference distribution of the normal assumption test (Tiefesldorf, 2002). Also, unlike the

randomisation test it can be used to test regression residuals.   More information about

this method can be found in Tiefelsdorf (2002).

3.4 Multivariate regression modelling in the presence of spatial dependence

It has been well established that Ordinary Least Squares (OLS) estimates of multivariate

regression parameters can result in biased variance estimates and inefficient regression

coefficients in the presence of spatial dependence (Anselin & Bera, 1998; Cliff & Ord,

1981; Cordy & Griffith, 1993; Doreian, 1981; Griffith, 1996; Hepple, 1976; Loftin &

Ward, 1983). This is due to the fact that spatial dependence violates the assumptions of

OLS.

To use OLS, the multivariate linear model has the form (in matrix notation):

$$\mathbf{Z(s)} = \mathbf{X(s)}\beta + \mathbf{e(s)}, \qquad\qquad 3.28$$

where $\mathbf{Z(s)}$ is a vector of n observations of the dependent variable at each location $\mathbf{s}$,

$\mathbf{X(s)}$ is a n by k matrix of observations of the explanatory variables, β is a k-element

vector of parameters, and $\mathbf{e(s)}$ is an n-element vector of disturbances or errors.

The following assumptions are necessary to ensure that OLS is the best linear unbiased

estimator.

The residuals must be normally distributed with a mean of zero and constant variance:

$$\mathbf{e(s)} \sim N(0, \sigma^2). \tag{3.29}$$

There should be no correlation between the explanatory variables and residuals:

$$\text{Cov}[\mathbf{X}_{ji}, \mathbf{e}_i] = 0. \tag{3.30}$$

The residuals must be independently distributed:

$$\text{E}[\mathbf{e(s)}\mathbf{e(s)}] = 0. \tag{3.31}$$

Finally, the explanatory variables must be independent:

$$\text{Cov}[\mathbf{X}_i, \mathbf{X}_j] = 0, \tag{3.32}$$

The assumptions of identically and independently distributed errors are often referred to

as the *ii*d assumptions. If these assumptions are true, then OLS is the best linear unbiased

estimator of the parameters β and σ^2 where

$$\hat{\beta}_{ols} = [\mathbf{X(s)}'\mathbf{X(s)}]^{-1}\mathbf{X(s)}'\mathbf{Z(s)}, \tag{3.33}$$

and

$$\hat{\sigma}_{ols}^2 = \frac{1}{n-k}[\mathbf{Z(s)} - \mathbf{X(s)}\hat{\beta}_{ols}]'[\mathbf{Z(s)} - \mathbf{X(s)}\hat{\beta}_{ols}]. \tag{3.34}$$

Using the estimated values of β and σ^2, a set of residuals can be calculated, which

in turn is utilized to calculate standard errors for each regression coefficient, as well as

test the significance of the coefficients. However, if the residuals are found to be spatially dependent, then the OLS assumptions have not been met and the inferences may be invalid (Cliff & Ord, 1981, p. 197).

There are two major causes of spatial dependence in the residuals of a linear regression model. First, if an explanatory variable is not included in the model, but is spatially dependent, the absence of this variable will most likely induce spatial dependence in the residuals. It may be possible to add an explanatory variable to the model that captures this spatial dependence. However, while it may reduce spatial dependence, it is unlikely to remove it entirely due to uncertainty of the precise nature of the spatial processes operating, and the limitation of the data available (Odland, 1988, p.60).

Second, spatial autocorrelation may also result if the functional form of the model is incorrect, for example, if a non-linear relationship has been modelled as a linear relationship (Cliff & Ord, 1981, p. 54; Odland, 1988). By correctly specifying the form of the relationship, spatial dependence may be removed.

If it is not possible to remove spatial dependence using the suggestions above, it may be necessary to include spatial autoregressive structures into the multivariate model. Before describing these models in section 3.4.2, the following section will show how Moran's *I* can be used to detect spatial dependence in the residuals of an OLS linear model.

3.4.1 How to test for spatial autocorrelation in the residuals

Testing for spatial autocorrelation in residuals requires a modification of the expected

value and variance of *I* used in section 3.3. This is because the variance and covariances

are not directly observable, but must be estimated from the residuals of a particular

regression model (Odland, 1988). The variance-covariance matrix of the OLS regression

model, under the assumptions of identical and independent errors, is estimated as follows

(Cliff and Ord, 1981, p.200):

$$
\begin{aligned}
\mathrm{E}\big[\hat{\mathbf{e}}(\mathbf{s})'\hat{\mathbf{e}}(\mathbf{s})\big] &= \sigma^2\big[\mathbf{I} - \mathbf{X}(\mathbf{s})\big(\mathbf{X}(\mathbf{s})'\mathbf{X}(\mathbf{s})\big)^{-1}\mathbf{X}(\mathbf{s})'\big] \\
&= \sigma^2\mathbf{M}.
\end{aligned}
\tag{3.35}
$$

Since **M** will have non-diagonal elements it can be seen from equation 3.35 that the

estimated errors are correlated with each other, even if the underlying population of

errors are uncorrelated.

To test the residuals for spatial autocorrelation, Moran's *I* has the same form as in

equation 3.23, although this time in matrix notation

$$
I_{res} = \frac{n}{[\mathbf{W}]}\frac{\hat{\mathbf{e}}(\mathbf{s})'\mathbf{W}\hat{\mathbf{e}}(\mathbf{s})}{\hat{\mathbf{e}}(\mathbf{s})'\hat{\mathbf{e}}(\mathbf{s})}.
\tag{3.36}
$$

The distribution of I_{res} has been shown to be asymptotically normal by Cliff and Ord

(1981, pp. 200 -203) and the expected value is given in equation 3.37 (Schabenberger &

Gotway, 2005, p. 314). Since **e**(**s**) is estimated from **X**(**s**), the expected value of *I* (shown

in equation 3.37) under the null hypothesis of identically and independently (i.i.d)

Guassian residuals, must take into account any spatial dependence that may be in **X**.

$$
\mathrm{E}[I_{res}] = \left[\frac{n}{(n-k)[\mathbf{W}]}\right]\mathrm{tr}\big[\big(\mathbf{X}(\mathbf{s})'\mathbf{X}(\mathbf{s})\big)^{-1}\mathbf{X}(\mathbf{s})'\mathbf{W}\mathbf{X}(\mathbf{s})\big].
\tag{3.37}
$$

Here k is the number of explanatory variables including the intercept. The expected

variance is considerably more complicated but has been derived in Cliff and Ord (1973),

Doreian (1981) and Schabenberger and Gotway (2005, p. 315).

The distribution of the variance-covariance matrix of I used to test its significance

is based on a normalisation assumption rather than randomisation. This is because

equation 3.36 is a function of the explanatory variables, **X**. As a result, the randomisation

procedure for testing autocorrelation statistics would require $n!$ permutations of the n

vectors $(Z(\mathbf{s}_i), X_2(\mathbf{s}_i), …., X_k(\mathbf{s}_i)$ (Cliff & Ord, 1981, p.200), however, it is not clear how

to do this while keeping a fixed level of spatial dependence in the explanatory variables

(Odland, 1988). Due to the complexities involved, Cliff and Ord (1981) conclude that

the only operational and efficient spatial autocorrelation tests available are Moran's I and

Geary's c, based on a normal assumption test.

3.4.2 Spatial autoregressive models

When spatial dependence is found in the residuals of an OLS model, a spatial

autoregressive model can be used to model spatial dependence structures. Besides

removing the problems associated with spatial dependence, these models can provide

information on the nature and strength of spatial processes in operation. Several

commonly used spatial autoregressive models in spatial econometrics are the error model,

the lag model and the Durbin model. All of these models can be estimated using a

maximum likelihood approach (Anselin & Bera, 1998). Spatial econometric approaches

assume a simultaneous autoregressive structure such that the n autoregressions occur

simultaneously (Anselin & Bera, 1998; Schabenberger & Gotway, 2005, p. 335).

3.4.2.1 Spatial error model

In this model, spatial autocorrelation is modelled in the error term as follows (Anselin & Bera, 1998):

$$\mathbf{Z}(\mathbf{s}) = \mathbf{X}(\mathbf{s})\beta + \mathbf{e}(\mathbf{s}), \quad \mathbf{e}(\mathbf{s}) = \lambda\mathbf{W}\mathbf{e}(\mathbf{s}) + \mathbf{v}, \qquad\qquad 3.38$$

$$\mathrm{E}\left[\mathbf{v}\mathbf{v}'\right] = \sigma^2\mathbf{I}, \qquad\qquad 3.39$$

where $\mathbf{W}$ is a n by n matrix of spatial weights, λ is the strength of the spatial dependence, and $\mathbf{v}$ the identically and independently distributed residuals (Doreian, 1981; Odland, 1988; Ord, 1975). If the spatial parameter, λ, is significant then significant spatial autocorrelation is present. A significant spatial parameter is assumed to be caused by spatial autocorrelation in the measurement errors or a missing explanatory variable (Anselin & Bera, 1998). The variance-covariance matrix of $\mathbf{Z}$ is given by Anselin & Bera, (1998) and Schabenberger & Gotway (2005) as:

$$\mathrm{Var}\left[\mathbf{Z}(\mathbf{s})\right] = \sigma^2\left(\mathbf{I} - \rho\mathbf{W}\right)^{-1}\left(\mathbf{I} - \rho\mathbf{W}'\right)^{-1}. \qquad\qquad 3.40$$

$(\mathbf{I} - \lambda\mathbf{W})^{-1}$ is a full matrix, therefore every pair of observations contains a non-zero value which decreases with the order of contiguity (Anselin & Bera, 1998).

3.4.2.2 Spatial lag model.

A spatial lag model may be developed if it is suspected or known that there is a spatial processes operating on the dependent variable such that $\mathbf{Z}(\mathbf{s})$ is a function of the surrounding values of $\mathbf{Z}(\mathbf{s})$ (Anselin & Bera, 1998; Doreian, 1981). A regressive-autoregressive lag model is defined as follows (Anselin & Bera, 1998):

$$\mathbf{Z}(\mathbf{s}) = \rho\mathbf{W}\mathbf{Z}(\mathbf{s}) + \mathbf{X}(\mathbf{s})\beta + \mathbf{e}(\mathbf{s}), \qquad\qquad 3.41$$

where $\mathrm{E}[\mathbf{e}(\mathbf{s})] = \mathbf{0}$ and $\mathrm{E}[\mathbf{e}(\mathbf{s})\mathbf{e}(\mathbf{s})'] = \sigma^2\mathbf{I}$.

If ρ is significantly different from zero then a spatial process may be operating.

The variance-covariance matrix shown in equation 3.42 is the same as for the spatial

error model (Anselin & Bera, 1998; Schabenberger & Gotway, 2005)

$$\text{Var}[\mathbf{Z}(\mathbf{s})] = \sigma^2 (\mathbf{I} - \rho\mathbf{W})^{-1}(\mathbf{I} - \rho\mathbf{W}')^{-1}. \qquad\qquad 3.42$$

Like in the error model, all pairs of observations have a non-zero covariance.

3.4.2.3 Durbin model

The Durbin model is derived from the spatial error model but includes a spatial lagged

structure and a *ii*d error term (Anselin and Bera, 1998, p. 249). It is defined as:

$$\mathbf{Z}(\mathbf{s}) = \lambda\mathbf{W}\mathbf{y} + \mathbf{X}\beta - \lambda\mathbf{W}\mathbf{X}\beta + \mathbf{v}(\mathbf{s}). \qquad\qquad 3.43$$

3.4.2.4 Testing the spatial parameter

The significance of the spatial model can be tested using the likelihood ratio test. This

tests whether the spatial autoregressive model is significantly different from the OLS

model (Schabenberger & Gotway, 2005). Thus the null hypothesis, H_0: $\theta = \theta_1$, is

compared to the alternative, H_1: $\theta = \theta_2$, where $\theta_1 = [\beta, \sigma^2]$ and $\theta_2 = [\beta, \sigma^2, \lambda]$. Since only

the spatial parameter is different this reduces to the following hypotheses: H_0: $\lambda = 0$ and,

H_1: $\lambda \neq 0$. The test statistic is

$$\varphi(\beta;\theta_1;\mathbf{Z}(\mathbf{s})) - \varphi(\beta;\theta_2;\mathbf{Z}(\mathbf{s})), \qquad\qquad 3.44$$

where $\varphi(\beta;\theta;\mathbf{Z}(\mathbf{s}))$ is twice the negative log-likelihood and is compared to the χ^2

distribution with one degree of freedom. Exactly the same approach can be used to test

the spatial lag model.

3.5 Summary

In section 3.1, the important concepts of strict, intrinsic and second-order spatial

stationarity were defined as they relate to the mean and expected variance and covariance

of a spatial stochastic process. Using these concepts, spatial dependence was explained as

the covariance among observations that are close to each other. Spatial dependence in

spatial data arises due to the inherent continuity of space, the operation of spatial

processes, and the interaction between reality and the sampling framework. It was also

shown that spatially dependent data provide an opportunity to explore spatial processes

that may be operating.

Section 3.2 described how spatial dependence can be explored over increasing

distances and in different directions using the semivariogram, covariogram and

correlogram. It then provided a definition of "closeness" in terms of the conditional

probability of an observation and its neighbouring observations. Spatial weight matrices

were then introduced as a mechanism for representing spatial relationships or covariance,

as well as some different methods by which they may be specified.

Section 3.3 provided two important spatial autocorrelation statistics, Moran's I

and Geary's c, that can be used to quantify spatial dependence using the spatial weights

matrices defined in the previous section. These statistics can be applied at the global

level, or to investigate local spatial dependence. Various estimation techniques for testing

the statistics were also introduced.

The final section, section 3.4, described why Ordinary Least Squares estimates of

linear models are likely to provide unreliable estimates in the presence of spatial

dependence. The use of Moran's I for detecting spatial dependence in the residuals of

OLS linear models was described and two popular spatial autoregressive models, SAR

and CAR, were presented as a means of improving the reliability of regression estimates.

Chapter Four: Methodology

Chapter four provides a detailed description of the study area, data and methodology used for this research.

4.1 Study Area

The study area (Figure 4-1) is found on the eastern slopes of the Alberta Rocky Mountains and Foothills, and is defined by the three Bear Management Areas (BMA) called Grande Cache, FMF Core and Clearwater, totalling 94 800 km^2 in area. Highway 16 defines the boundary between Grand Cache and the FMF Core, and FMF Core and Clearwater are separated by Highway 11. Highway 3 is on the south boundary of Clearwater. The Bear Management Units were delineated based on genetic distinctions within the Alberta population (Stenhouse, 2007, p. 192). Thus each BMA is a distinctive population unit. These population units were selected for study as they had the greatest number of complete grizzly bear datasets available, making them most suitable for the systematic examination of spatial dependence in the grizzly bear health data.

A smaller study area is hatched in Figure 4-1. This additional study area was defined since a grizzly bear movement cost surface was available for this area. This allows the exploration of least cost distance neighbours. More information on the smaller study area and cost surface is given in section 4.3.3. The whole study area is referred to as study area A, and the smaller area as study area B.
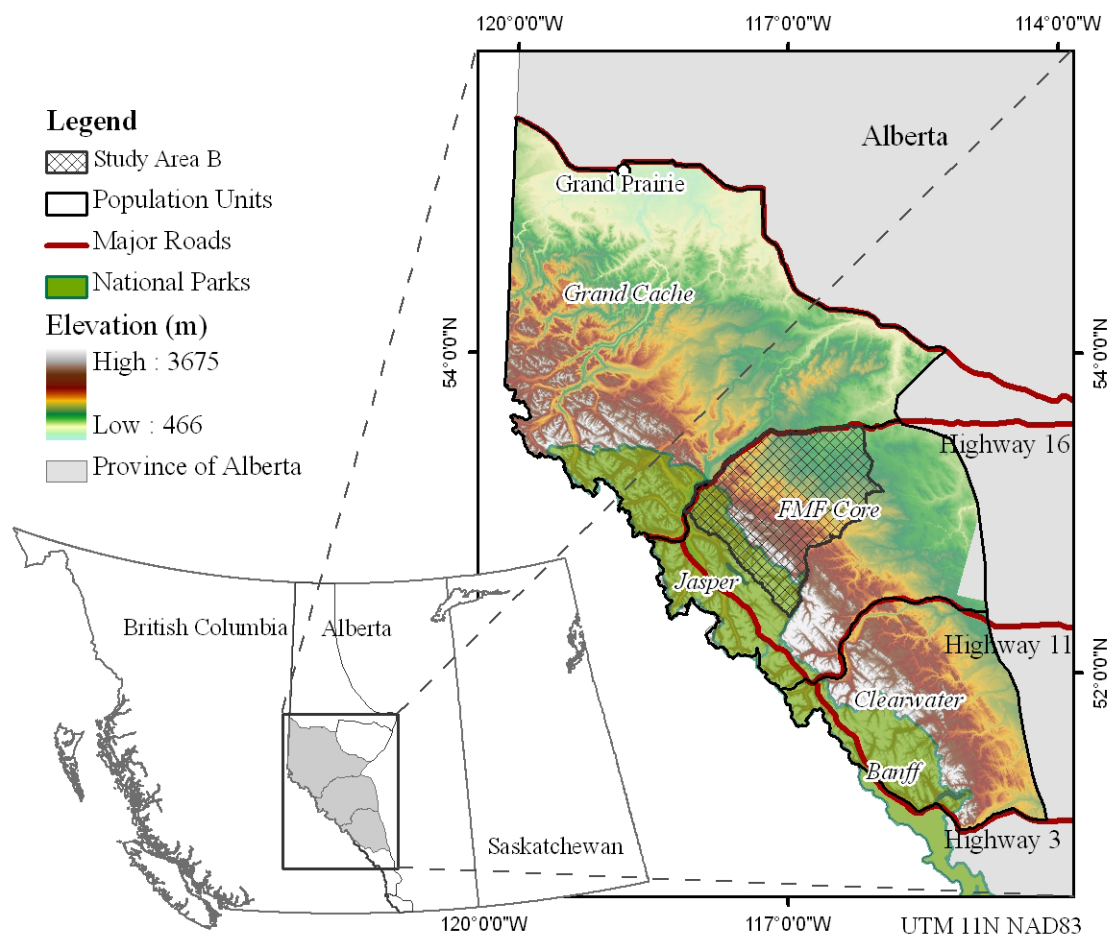
Figure 4-1. Study area comprising of three grizzly bear population units

The study area falls within the Cordilleran and Boreal climatic regimes of Alberta (Strong, 1992). The Cordilleran regime falls over the Rocky Mountains extending from British Columbia to the eastern slopes in Alberta.   The northwest-southeast orientation of the mountains block the winds arising from the Pacific ocean, causing rainshadows on the leeward sides of the mountains and in interior valleys (Strong, 1992).

The Cordilleran regime consists of three natural subregions, the Montane, Subalpine and Alpine (Natural Regions Committee, 2006; Strong, 1992). These can be seen in Figure 4-2. The Montane Subregion occurs at the lowest elevation in the foothills

and major valleys of the Rocky Mountains. A diverse variety of vegetation types are found in this ecoregion, including coniferous and broadleaf trees, as well as grasses (Achuff, 1984; Strong, 1992).
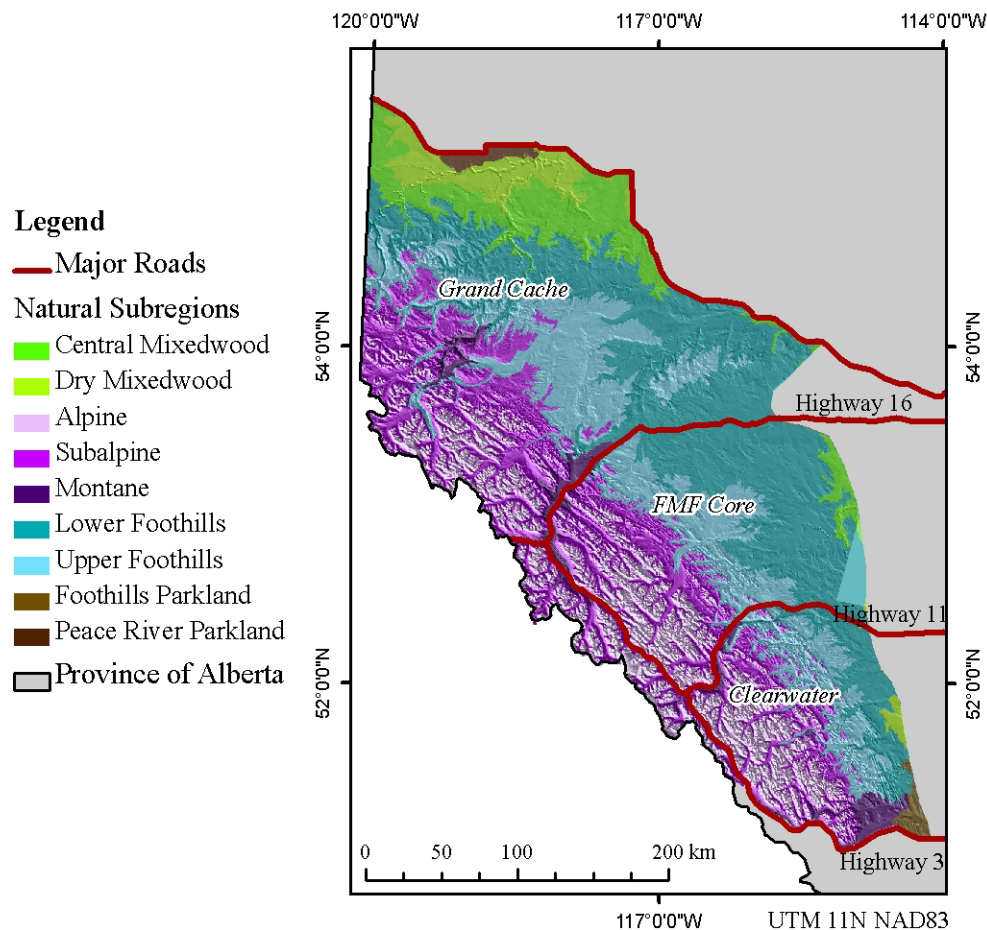
Figure 4-2. Natural regions of study area (Government of Alberta)

The Subalpine Subregion is found above the Montane, ranging between 1,450 m and 2,180 m on average (Strong, 1992, p. 36). The Subalpine Subregion is dominated by coniferous forests with broadleaf deciduous trees being found only in warmer sites (Achuff, 1984, Strong, 1992). Shrubs and herbaceous vegetation are also found in the upper subalpine areas (Achuff, 1984).

The highest subregion is the Alpine, which is nearly treeless consisting of glaciers, colluvial talus and frost-shattered bedrock with lichens (Achuff, 1984; Strong, 1992). It also includes patches of low-growing shrubs and grassland. Deformed and stunted arboreal species may occur within protected sites.

The Boreal climatic regime is found to the west and north of and adjacent to the Rocky Mountain Foothills and consists of the Foothills and Boreal Forest Natural Regions (Strong, 1992, Natural Regions Committee, 2006). The Boreal region is characterised by undulating and rolling topography. The Upper Foothills consists mostly of closed canopy coniferous vegetation, while a mix of deciduous boreal and coniferous cordilleran vegetation occur in the Lower Foothills (Strong, 1992, pp. 41, 43, Natural Regions Committee, 2006). On the northern and eastern outskirts of the study regime, the Central Mixedwood and Dry Mixedwood Subregions are found. Much of the Dry Mixedwood Subregion has been cultivated, while the Central Mixedwood consists of closed-canopy mixedwood and aspen, and a variety of other tree species (Natural Regions Committee, 2006).

The study area has been highly transformed, fragmented and disturbed by human activities such as settlement, agriculture, forestry, coal and petroleum extraction, hunting, trapping, and all-terrain vehicle use (McLellan, 1998; Stenhouse et al., 2005). These activities are supported by an extensive linear network of roads and seismic lines for oil and gas exploration (Stenhouse, et al., 2005). The FRI has shown that human activities within the study region are steadily increasing as can be seen in Table 4-1. Only nineteen percent of the study area falls within in the two national parks of Jasper and Banff.

Table 4-1. Land use change in the study area

Population units	Years	Road density	Cutblock proportion	Pipeline density	Wellsite density	Mine area
Grand Cache (McDermid et al., 2008)	2005 – 2008	15 %	21 %	13 %	44 %	N/A
FMF Core and Clearwater (Linke et al., 2009; Linke et al., 2009; McDermid et al., 2008)	1998 - 2005	28 %	98 % (total area = 2,300 km^2)	5 %	56 % (total = 8,162 km^2)	13-fold increase

4.2 Datasets

4.2.1 GPS Data

Grizzly bear location data was acquired from GPS radio collars placed on more than 150 bears between 1999 and 2008 by the FRI. Many bears were collared for two or more years. The bears were captured between April and October by various means including helicopter, snare, ground dart and culvert trap. The collars were programmed to provide position data at regular intervals on a 24-hour basis for approximately 9 to 10 months (Stenhouse & Munro, 2000, p. 24). However, in reality the sampling interval and total duration of data collected varied greatly among bears, as well as inter-annually. This was caused by variety of factors. The GPS units were not always able to acquire position fixes and sometimes delivered inaccurate positions. This was mostly caused by rugged mountain terrain and north facing slopes. Also, the sampling interval changed from year-to-year, ranging between 4 hours and 20 minutes, dependent on the battery power and GPS model. Finally, in some cases, the GPS collars had mechanical failure, or fell off the bear before the end of the summer season.

The GPS tracking data of 94 bears found within the study area A, and which also had accompanying health data were used for this study.   As seen in Figure 4-3, 27 of these were adult females (AF), 10 were adult females with cubs (AFC), 15 were subadult females (SF), 25 adult males (AM) and 17 subadult males (SM).
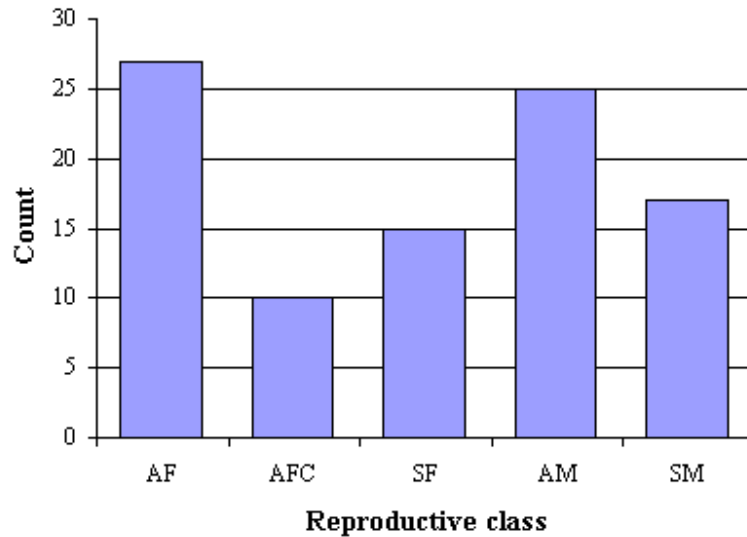
Figure 4-3. The number of bears in each reproductive class. AF = adult females, AFC = adult females with cubs, SF = subadult females, AM = adult males, SM = subadult males

4.2.2 Environmental data

Numerous geographic environmental datasets were provided by the FRI and used to generate environmental variables for this study. They are shown in Table 4-2. The datasets provide information about vegetation structure and composition, land cover, topography, water, and human features.

Table 4-2. A description of environmental datasets used

Dataset	Description	Range of values	Raster /Vector	Reso-lution /Scale
Canopy Closure	The canopy gap fraction in each 30m pixel. This is a continuous variable.	0 - 100	Raster	30 m
Percent Conifer	The percentage conifer trees in each 30m pixel. A continuous variable.	0 - 100	Raster	30 m
Forest Age	Forest age is given as years AD.	1200 - 2007	Raster	30 m
Land Cover	Land cover consisting of 1. Upland trees 2. Wetland trees 3. Upland herbs 4. Wetland herbs 5. Shrub 6. Water 7. Barren 8. Snow/Ice 9. Cloud 10. Shadow	1 – 10	Raster	30 m
Regenera-ting forests	Presence (1) or absence (0) of regenerating forests. Regenerating forests are defined as cut blocks, or wildfires after 1950.	0 / 1	Raster	30 m
Agriculture	Presence (1) or absence (0) of agricultural land. Its purpose is to separate agricultural zones from natural herbaceous areas (natural grasslands, alpine meadows, etc).	0 / 1	Raster	30 m
Water-bodies	Large open water bodies, including wide river beds.	N/A	Polygon	1: 50,000
Streams and Rivers	Rivers, creeks and streams.	N/A	Line	1: 50,000
Digital Elevation Model	Elevation in meters above sea level.	218 - 3945	Raster	30 m
Well sites	Well sites	N/A	Point	?
Roads	A complete road network for Alberta provided by the Alberta Sustainable Resource Development Department. Features added by the FRI GBP.	Road types.	Line	1: 50,000

All datasets are in UTM Zone 11 N on the NAD 1983 datum. Landsat 5 TM and

Landsat 7 ETM+ acquired between 1999 and 2005 were the primary image datasets used

for mapping (Laskin et al., 2006). The definition of the land cover classes are given in

Table 4-3.

Table 4-3 Definition of land cover classes

Land Cover	Class Description
Upland Trees	Vegetated sites with tree crown closure > 5%; dry or mesic
Wetland Trees	Vegetated sites with tree crown closure > 5%; wet
Upland Herbs	Vegetated sites with herbaceous cover > 5%; dry or mesic; includes pipelines.
Wetland Herbs	Vegetated sites with herbaceous cover > 5%; wet
Shrubs	Vegetated sites with shrub cover > 5%;
Shadow	Ground features obscured by shadow
Water	Non-vegetated sites with water cover > 50%
Barren Land	Non-vegetated sites with barren cover > 50%; includes natural (rocks and soil) or manmade (cutblocks, permanent roads with 25 m buffer, well sites buffered by 70 m) non-vegetated sites
Snow/Ice	Non-vegetated sites with snow/ice cover > 50%
Cloud	Ground features obscured by cloud cover

4.2.3 Health data

The FRI conducted a variety of procedures to collect data to assess the health of

individual bears. This included physical examination and measurement, physiological

measurement, extraction of the pre-molar for age determination, and collection of blood

samples (Janz et al., 2006, p. 56). The complete set of 110 variables was reduced to nine

based on biological knowledge and data reduction techniques by Cattet et al. (2007). The

final set can be seen in Table 4-4. These variables indicate healthy functioning with

respect to growth, immunity and stress, although it is difficult to interpret some of these

variables separately from each other (Cattet et al. 2007, personal communication). The

health data was also accompanied by information on age, sex, reproductive class, date

of capture and capture method.

Table 4-4. Health variables for grizzly bears captured (Cattet & Vijayan, 2007; Cattet, 2008, email correspondence)

Functional Health Group	Variables	Range of values
Growth	o straight-line body length in cm o body condition index (BCI) o serum concentration of alkaline phosphatise	o $60 \leq value \leq 230$ o $-4.000 \leq value \leq +4.000$ o $4 \leq value \leq 300$
Immunity	o White blood cell count, lymphocyte count, o percentage of neutrophils o percentage of monocytes,	o $35.0 \leq value \leq 100.0$ o $0.0 \leq value \leq 35.0$ o $10 \leq value \leq 60$
Stress	Serum concentrations of o heat-shock protein 60 o heat-shock protein 70 o gamma-glutamyltransferse (GGT)	o $0.0 < value \leq 35.0$ o $0.0 < value \leq 20.0$ o $0 \leq value \leq 300$

The health data collected was not entirely systematic due to the inherent

unpredictability of the process of capturing bears in the wild. As a result, some bears had

only one set of health measurements available, while others had several, sometimes from

the same year. Also, the bears were not captured at the same time of year. While most

health measurements were obtained in May at the same time that GPS collars were

attached, a large proportion of measurements were acquired in April, and between June

and October. This is a complicating factor as grizzly bears are known to gain

considerable weight in late summer and fall before hibernation (Schwartz et al., 2003),

for example. Finally, not all health records were complete. There were several cases

where GPS data was available for a particular bear, that had no, or incomplete health

records. This situation is also reversed, where GPS data were not always available for bears that had complete health records. Further, the year in which health data was collected does not always match the years for which tracking data were available. Finally, health data collected early in the year, May for example, reflects the bear's condition from the previous year, not the upcoming year from when GPS data was collected.

4.3 Methodology

4.3.1 Home range estimation

The delineation of the home range allows the identification of resources used by the bears and other environmental conditions that may have an impact on their health. Considering the non-systematic nature of the GPS data collected, it was decided to estimate multi-annual, rather than annual home ranges for this study. An inspection of the grizzly bear GPS points and annual home ranges revealed that there was considerable overlap in the extent of a bear's home range from year to year. Blanchard and Knight (1991) found that adult female bears have a high degree of home range fidelity, while male home ranges are more variable. In order to obtain a better understanding of home ranges, GPS data were combined to estimate a single multiannual home range. However, annual GPS datasets were not aggregated for bears transitioning from subadult to adult as these bears are more likely to disperse at this stage (Blanchard and Knight, 1991). This approach negated the difficulty of matching health data to temporally mismatched GPS tracking data. Only the

GPS data from bears that had health data were used. A total of 94 home ranges were computed.

Multiannual home ranges were estimated using kernel density estimation. As described in Chapter 2, this method is recommended by several authors and has been one of the most popular home range estimation processes since it was introduced in 1989 by Worton. KDE is appropriate as it is non-parametric and can estimate multi-modal utilisation distributions and enable the identification of core areas where the bear spends more time. ABODE beta v.4., an application written for ArcGIS by Laver (2005), was used to compute KDE home ranges. The parameters used are shown in Table 4-5.

Table 4-5. Kernel Density Estimation Parameters

Cell size	Bandwidth	Fixed/Adaptive	Kernel	Standardize data	Contouring method
100 m	LSCV	Fixed	Biweight	Unit variance	Volume

The estimated home range is most sensitive to the choice of the bandwidth and was therefore estimated using LSCV (see Chapter 2, section 2.5.2). LSCV is appropriate for estimating bandwidths for multimodal home ranges.

A fixed probability contour was not used to define the home range as there is no objective method to define this. Rather the core area of the home range was estimated using the method suggested by Seaman and Powell (1990) as described in section 2.5.5. Examples of the core home ranges and utilisation surfaces are shown in Figure 4-4.
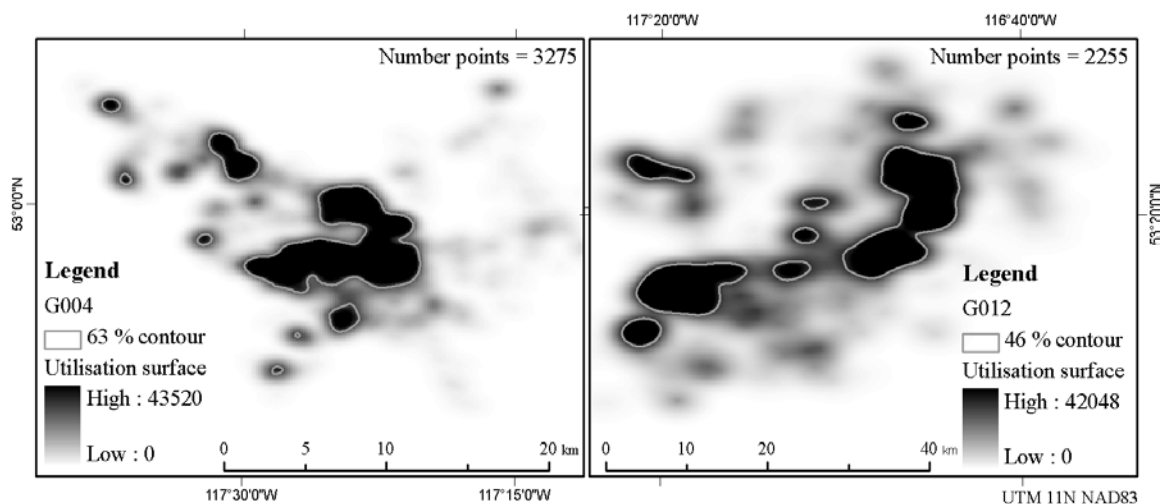
Figure 4-4. Utilisation surfaces and core home ranges

The utility distribution surfaces computed for each home range were saved to be used as a weighting surface for summarising the environmental variables for each core home range. This is described in detail in section Table 4-3.

A visual inspection of the core home ranges within the mountains suggested that KDE had overestimated the true extent of the home ranges. The raw core home ranges extended into barren areas of rock, snow and ice, which although occasionally crossed by the bears, do not provide any resources to them (Munro, et al., 2006). These high alpine areas should be distinguished from alpine meadows which provide food to the bears (Nielsen, et al., 2006). This situation is illustrated in Figure 4-5.
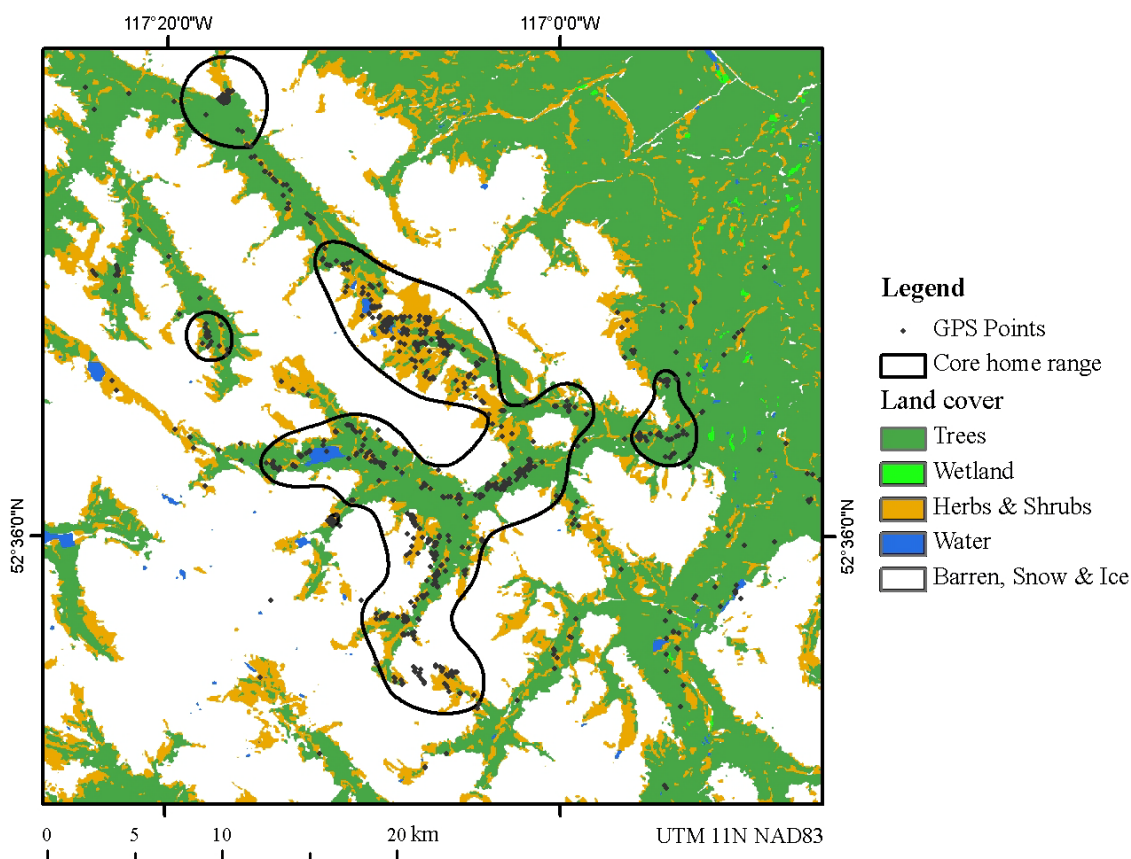
Figure 4-5. Example of core home ranges in the Alpine and Subalpine Subregions

In Figure 4-5, a core home range is outlined in black and suggests that bears occupy the barren alpine regions shown in white. However, the black GPS points indicate that the bear seldom goes into these areas. For this reason, to avoid the inclusion of non-utilised barren areas in the home range which would bias the composition calculations of each, non-vegetated alpine regions were removed from the mountain home ranges.

It was first necessary to define at what elevation the Alpine Subregion began. According to Strong (1992) the boundary between the Alpine and Subalpine Subregions decreases in elevation in a northward direction, and eastwards from the cardinal divide,

as defined by equations 4.1 and 4.2. Equation 4.1 describes the decline of the alpine

zone in the north direction with an origin at the 49th parallel, and 4.2, in the east direction.

$$E = 3910.49 - 35.61\phi , \hspace{6cm} 4.1$$

$$E = 3910.49 - 35.61d , \hspace{6cm} 4.2$$

where elevation is in meters, ϕ is latitude in decimal degrees, and d is the distance in

kilometres from the continental divide in an easterly direction. Using these two equations

a sloping alpine elevation plane was computed. Elevations in the DEM that were higher

than the plane were selected and then intersected with the barren, snow/ice, shadow and

cloud classes from the land cover layer. These barren alpine regions were then removed

from the home ranges with which they intersected. This process is illustrated in the

Figure 4-6.
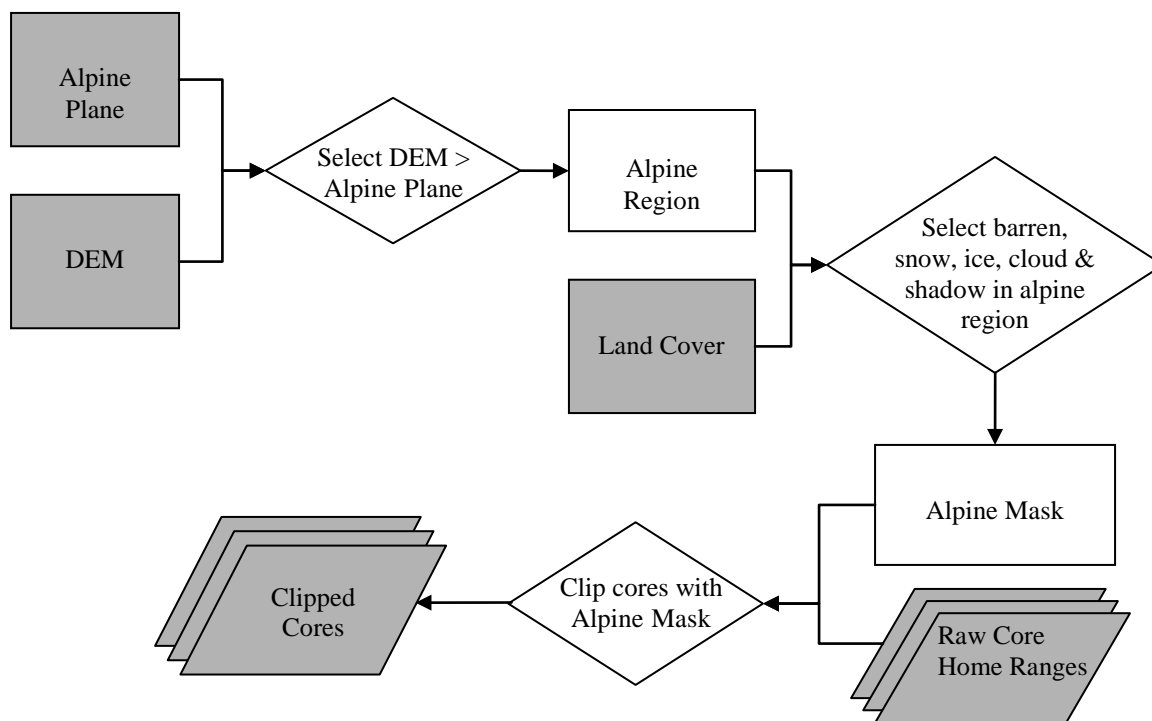
Figure 4-6. The process for correcting the core home ranges in the alpine regions

The coordinates of the cell with the greatest utilisation value from each utilisation grid were used as centroids for computing various spatial neighbourhoods and weights described later. The final home ranges and their centroids can be seen in Figure 4-7. The core home ranges were defined by probability contours ranging from 35 % to 76%, with a mean of 57 % and median of 56 %. Core areas ranged between 8 km^2 and 2,328 km^2, with a mean of 252 km^2 and median equal to 124 km^2. The area distribution was strongly skewed left.
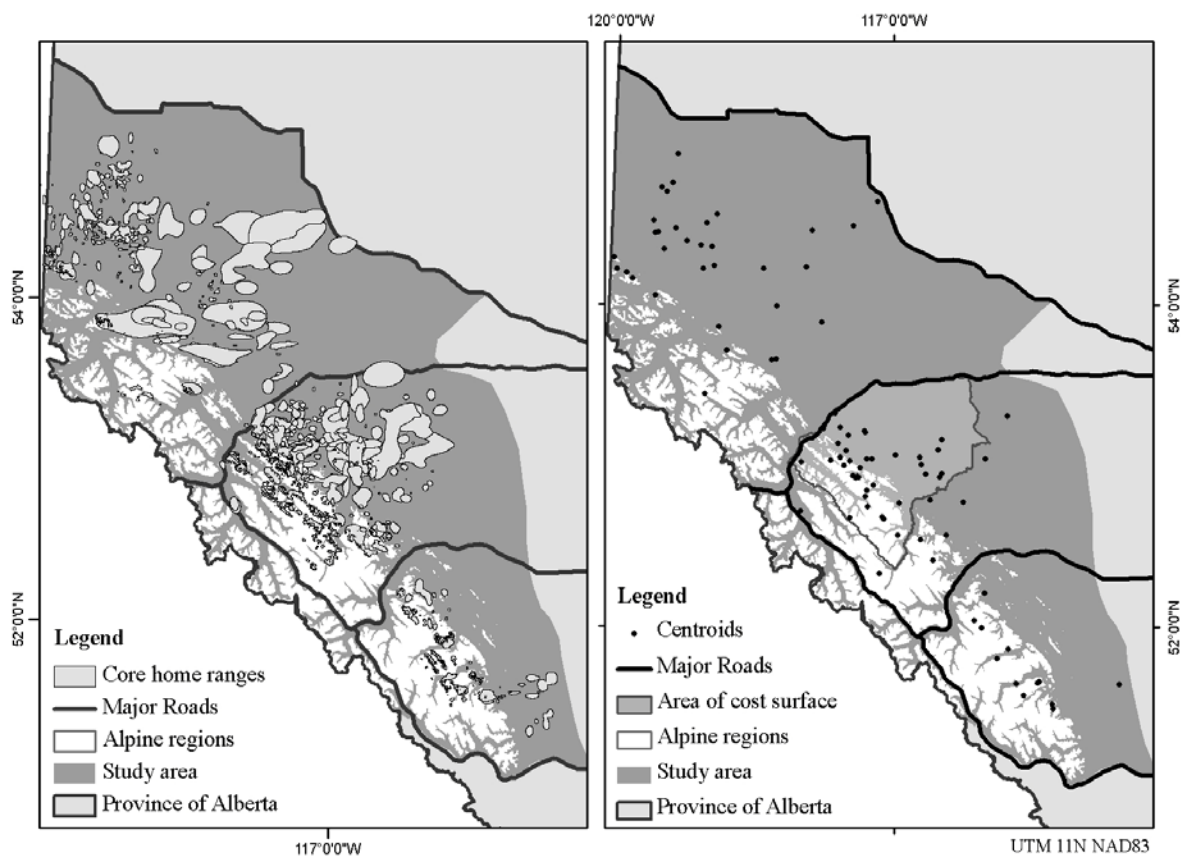
Figure 4-7. Core home ranges and centroids

4.3.2 Environmental variables

Using the environmental datasets listed in Table 4-2, the desired environmental variables

were computed for each core home range area. The environmental variables can be

categorised into four groups: habitat types, topography, water availability and human

disturbance. The utility distribution surface of each core home range generated by the

KDE was used as a weighting surface to weight the relative contribution of the

environmental attribute at the position of each grid cell. Thus, it was first necessary to

convert all vector environmental GIS layers into raster format. The raster environmental

datasets were then summarised per core either as a weighted "average" for numerical

variables, or for categorical variables as a weighted "percentage" of the area.   The

formula for the weighted average is shown below.

$$EV_{ave} = \frac{\sum_i^m u_i EV_i}{\sum_i^m u_i}, \qquad\qquad 4.3$$

where *EV* is a numerical environmental variable, *u* is the utilisation value from the

utilisation grid, and *i* indicates a particular grid cell.

The categorical variables were reclassified into separate binary GIS layers where

1 indicates the presence of the class of interest, and 0, its absence. The formula for the

weighted percentage area is almost identical to 4.4,

$$EV_{per} = \frac{\sum_i^m u_i EV_i}{\sum_i^m u_i} \times 100, \qquad\qquad 4.4$$

where EV_i is one or zero indicating presence or absence.

Habitat types were based on those compiled for west-central Alberta by Munro et al. (2006). The habitat types, their descriptions and the resources that they provide to grizzly bears are shown in the Table 4-6.

The alpine-subalpine, shrub and herbaceous habitat types were merged together as they provide similar food resources to grizzlies. Also, since elevation and slope (described hereafter) already provide a measure of mountainous regions versus foothills, the herbaceous-shrub class were not split into two geographic regions as these would make the same distinction. Nielsen et al., (2006) also followed this approach, grouping together subalpine, alpine and herbaceous vegetation in their habitat-based conservation framework analysis.

Table 4-6. Definition of habitat types (Munro et al., 2006)

Habitat type	Description	Resources
Alpine - subalpine	Herbaceous areas >1,700 m where clusters of trees (< 20% crown closure) are mixed with grasses, sedges, and forbs.	Roots
Shrub	Areas greater than 50% shrub cover.	Roots
Herbaceous	Herbaceous areas <1,700 m including mine site reclamation.	Roots, Fruit
Mixed forest	Forested areas having both coniferous and deciduous trees with less than 80% dominance of either type.	Fruit, Bedding
Open forest	Coniferous or deciduous forests with < 60% crown closure.	Fruit, Ungulates, Bedding
Closed forest	Coniferous or deciduous forests with > 60% crown closure.	Ungulates, Bedding
Wet forest	Wet treed areas (semiopen to closed) typically dominated by black spruce (Picea mariana) and tamarack (Larix laricina).	Ungulates, Ants, Insects, Bedding
Regenerated forest	Open or partially timbered site where timber harvest has disturbed natural vegetation	Insects
Anthropogenic	Areas altered by humans, including residential and industrial (oil and gas well sites, pipelines, and transmission lines).	Herbaceous grazing, Green vegetation
Nonvegetated	Nonvegetated areas including rock, water, ice, shadow, and cloud.	Ungulates

The forest regions in contrast were both aggregated and separated into the following classes and sub-classes for additional exploration. Subsets of these classes have been used in various studies by Munro et al. (2004) and Nielsen et al. (2006).
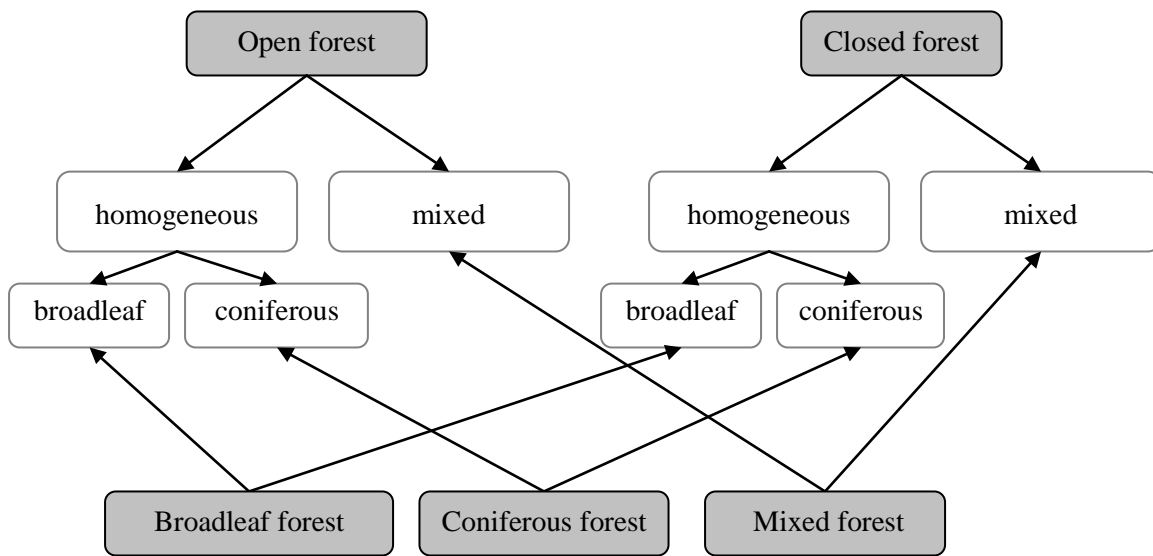
Figure 4-8. Forest classes and subclasses

The method for creating the final habitat types are described in detail in Table 4-7.

Although, elevation has no direct impact on health, it is a surrogate for plant growth, temperature and moisture (Austin, 2007). These in turn affect the availability of food. Areas of high elevation and rugged terrain tend to have a lower density of human activities so it also acts a surrogate for human disturbance.

Table 4-7. Habitat types (adapted from Munro et al., 2006)

Habitat type	Method
Alpine-subalpine herbs & shrubs	o Select *shrub* and *upland herb* classes from land cover dataset. o Remove *regenerating forests* that overlap with this layer.
Broadleaf forests	o Select *upland trees* from land cover where *percent conifer* < 20 %. o Remove *regenerating forests* that overlap with this layer.
Coniferous forests	o Select *upland trees* from land cover where 80 % < *percent conifer* o Remove *regenerating forests* that overlap with this layer. .
Mixed forests	o Select *upland trees* from land cover where 20 % < *percent conifer* < 80 %.
Open forests	o Select *upland trees* from the land cover, where *canopy cover* < 60 %. o Remove areas that are *regenerating forests*.
Open mixed forests	o Using open forests, select areas where 20 % < *percent conifer* < 80 % o Remove *regenerating forest*.
Open homogeneous forests	o Select *upland trees* from the land cover, where *canopy cover* < 60 % o Select areas where *percent conifer* < 20 % and 80 % < *percent conifer* o Remove *regenerating forest*.
Closed forests	o Select *upland trees* from the land cover, where *canopy cover* > 60 %. o Remove areas that are *regenerating forests*.
Closed mixed forests	o Select *upland trees* from the land cover, where *canopy cover* > 60 %. o Select where 20 % < *percent conifer* < 80 %. o Remove *regenerating forest*.
Closed homogeneous forests	o Select *upland trees* from the land cover, where *canopy cover* > 60 %. o Select where *percent conifer* < 20 % and 80 % < *percent conifer* o Remove *regenerating forest*.
Regenerating forests	o Use the regenerating forest layer. o Exclude *agricultural lands*. o Due to clear distinction between new regenerating forest (fresh cutblocks or burns) and older regenerating forest (which has more trees, older cuts and fires) this class was also split into two.
New regenerating	o Select regenerating forest where barren, herbs or shrubs exist and/or *canopy closure* * < 20 %
Old regenerating	o Select all other regenerating forest not selected above.
Wet trees	o Select w*etland trees* from the land cover. o Remove *regenerating forest*.
Wet herbs	o Select *wetland herbs* from the land cover o Remove *regenerating forest*
Wetlands	o wet trees + wet herbs

Other indirect measures that were derived from elevation were slope and three aspect classes: eastness, northness and northeastness. These represent the degree to which sloped terrain faces east, north or northeast. Northeastness was computed in addition to northness and eastness, as temperature and moisture are strongly related to the degree to which a slope faces northeast or southwest. Southwest slopes exhibit xeric conditions, while northeast slopes are cool and mesic (Nielsen et al., 2002).

To assess water availability, the waterbodies, streams and rivers layers were converted to raster and then merged together. This layer was used to compute to measures of water availability: 1) the percentage water in the home range and 2) the average distance to water.

Human disturbance was measured by several distance surfaces to roads, wells, roads and wells, and towns. A list of the final environmental variables, their abbreviations, descriptions and units is given in Table 4-8.

4.3.3 Cost Surface

A 30 m cost surface indicating the difficulty to move across a unit cell from the perspective of grizzly bear was generated by the FRI for part of FMF Core Population Unit. The cost surface covers study area B and is shown in Figure 4-9. Using the cost surface it was possible to compute the shortest route between every pair of centroids considering factors such as mountain ridges, steepness and roads which may impede bears' travel. Using least cost distances a set of nearest neighbours and distance neighbourhoods were created in addition to compare to those based on Euclidian distances.

Table 4-8. Complete list of environmental variables

Variable	Description	Units
MaxX	*x* coordinate of the point of maximum use on the utilization surface	km
MaxY	*y* coordinate of the point of maximum use on the utilization surface	km
Elev	Average elevation above sea level	km
Slope	Average slope, where slope is measured as a percentage elevation change over horizontal distance.	% change
Northness	Average degree to which the slope faces north.	unitless
Eastness	Average degree to which the slope faces east.	unitless
Neastness	Average degree to which the slope faces northeast.	unitless
Per_Wat	Percentage water in the home range	%
Dist_Wat	Average distance to waterbodies and rivers	km
Dist_Town	Average distance to towns	km
Dist_Road	Average distance to roads	km
Dist_Well	Average distance to wells	km
Dist_Rd_Wll	Average distance to roads and wells	km
PerCon	Average percentage conifer	%
CanClo	Average canopy closure	unitless
FstAge	Average forest age	years
Herbs	Percentage herbaceous and shrubby vegetation	%
OpMixFst	Percentage open mixed forest	%
OpHomFst	Percentage open homogeneous forest	%
CldMixFst	Percentage closed mixed forest	%
CldHomFst	Percentage closed homogeneous forest	%
OpFst	Percentage open forest	%
CldFst	Percentage closed forest	%
HomFst	Percentage homogeneous forest	%
MixFst	Percentage mixed forest	%
DecFst	Percentage deciduous forest	%
ConFst	Percentage coniferous forest	%
OpDecFst	Percentage open deciduous forest	%
CldDecFst	Percentage closed deciduous forest	%
OpConFst	Percentage open coniferous forest	%
CldConFst	Percentage closed coniferous forest	%
WetHerbs	Percentage wet herbs	%
WetFst	Percentage wet forests	%
Wetlands	Percentage total wetlands	%
RegBar	Percentage regenerating barren lands	%
RegFst	Percentage regenerating forests	%
RegAll	Percentage total regenerating area	%

Thirty-nine individual grizzly bears with health data were available for this smaller

region.
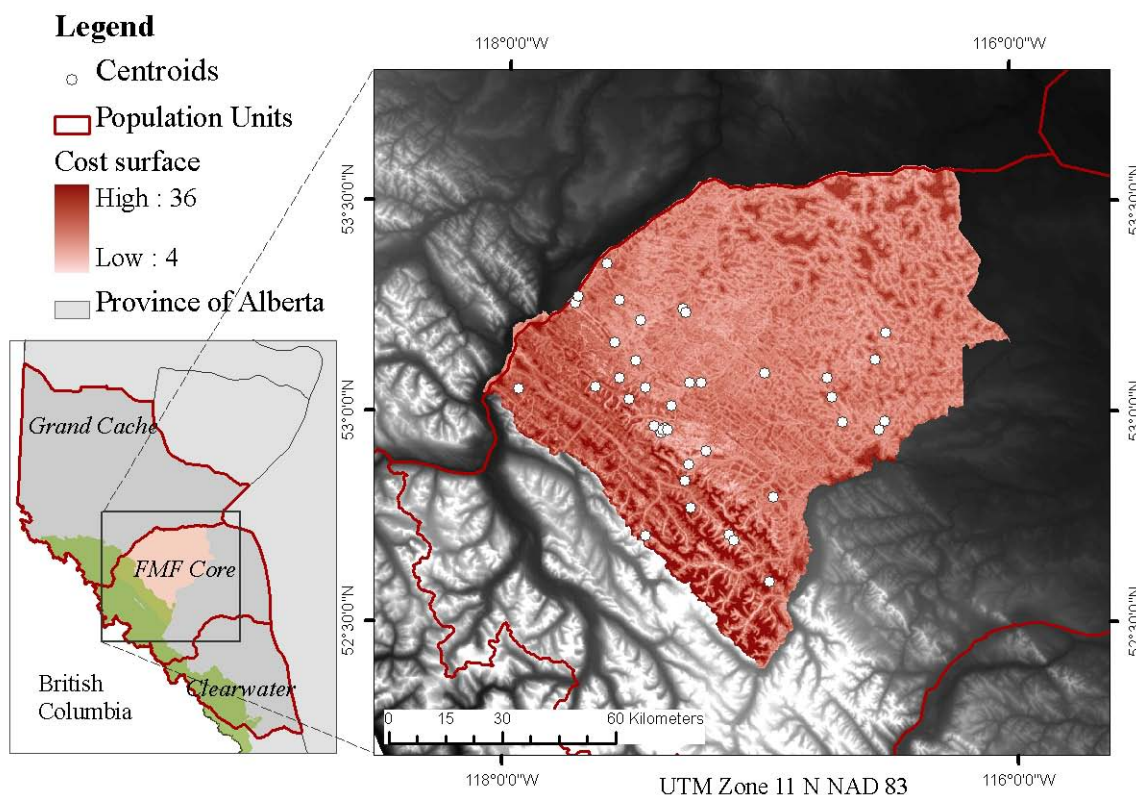
Figure 4-9. The movement cost surface for study area B

4.3.4 Choice of health variable

It was not immediately obvious how to use all the health records available, nor how to

combine these with the home range data due to the fact that some bears were captured

and measured several times in one year, and/or over several years, while others were only

captured once. Furthermore, the health measurements were not all obtained at the same

time of year, nor did they always match the time frame over which the GPS data were

collected. To overcome this difficulty, average values for each bear were computed,

using the first and/or only measurements of each year. By using the average values for

each bear, the effect of annual fluctuations would be reduced, thereby providing an overall indication of health for each bear. This approach is also consistent with the estimation of multiannual home ranges, so that one set of health variables is associated with one set of environmental variables for each bear.

Out of the nine health variables shown in Table 4-4, it was necessary to select one to act as the dependent variable for multivariate regression modelling based on its potential to reflect the effect of environmental conditions on grizzly bear health.

The stress variables were considered an unsuitable choice as there are several challenges associated with understanding this highly complex phenomenon. Cattet et al. (2007) discuss the difficulties of measuring long-term stress directly, especially when capturing bears to acquire blood and tissue samples for stress measurements increases short-term stress. Measures of long-term stress in grizzly bears that are unaffected by the method of capture are in the process of being developed by Cattet et al. (2007). Further, individual animals may experience different stress responses to the same stressors based on their specific early experiences, genetics, age, physiological state and the season (Moberg & Mench, 2000).

Immune functioning is affected by both long and short-term stress. While long-term or chronic stress depresses immunity, it has also been found that acute stress can have the opposite effect (Cattet et al., 2007). Cattet et al. (2007) have found that there is a positive association between stress and immunity using the FRI data. This counterintuitive result is being explored further. Cattet (2008, personal communication) also suggests that the immunity variables must be interpreted along with other variables.

Due to this complexity of interpreting immune responses, the immunity variables were not selected for use.

It was therefore decided to focus on the growth variables which are easier to interpret and not affected by the capture process. Measures of growth are useful indicators of the overall health of individuals and the potential success of a population. Also, access to high-quality and abundant meat, such as salmon, is strongly associated with increased body mass, reproductive success and increased population density (Hilderbrand et al., 1999; Schwartz et al., 2003). Low scores in body growth variables can therefore signify a shortage or lack of access to quality food which could be caused by human disturbance. Stress can also divert metabolic resources away from growth towards various coping mechanisms, thus resulting in reduced growth (Elsasser et al., 2000, p. 79, 86, 87). This in turn could have long-term negative impacts on reproduction and ultimately population density. This relationship is illustrated in the diagram below.
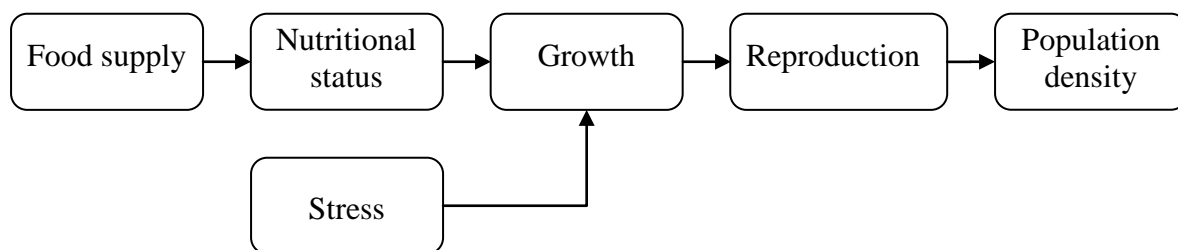
Figure 4-10. Relationship between growth, habitat and population density (Hildebrand et al., 1999; Elsasser et al., 2000)

Straight-line length was chosen as the dependent variable, after evaluating the suitability of all three growth variables (straight-line length, body condition index and serum alkaline phosphatase concentration).

Serum alkaline phosphatase concentration was eliminated as an appropriate choice as its interpretation relies on the interpretation of several other variables (Cattet, 2008, email correspondence).

Body condition index (BCI) was a promising candidate. Body condition measures the relationship between the combined mass of fat and skeletal muscle against straight-line length, and is an indicator of long-term trends in food availability (Cattet et al., 2002). However, it is also influenced by the time since den emergence. At emergence, body condition is at the lowest and improves as the season progress until it is at its best in October (Cattet et al., 2002).

Straight-line length (SLL) has been shown to be an accurate indicator of skeletal (bone) mass and total body mass, i.e., the natural logarithms SLL, skeletal mass and total body mass, result in a linear relationship between SLL and skeletal mass, and between SLL and total body mass (Cattet et al., 2002). Hence, SLL is also an indicator of body size (Cattet et al., 2002). SLL has the ability to capture long term effects without seasonal fluctuations. Finally, SLL was selected as the variable of choice as an initial investigation of the correlation between straight-line length and environmental variables revealed that it had stronger relationships with the environmental variables than BCI. Also, more records were available for SLL than BCI for the study area. For these reasons, SLL was chosen as the dependent variable for model development; although BCI warrants further investigation in future work.

To facilitate the interpretation of straight-line length as an indicator of good or poor health, and to allow males, females, adults and subadults to be considered simultaneously, SLL was transformed to values between 0 and 1. These transformed

values represent the degree of growth on a continuum, where 1 indicates the best possible growth and 0, the worst. The transformation of the raw SLL values to scaled values was based on thresholds indicating the transition between poor, ok and good values, provided by Marc Cattet, a veterinary scientist with the Canadian Cooperative Wildlife Health Centre, in 2008. These are shown in Table 4-9.

Table 4-9. Thresholds for good and poor values (Cattet, 2008)

Health Component	Variable	Expert identified thresholds for poor values	Expert identified thresholds for good values
Growth	straight-line length	• adult female < 152 • subadult female < 137 • adult male < 174 • subadult male < 141	• adult female > 164 • subadult female > 154 • adult male > 186 • subadult male > 160

The approach used was based on Fuzzy Set Theory (Zadeh, 1965). Fuzzy Set Theory allows quantitative work to be conducted on fuzzy data or with fuzzy concepts. In contrast to Boolean logic which requires statements to be true or false, Fuzzy Set Theory permits statements to be true with a certain possibility, or properties to partially belong to one or more sets (Burrough & McDonnell, 1998). The possibility of being true, or the degree of membership of an object, z, to a particular set, A, can be assigned using a mathematical membership function (MF^F). Formally, a fuzzy set is thus defined as follows (Zadeh, 1965)

$$A = \left(z, MF_A^F \left(z \right) \right) \quad \text{for all } z \in Z .$$ 4.5

The degree of membership, or truthfulness, of a statement falls between $[0,1]$. The closer it is to one, the more z belongs to A. In this research, the transformed value of SLL,

ranging between 0 and 1, indicates the degree to which the observed SLL can be considered a good health score.

In this research a sinusoidal function was used as the membership function to assign each of the variables to the interval [0, 1]. Three forms of the sinusoidal membership function are shown in Figure 4-11, and are defined by the following equations (Burrough & McDonnell, 1998)

$$MF^F(z) = \frac{1}{1+\left(\dfrac{z-b_1-d_1}{d_1}\right)^2}, \quad \text{if } z < b_1 + d_1 \tag{4.6}$$

$$MF^F(z) = 1, \quad \text{if } b_1 + d_1 \leq z \leq b_2 - d_2 \tag{4.7}$$

$$MF^F(z) = \frac{1}{1+\left(\dfrac{z-b_2+d_2}{d_2}\right)^2}, \quad \text{if } z > b_2 - d_2. \tag{4.8}$$

The combination of equations 4.6 and 4.7 results in Figure 4-11 a), 4.7 and 4.8 gives c), and b) is constructed from all equations. b_1 and b_2 correspond to the values at which the membership function equals 0.5 (Burrough & McDonnell, 1998). d_1 and d_2, control how gradually or rapidly the transition occurs between 0 and 1 by defining the width of the transition zone (Burrough & McDonnell, 1998). These can be informed by the observation precision.
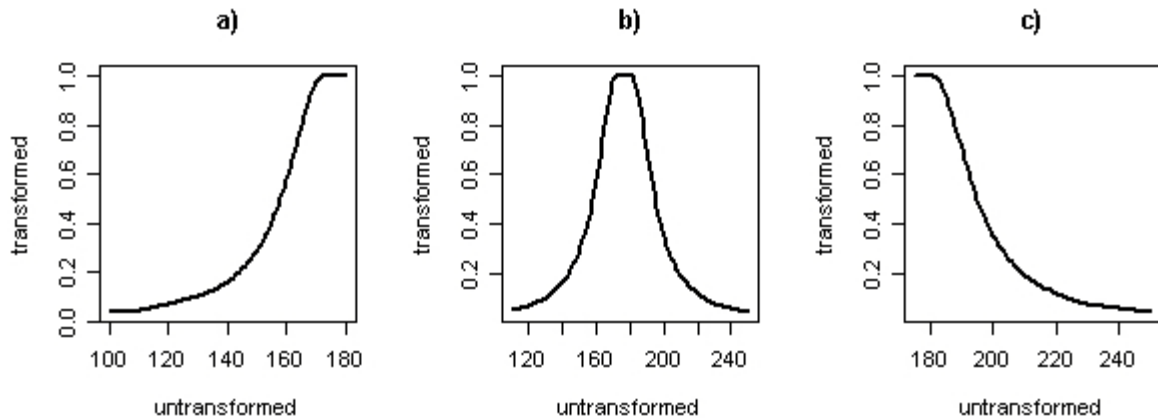
Figure 4-11. Sinusoidal membership functions

Since a longer straight-line length is considered better than a shorter length, only the left-sided sinusoidal function was needed (equations 4.6 and 4.7, shown in Figure 4-11 a)). In this study b_1 is the average of the thresholds for good and poor, and d_1 is the measurement precision estimated at 9 % of the measured value (Cattet, 2008):

$$b_1 = (good + poor)/2$$
$$d_1 = 0.09b_1.$$

4.9

Due to differences in straight-line length among adult males, adult females, subadult males and subadult females (Schwartz, et al., 2003; Cattet, 2008, personal communication), different thresholds were used for each reproductive group resulting in different curves for each. The final membership function curves for each reproductive group are shown in Figure 4-12.

Adult Females

Subadult Females

Adult Males

Subadult Males
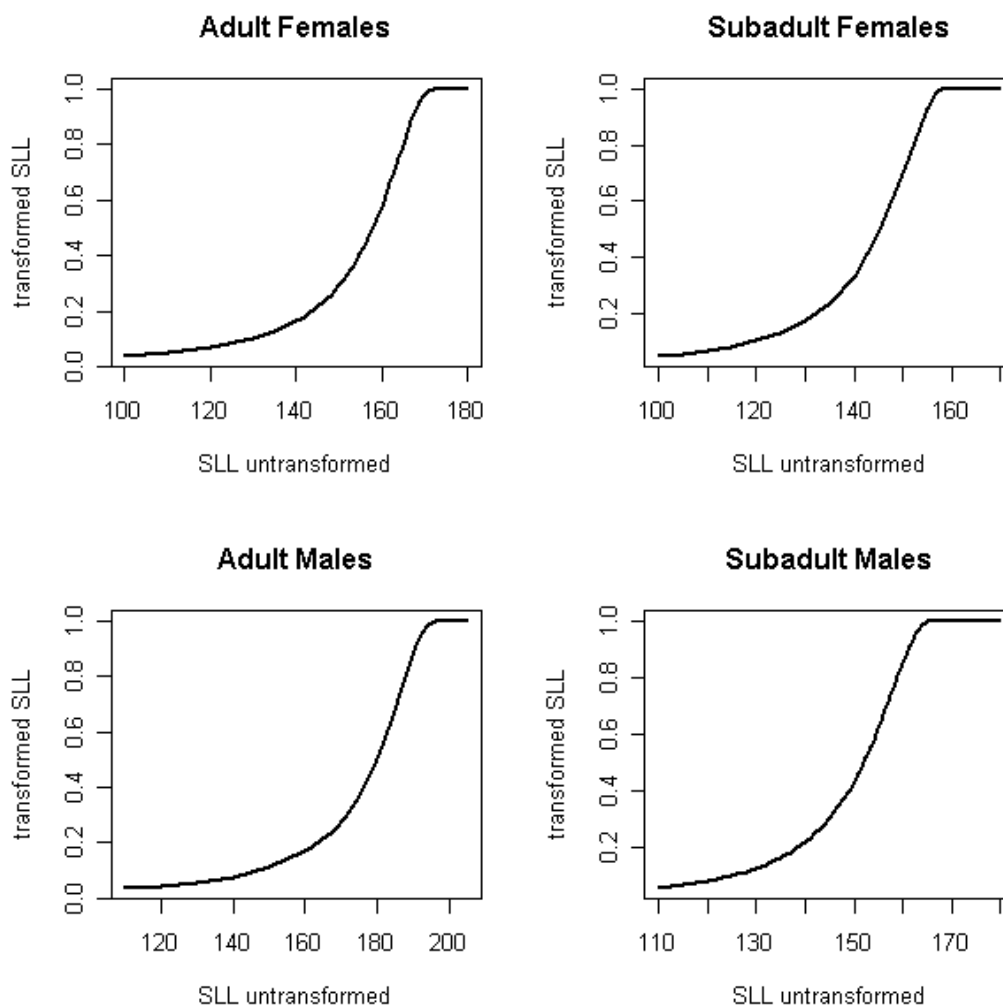
Figure 4-12. Membership functions for straight line length in each reproductive group

After transformation there were no statistical differences between reproductive classes. Boxplots of the transformed straight-line length per reproductive class and results of an ANOVA assessment are shown in Figure 4-13 and Table 4-10.
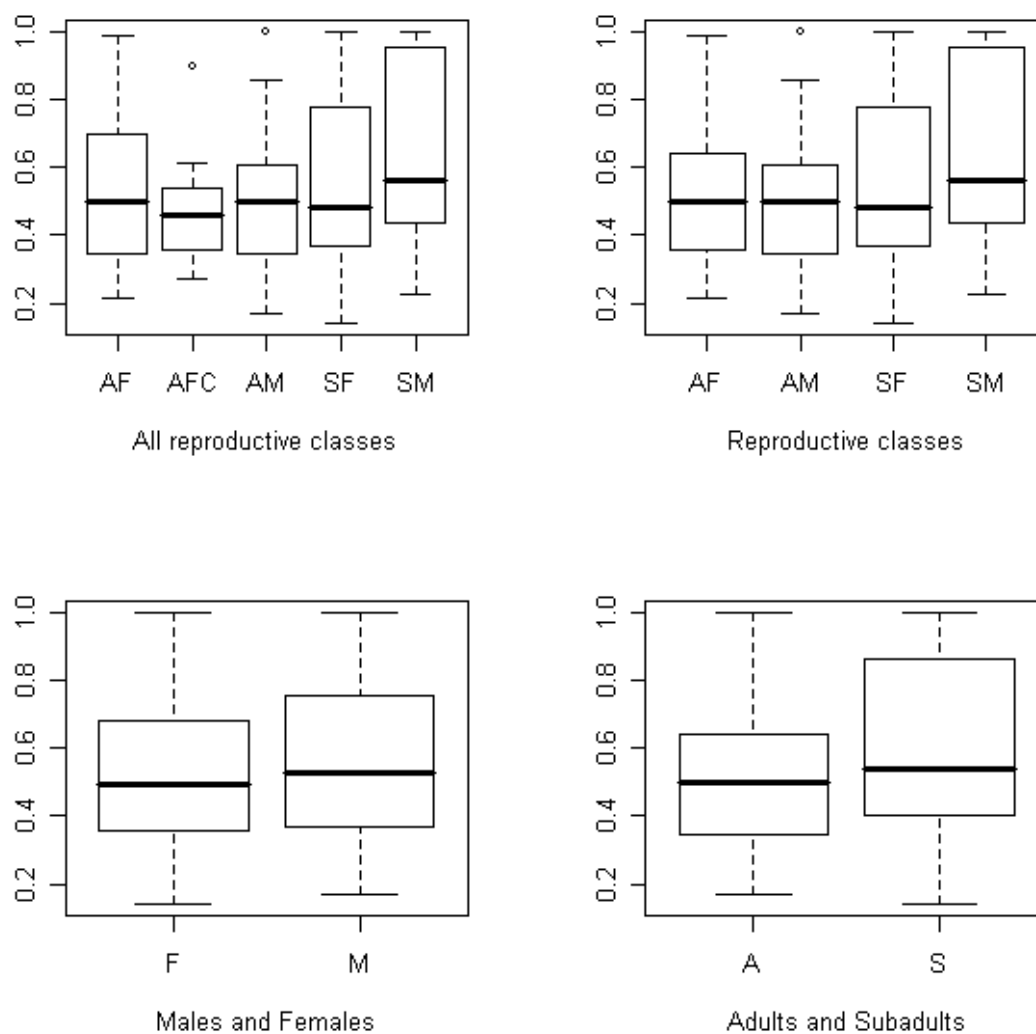
Figure 4-13. Boxplots of SLL100 for reproductive classes. AF = adult females, AFC = adult females with cubs, AM = adult males, SF = subadult females and SM = subadult males.

Table 4-10. Summary of ANOVA results for SLL100

Source of variation	Sum of squares	Degrees of freedom	Mean square	F value	Pr (> F)
AF, AFC, SF, AM, SM	0.2079	4	0.0520	0.9157	0.4585
Residuals	5.0517	89	0.0568		
4 classes: AF, SF, AM, SM	0.1947	3	0.0649	1.1534	0.3321
Residuals	5.0649	90	0.0567		
Males vs Females	0.0415	1	0.0415	0.7315	0.3946
Residuals	5.2181	92	0.0567		
Adults vs subadults	0.1352	1	0.1352	2.4274	0.1227
Residuals	5.1244	92	0.0557		

4.3.5 Linear regression models

After completing home range estimation, the computation of environmental variables per home range, and the selection and transformation of an appropriate health variable, it was possible to create OLS linear regression models. Several multivariate models were developed, starting from universal models in which all variables that were not highly correlated with each other ($r < 0.7$) or a linear combination of each other were included. Backward elimination was used to remove variables sequentially such that each variable removed would cause the largest decrease in the AIC score (Burnham & Anderson, 1998; Golberg & Cho, 2004). Those models with the lower AIC scores and a higher adjusted coefficient of determination were considered more predictive and explanatory. This process was stopped once the removal of another variable would cause Akaike's information criterion (Akaike, 1973) to increase. Akaike's information criterion (AIC) is defined as (Burnham & Anderson, 1998)

$$\text{AIC} = -2\log\left(\hat{\sigma}^2\right) + 2K, \qquad\qquad 4.10$$

where $\hat{\sigma}^2$ is the estimated variance, and K is the number of estimated parameters including the intercept and the variance. If the sample size is small, AIC is adjusted for a small sample size using the following equation

$$\text{AIC}_c = \text{AIC} + \frac{2K(K+1)}{n-K-1}, \qquad\qquad 4.11$$

where n is the sample size. Generally, the AICc is advocated when $n/k < 40$ (Burnham & Anderson, 1998).

R, version 2.6.2 (The R Foundation for Statistical Computing, 2008), was used for this analysis.

Models were screened for outliers using a variety of diagnostic plots. If any observations were found to have a Cook's distance greater than one, they were examined (Golberg & Cho, 2004, p. 273). Cook's distance measures the effect of an observation on all the coefficient estimates (Golberg & Cho, 2004, p. 272). Those observations with a large Cook's distance and leverage were investigated to determine if these observations were perhaps not part of the same population as the other observations, or perhaps erroneous. If there was no justifiable reason to remove them from the study, they were retained in the model, even if they reduced the overall fit of the model.

The models were also checked for multicollinearity among the explanatory variables, or regressors, which can cause large variances and covariances of the estimated coefficients (Faraway, 2002, p. 291; Montgomery & Peck, 1982). As a result of this, t-tests are more likely to fail to identify important variables. Multicollinearity occurs when there is near linear dependencies between two or more regressors in the model (Montgomery & Peck, 1982, p. 287).

Three methods were used to check for the presence of multicollinearity. These were the examination of i) the correlation matrix of the predictors, ii) the variance inflation factors, and iii) condition numbers (Faraway, 2002, pp. 116 - 118; Montgomery & Peck, 1982, pp. 288 - 300). Typically, if correlations are greater than 0.9, multicollinearity is a problem (Golberg & Cho, 2004, p. 385). In this case one or more of the offending variables were removed from the model. The variance inflation factor (*vif*) of the jth regressor is given by (Montgomery & Peck, 1982, p. 300)

$$vif_j = \frac{1}{1 - R_j^2},$$
<div style="text-align: right">4.12</div>

where R_j^2 is the coefficient of determination obtained when the jth variable is regressed

on the remaining regressors. In a perfectly orthogonal dataset $R_j^2 = 0$ and the variance of

parameter estimates is minimized.   If vif_j is greater than 10, it is likely that

multicollinearity is present and that the jth parameter is poorly estimated (Montgomery

and Peck, 1982, p.300). The condition score, κ_j, are computed as follows (Faraway,

2002)

$$\kappa_j = \sqrt{\frac{\lambda_{\text{max}}}{\lambda_j}} \hspace{4cm} 4.13$$

where λ_j are the eigenvalues and λ_{max} is the maximum eigenvalue of the variance-

covariance matrix of the estimated coefficients. If one or more condition numbers are

equal to or greater than 30, then at least one near linear dependence exists among the

explanatory variables (Faraway, 2002, p. 117).

A problem with this method is that it is not clear which design matrix to use (Golberg &

Cho, 2004, p. 380). It has been recommended to center and scale the design matrix

before calculating the eigenvalues and condition numbers (Golberg and Cho, 2004). In

this study the design matrix was centered and scaled such that the variance equalled one

before calculating the condition numbers.

Once the issues of outliers and multicollinearity were satisfactorily resolved, a

series of diagnostics plots were created to examine the residuals for heteroskedasticity

and non-normality.

To determine the relative likelihood of each model given the data, the weights of each model was computed and then ranked. First the differences between all AIC scores and the lowest AIC score were computed (Burnham & Anderson, 1998, p. 71):

$$\Delta_i = AIC_i - AIC_{min}.$$
<div align="right">4.14</div>

The differences were then used to calculate the Akaike weights as follows (Burnham & Anderson, 1998, p. 75)

$$w_i = \frac{\exp\left(-\frac{1}{2}\Delta_i\right)}{\sum\limits_{r=1}^{n}\exp\left(-\frac{1}{2}\Delta_r\right)},$$
<div align="right">4.15</div>

where Δ_r is the sum of all Akaike differences, Δ_i. Further, the evidence ratio can be computed as the Akaike weight of one model over the weight of the other (Burnham & Anderson, 1998, p. 75). This measures the relative likelihood of model pairs and is useful for comparing any two models. If the ratio is small for a pair of models then there is weak support that one model is better than the other. If the ratio is large then the model with smaller weight has strong evidence against it. A ratio of less than three is considered to be poor support for selecting one model over the other (Burnham & Anderson, 1998, p. 75).

Once the models were ranked and compared using Akaike's weights and the evidence ratio, it was then possible to select the best model for testing for spatial dependence in the residuals. This is discussed further in the next section.

This process was carried out for the entire study area A, and repeated for study area B.

4.4 Developing spatial weights

A variety of spatial neighbourhood weights were developed to test the residuals of the best models for spatial dependence using Moran's *I.* The neighbourhoods tested are demonstrated conceptually in Figure 4-14. *K*-nearest neighbours, distance thresholds, inverse distance weights, Gabriel graphs, Delaunay networks, proportion overlap between home ranges and family relatedness were used to inform spatial weight matrices.

The cost surface was employed to develop least cost distance decay weights for the subset of data which fell over its coverage. These observations were tested for spatial dependence using both Euclidian and least cost distance decay weights for comparison.

For overlap neighbours, the proportion of overlap between core home ranges was used to define weights. These were calculated in two ways

$$O_{1i} = \frac{A_{ij}}{A_i},$$
<div align="right">4.16</div>

and

$$O_{2i} = \frac{A_{ij}}{A_i + A_j}.$$
<div align="right">4.17</div>

These will be referred to as overlap # 1 and overlap # 2 for simplicity.

Family relationships were also used to define weight matrices. Genetic relatedness was expected to cause similarity or dependence in SLL among related bears. Weights were equal to the inverse of the number of degrees of separation to a maximum of two degrees of separation. This allowed the inclusion of family relations between grandparents and offspring, as well as aunts/uncles and nieces/nephews.

The point of maximum use from each home range utilisation surface was used as the centroid from which to determine distance-based neighbourhoods, including *k*-nearest neighbours, distance-threshold and distance decay weights.

a) *k* nearest neighbours

$k = 2$

Mutual 1st /2nd nearest neighbours

1st/2nd nearest neighbour

b) Distance neighbourhoods

Neighbours within distance d

c) Least-cost distance weights

Least cost distance neighbours

River

Mountain

d) Delaunay network

e) Proportion overlap

Centroid   Home Range   Neighbours
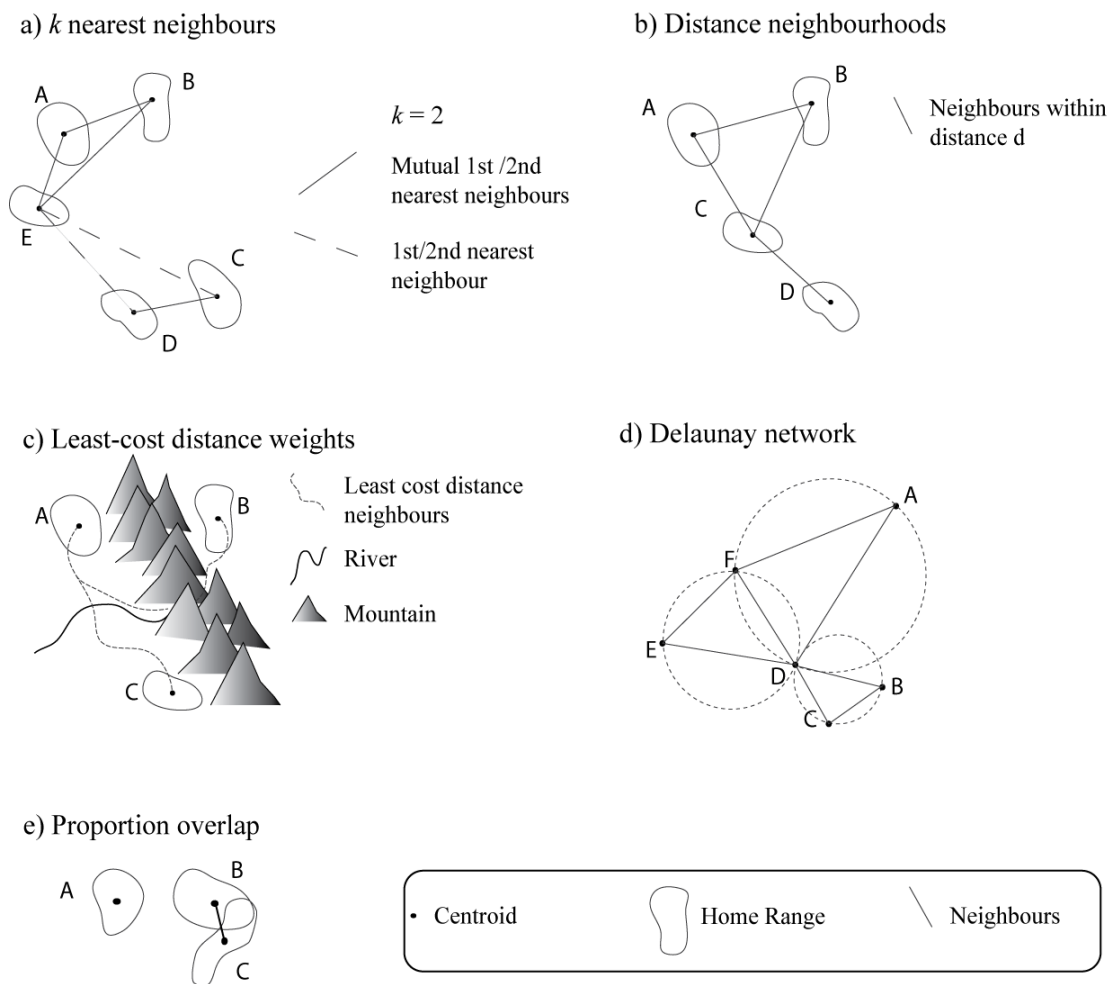
Figure 4-14. Spatial neighbourhoods

4.5 Developing spatial autoregressive models

Those spatial weight matrices for which significant spatial dependence was detected ($p < 0.05$), were selected to test spatial error, lag and Durbin models (See Chapter 2, section 2.4.2). Simultaneous autoregressive models were used rather than conditional as the

former do not require the spatial matrices to be symmetric and are commonly applied

in spatial econometric approaches (Anselin & Bera, 1998, p. 255). Again R, version

2.6.2 (The R Foundation for Statistical Computing, 2008), was used for this analysis.

The log-likelihood ratio test was used to evaluate whether the inclusion of a

spatial parameter was a significant improvement over the ordinary linear model. The

OLS and spatial autoregressive models were ranked and their relative strength was

assessed using AIC and Akaike weights. For the spatial autoregressive model, equation

4.10 is slightly modified for maximum likelihood estimation (Burnham and Anderson,

1998, p. 61):

$$\text{AIC} = -2\log(\mathcal{L}(\hat{\theta} \mid z)) + 2K, \qquad\qquad 4.18$$

where $\log((\mathcal{L}(\hat{\theta} \mid z))$ is the log-likelihood of the maximum likelihood estimation of the

parameters, $\hat{\theta}$ (includes explanatory variables, intercept, variance and spatial

parameter(s)), given z (Burnham & Anderson, 1998). It can be adjusted in the same

manner as equation 4.11 for small sample sizes.

Chapter Five: Results and Discussion

The results of this research are presented in this chapter along with a detailed discussion relating these to the hypotheses and objectives listed in chapter one. Findings for study area A and B (see Figure 4.1) are shown separately in sections 0 and 5.2 respectively. The results of the Moran's I tests for dependence in the transformed straight-line length variable are shown in section 5.1.1. OLS model descriptions, parameter estimates and diagnostics tests are found in section 5.1.2 and 5.2.1. Moran's I tests for spatial dependence in the residuals of the OLS models are presented in section 5.1.3 and 5.2.2. Those spatial weight matrices that were able to capture significant dependence were used to develop the spatial autoregressive models shown in section 5.1.4 and 5.2.3.   The significance of the selected environmental parameters, spatial neighbourhoods and spatial autoregressive models are discussed in depth in section 5.3. Finally, the findings of this research are summarised.

5.1 Results for study area A

5.1.1 Spatial dependence in the dependent variable

The dependent variable, transformed straight-line length (SLL100) was found to have strong positive spatial dependence using several spatial neighbourhoods. All nearest neighbour (NN) neighbourhoods from first to twenty-second were tested and all found to

have significant dependence. Thirteen NN had the smallest probability of being

generated from a random process, $p = 1.6\text{e-}7$ and Moran's $I = 0.16$. Distance threshold

neighbours were also found to have significant positive dependence.

Neighbourhood weights were also based on the proportion of overlap between

neighbours based on the following two equations $O_{1i} = \dfrac{A_{ij}}{A_i}$ (overlap # 1) and

$O_{2i} = \dfrac{A_{ij}}{A_i + A_j}$ (overlap # 2) as were described in Chapter 4 in equation 4.15 and 4.16.

Both of these weight neighbourhoods showed significant positive spatial dependence, $p =$

0.0005 and $p = 0.001$ respectively. The family-based neighbourhoods did not detect

significant dependence, but this was most likely due to the fact that 57 observations had

no family information available. The results are summarised in Table 5.1

Table 5-1. Moran's *I* tests for SLL100

Neighbourhood & weights	Test	Observed Moran's *I* (I_{obs})	Pr ($I < I_{obs}$)
13 NN – row standardised	Randomisation	0.16	1.6e-7
0.6 x, 0.75 x, 1.25 x, 1.75 x and 2 x 48 km	Randomisation	0.04 to 0.16	0.0006 to 0.016
Overlap # 1	Randomisation	0.27	0.0005
Overlap # 2	Randomisation	0.25	0.001

Moran's *I* tests rely on the assumption of a constant mean and variance in the

tested variable (Schabenberger and Gotway, 2005, p. 22). Any spatial clustering in

SLL100 may be due to one or more spatially autocorrelated environmental variables.

Thus, OLS regression models relating SLL100 to environmental variables were

developed and the residuals of these models were tested for spatial dependence. The

results are shown in section 5.1.2 and 5.1.3.

5.1.2 OLS Linear model

It was intended that several universal models be created that include representative

variables from each of the categories: terrain, water availability, habitat type and human

disturbance. However, several variables were highly correlated with each other thereby

limiting which variables could be included within the same models. The variables slope

and elevation were found to be highly correlated to each other and with distance to roads

and wells, closed canopy, wetland types, regenerating land types, herbaceous and

shrubby vegetation, as well as open mixed and deciduous forests. The correlated

variables are shown in Table 5-2.

Table 5-2. Correlation between explanatory variables

Variables	Elevation	Slope
SLL100	-0.6229	-0.6883
Elevation	1.0000	0.8848
Slope	0.8848	1.0000
Distance to roads	0.8561	0.8411
Distance to wells	0.9051	0.8757
Distance to roads & wells	0.8565	0.8401
Canopy closure	-0.7202	-0.5692
Herbaceous and shrubby veg	0.8804	0.7717
Open mixed forest	-0.7364	-0.6223
Open deciduous forest	-0.7366	-0.5560
Wetland herbs	-0.8464	-0.9075
Wetland forests	-0.6687	-0.7487
Wetlands (herbs + forests)	-0.6753	-0.7617
Regenerating barren lands	-0.8242	-0.7720
Regenerating forests	-0.7367	-0.6332
Regenerating (forests + barren)	-0.7951	-0.7184

This precluded the combination of elevation, slope, disturbance measures (distance to roads, wells, and or roads and wells), herbaceous and shrubby vegetation, and the various wetland and regenerating vegetation classes in the same model. Canopy closure, open mixed forest and open deciduous forests were also highly correlated with elevation, but less than 0.7 for slope.

Considering these constraints, the candidate models shown in Table 5-3 were obtained using a process of backward elimination (Golberg & Cho, 2004) and were ranked using Akaike's weights (Burnham & Anderson, 1998). The highest ranked model is model E with three variables: slope (Slope), open deciduous forest (OpDecFst) and distance to water (Dist2Wat).

Table 5-3. Ranked candidate OLS linear models for study area A

Model	Variables	K	AIC	Δ_i	w	Evidence ratio
E	Slope + OpDecFst + Dist2Wat	4	825.21	0	0.277	1.000
D	Slope + OpDecFst + Northeast + Dist2Town	5	826.16	0.952	0.172	1.610
I	Slope + OpDecFst + Northeast	4	826.51	1.296	0.145	1.912
J	Slope + OpDecFst	3	826.83	1.615	0.124	2.242
F	Slope + log(OpDecFst+0.01) + Northeast + MaxX	5	827.84	2.623	0.075	3.712
G	Slope + log(OpDecFst+0.01) + Northeast	4	828.70	3.486	0.048	5.713
A	Slope + Northeast	3	828.90	3.692	0.044	6.335
B	Slope + East	3	829.02	3.811	0.041	6.721
K	Slope + OpMixFst+Northeast + Dist2Wat	5	829.23	4.022	0.037	7.472
H	OpDecFst + WetAll + RegAll + Dist2Wat	5	829.53	4.320	0.032	8.670
C	Elev + Dist2Wat	3	833.39	8.180	0.005	59.728

Model E is very similar to models D, I, and J, which have $\Delta_i < 2$. According to Burnham and Anderson (1998, p. 70), those models with AIC differences of two or less from the best model are well-supported by the data, while those models that have $\Delta_i > 4$

are unlikely to be the best models given the data. Also, the evidence ratio, which compares the relative likelihood of each model, shows that model E is just over two times more likely than model J.

The key variables which distinguish the top four from the other models are slope and open deciduous forest (untransformed). The top model, E, was examined more closely for fit and diagnostics. Table 5-4 provides the parameter estimates of model E, as well as its overall fit and AIC score.

Table 5-4. Model E parameter estimates and fit

Variable	Coefficient	Std.Error	t-Statistic	Pr(>|t|)	
Intercept	76.5402	6.056108	12.63851	< 2.00E-16	***
Slope	-1.6715	0.390553	-4.27991	4.66E-05	***
OpDecFst	5.0631	1.997701	2.534462	0.0130	*
Dist2Wat	-2.9453	1.56789	-1.87849	0.0636	.
Signif. codes: 0 '***' 0.001 '**' 0.01 '*' 0.05 '.' 0.1 ' ' 1					

F-statistic:	19.092	**Pr(>F)**		1.15e-09
Number of observations	94	**Degrees of freedom**		90
Number of variables	4	**R-squared**		0.389
AIC	825.213	**Adjusted R-squared**		0.369
Mean dependent variable	54.311	**Log Likelihood**		-407.606
S.D. of dependent variable	23.654	**Sum of squared residuals**		32141.200
Sigma-squared	357.124	**Sigma-square ML:**		341.928
S.E. of regression	18.898	**S.E. of regression ML**		18.491

Slope is by far the most significant predictor with a coefficient of -1.67 and a probability of $p < 0.0001$. This means that as the slope increases, straight line length decreases. Open deciduous forest is positive with a coefficient of 5.06 and $p < 0.05$. Distance to water has a negative coefficient of – 2.95 and a probability of $p < 0.1$.

Although the adjusted R^2 is only 0.36, the model is highly significant since the F-test[1]

has $p = 1.14\text{e-}009$.

Various diagnostics were conducted to test the normality and heteroskedasticity of

the residuals. Also, the possibility of multicollinearity was examined using the

multicollinearity condition number, the correlation matrix of the parameter estimates, and

the variance inflation factors. These diagnostics are shown in Table 5-5 and Figure 5-1.

Table 5-5. Diagnostics of model E

Regression Diagnostics			
Multicollinearity condition number			6.516736
Test of normality of errors			
Test	df	value	p-value
Jarque-Bera	2	1.133947	0.56724
Diagnostics for Heteroskedasticity			
Random Coefficients			
Test	df	value	p-value
Breusch-Pagan test	3	3.847241	0.278439
Koenker-Bassett test	3	4.031967	0.258033
Specification Robust Test			
Test	df	value	p-value
White	9	11.14075	0.266185
Correlation Matrix			
	Intercept	Slope	OpDecFst	Dist2Wat
Intercept	1	-0.547	-0.495	-0.542
Slope	-0.547	1	0.446	-0.302
OpDecFst	-0.495	0.446	1.000	-0.059
Dist2Wat	-0.542	-0.302	-0.059	1
Variance Inflation Factors			
Intercept	Slope	OpDecFst	Dist2Wat
2.0283	1.3797	1.2584	1.1091

The tests for heteroskedasticity and non-normality of errors are not significant.

The multicollinearity condition number is well below 10, the correlations are lower than

---

[1] The F-test tests whether the variance explained by the regression is statistically different from the variance caused by error (Underhill & Bradfield, 1996). If the F-test is statistically significant it can be concluded that there is a significant relationship between the dependent variable and explanatory variables.

0.9 and the variance inflation factors are well below 10. These all indicate that multicollinearity is not present to any significant degree since these values are all within their normal bounds.

The diagnostics plots in Figure 5-1 seem to confirm these results. Observation 45 draws attention as a potential outlier due to the fact that it has a much larger Cook's distance than the other observations. However, Cook's distance is well below 1 (Golberg & Cho, 2004) and does not have a particularly large leverage; hence it has been retained for this research.
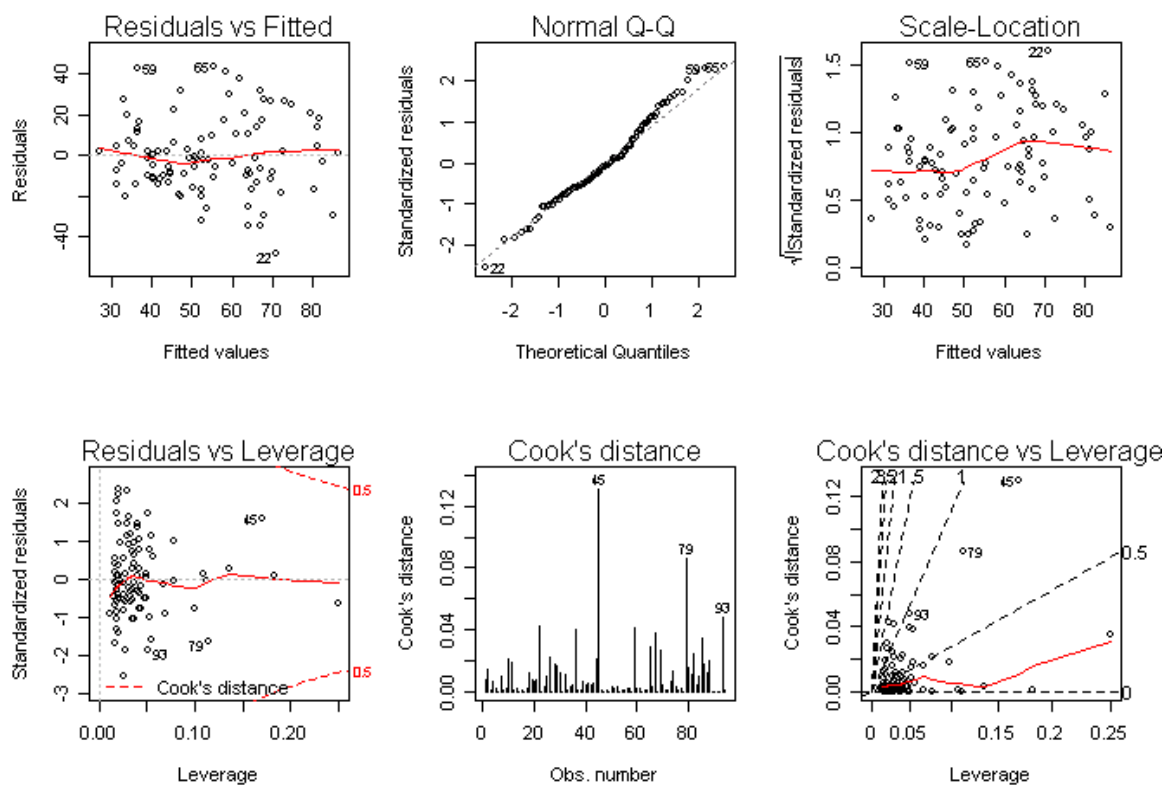
Figure 5-1. Diagnostic plots of Model E

Figure 5-2 shows the spatial distribution of the explanatory variables of model E. To facilitate visualisation, Voronoi polygons were generated from the core home range centroids.
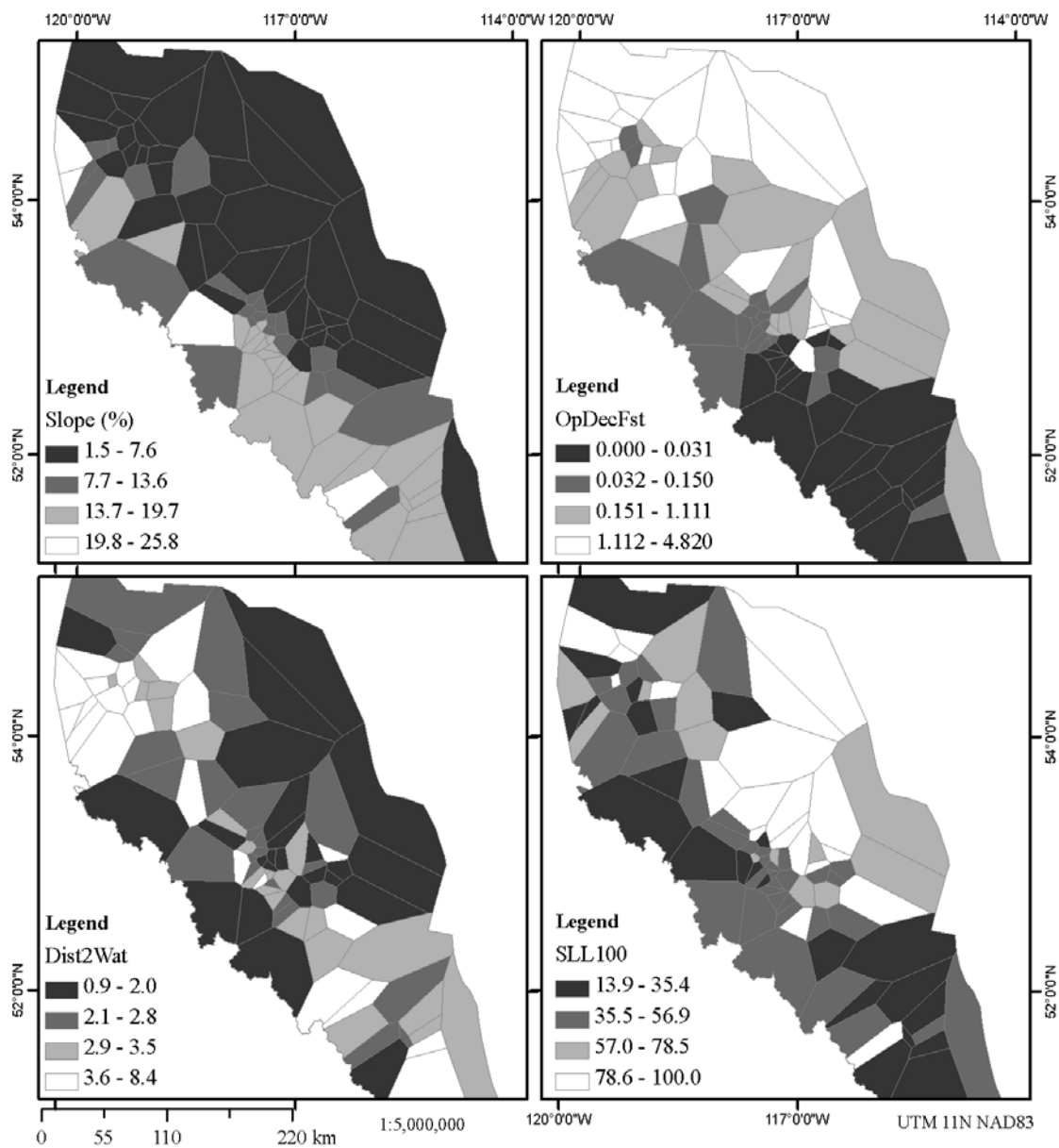
Figure 5-2. Spatial distribution of slope, open deciduous forest, distance to water and SLL100

SLL100 appears to be positively spatially autocorrelated with lower values towards the mountains and higher values towards the mid-northeast. This corresponds to the Moran's *I* findings in section 5.1.1. There are also patchworks of contrasting SLL100 values appearing in the northwest especially. It can also be seen from the figure that slope is highly spatially autocorrelated, as is open deciduous forest (OpDecFst) and distance to water (Dist2Wat). This visual pattern in each of the explanatory variables was confirmed using Moran's *I* with one to twenty nearest neighbours. All neighbourhoods were found to have highly significant positive spatial dependence. The results for five nearest neighbours are shown in Table 5-6.

Table 5-6. Results of Moran's *I* tests for slope, open deciduous forest and distance to water in study area A

Variable	Neighbourhood	Test	Observed Moran's I (I_{obs})	Pr ($I_{obs} > I$)
Slope	5 NN – row standardised	Randomisation	0.6786	< 2.2e-16
Open deciduous forest	5 NN – row standardised	Randomisation	0.4362	1.792e-15
Distance to water	5 NN – row standardised	Randomisation	0.4184	2.560e-14

The model E-predicted SLL100 values shown in Figure 5-3 roughly fit the trend of the observed SLL100, with lower values in the mountains higher values towards the north and east. However, it does not reproduce the range of values observed in the raw data, strongly under predicts SLL100 in the middle east of the region and does not seem to capture the heterogeneity observed in SL100. The residuals (also in Figure 5-3) appear to have some clustering as well as contrasting values adjacent to each other.
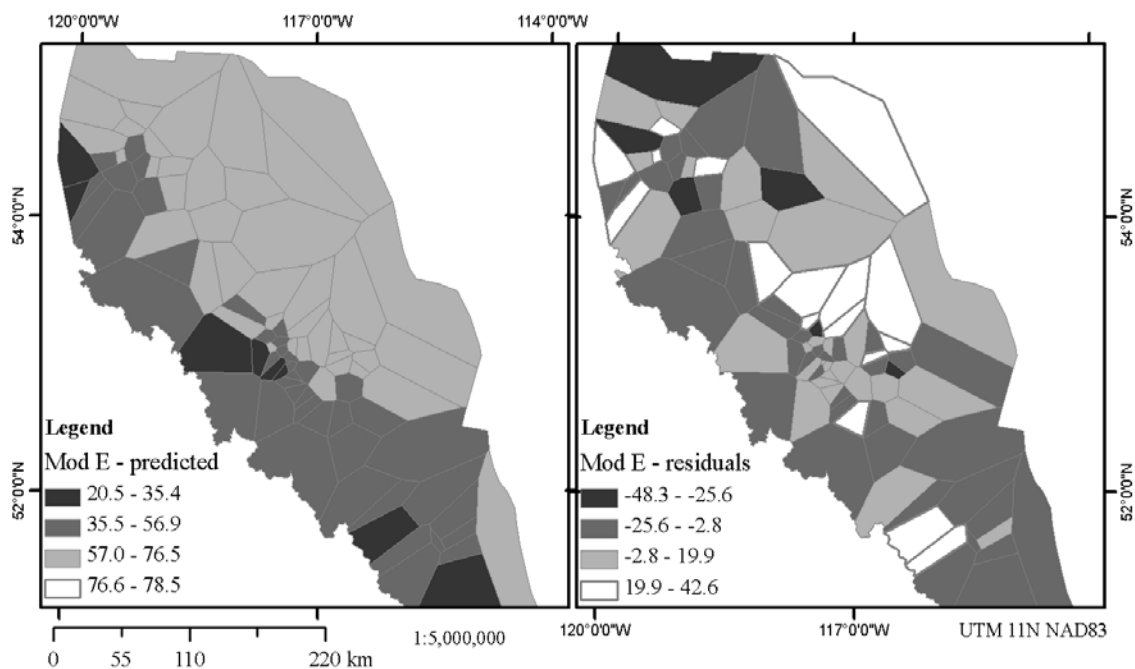
Figure 5-3. Predicted values and residuals of model E

5.1.3 Spatial dependence tests

Due to the fact that significant spatial dependence was found in the SLL100 data (section

5.1.1), it was deemed necessary to test whether model E had accounted for the spatial

dependence present in the data, or whether it still remained in the residuals.

Moran's *I* was therefore computed for the residuals of model E using one to

twenty nearest neighbours (NN). Significant *negative* spatial dependence was found for

three to eight NN. Negative dependence is a rare finding, but does reflect the contrasting

residuals seen in Figure 5-3. Those significant NN neighbourhoods and the Moran's *I*

results are shown in Table 5-7. All neighbourhoods were row-standardised and Moran's

I was tested using a normal assumption (Normal), exact (Exact) and a Saddlepoint

(Saddle) approximation test.

Table 5-7. Moran's *I* tests on model E residuals using nearest neighbour weights

Neighbourhood & weights	Test	Observed Moran's *I* (I_{obs})	Pr ($I < I_{obs}$)
3 NN – binary & row standardised	Normal	- 0.1789	0.0195
	Exact		0.0118
	Saddle		0.0118
4 NN – binary & row standardised	Ordinary	-0.1405	0.0.370
	Exact		0.0252
	Saddle point		0.0252
5 NN - binary & row standardised	Ordinary	-0.1367	0.0223
	Exact		0.0102
	Saddle point		0.0102
6 NN - binary & row standardised	Ordinary	-0.1023	0.0583
	Exact		0.0403
	Saddle point		0.0404
8 NN - binary & row standardised	Ordinary	-0.0891	0.0574
	Exact		0.0355
	Saddle point		0.0356

Three and five NN resulted in the most significant *p*-values for the observed Moran's *I*. Neighbour distances ranged between 0.3 km and 66 km of each other for three NN, and between 0.3 km and 92 km for five NN. The spatial arrangement of these neighbourhoods is shown in Figure 5-4. From this figure it appears that these nearest neighbour configurations distinguish three spatial groups that correspond to the three population units separated by Highway 11 and Highway 16. There is evidence that these populations are genetically distinctive (Stenhouse, 2007).

Neighbourhoods defined by distance thresholds were also tested. Distance thresholds were based on multiples of the largest nearest neighbour distance of 48.425 km. Multiples used were 0.6, 0.75, 1, 1.25, 1.5, 1.75 and 2 and neighbourhood weights were row-standardised. The only neighbourhood found to be significant was 1.5 times the

maximum nearest distance, i.e. 72.638km. Negative spatial dependence was detected.

The results are shown in Table 5-8.

3 Nearest Neighbours

5 Nearest Neighbours
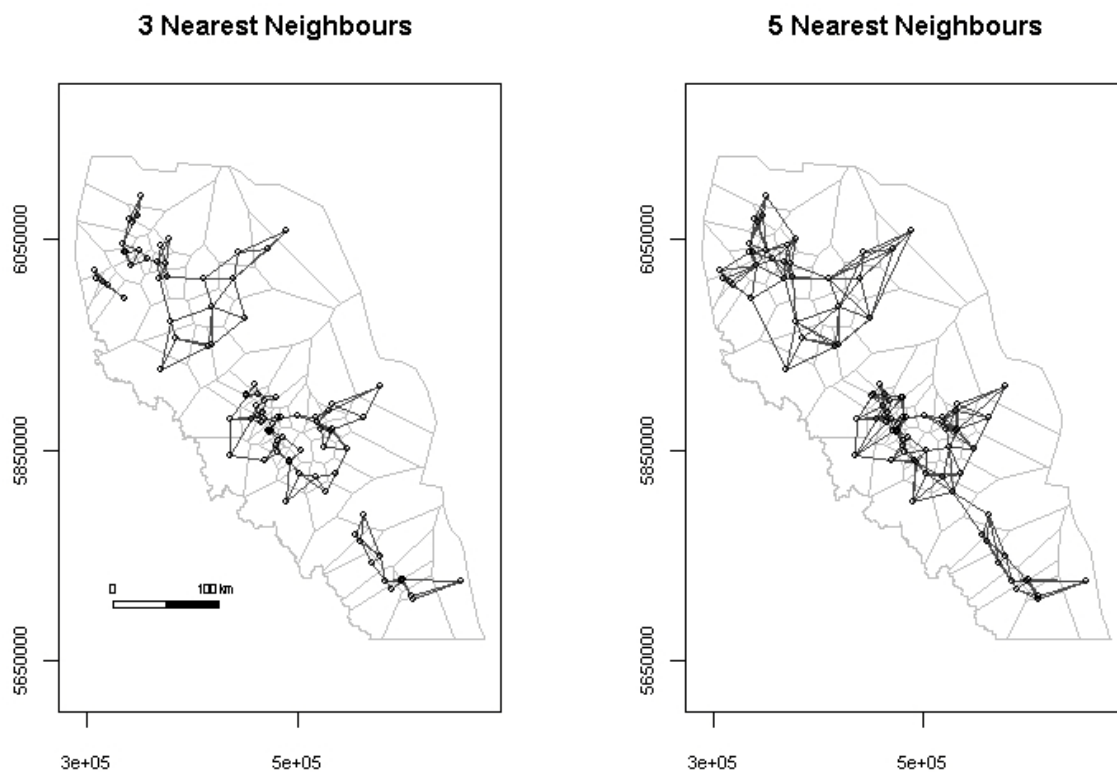
Figure 5-4. Three and five nearest neighbours

Table 5-8. Moran's *I* tests on Model E residuals using distance threshold neighbourhood, where threshold = 73 km.

Neighbourhood	Test	Observed Moran's I (I_{obs})	p-value ($I_{obs} > I$)
Distance threshold = 1.5 x max. NN dist – binary weights	Normal Exact Saddle	-0.0625	0.9550 0.9705 0.9717

The spatial distribution of this neighbourhood configuration is shown in the figure

below.
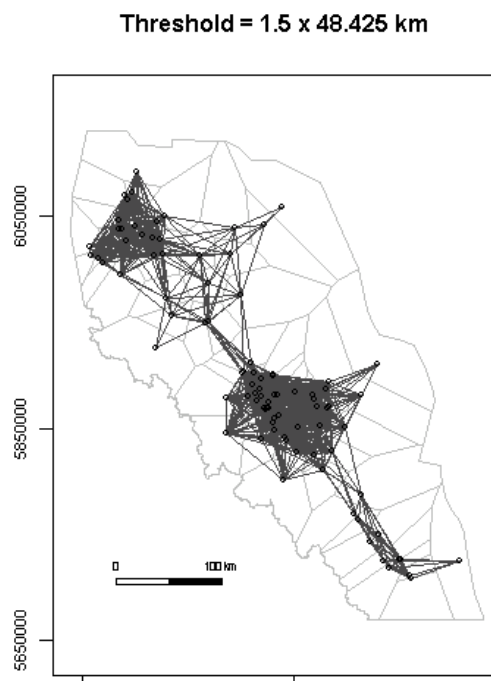
Figure 5-5. Distance threshold neighbours. Threshold = 73 km

The scales of three and five NN neighbourhoods and the distance threshold

neighbourhoods shown in Table 5-9 are very similar. Although the distance threshold

neighbourhood has connections between population units, the within group connections

occurred at a much higher frequency.

**Table 5-9. Neighbourhood distances for 3 NN, 5 NN and distance threshold
neighbourhoods**

	Minimum distance	Median distance	Maximum distance
3 NN	0.3 km	13.1 km	66.5 km
5 NN	0.3 km	16.6 km	91.7 km
Distance threshold = 72.9 km	0.3 km	41.5 km	72.9 km

The relative neighbour graph, Gabriel graph and Delaunay network graph

neighbourhoods, the overlap neighbourhoods # 1 and 2, and the family neighbourhood

did not detect significant spatial dependence.

5.1.4 Spatial autoregressive models

Spatial lag, error and Durbin models were developed using those spatial neighbourhoods that showed significant spatial dependence. All neighbourhood weights were row-standardised, forcing an upper limit of 1 for the estimated spatial parameter. The explanatory variables from model E (slope, open mixed forest and distance to water) were used to develop the spatial autoregressive models. Only simultaneous autoregressive (SAR) models were implemented as these do not require symmetrical weight matrices. The SAR models were ranked according to their Akaike weights and are shown in Table 5-10. All models have a significant spatial parameter ($p < 0.05$) according to the log-likelihood test.

The top eight top models have considerable support as the best models. Their Akaike differences are less than three and the evidence ratio is less than four. After these eight, there is quite a jump in the Akaike differences and evidence ratios. Therefore these models are not well supported by the data. Six out of the top eight spatial models are error models and two are lag models, while Durbin models fair the worst due to the larger number of parameters estimated. Almost every spatial neighbourhood appears once in the top eight models except seven NN. Only five NN appears twice, including rank one model.

Table 5-10. Ranked spatial autoregressive models for study area A

Rank	Model	Neighbourhood	Type	k	AIC	AICc	Δ$_i$	w$_i$	Evidence ratio	lamda/ rho	p - value
1	5NN_err	5 NN row standard	error	6	818.11	820.74	0.00	0.200	1.000	-0.706	0.0025
2	Dist_thre_72km_err	dist threshold = 73 km	error	6	818.56	821.19	0.45	0.160	1.252	-1.507	0.0033
3	3NN_err	3 NN row standard	error	6	819.26	821.89	1.15	0.113	1.777	-0.465	0.0048
4	8NN_err	8 NN row standard	error	6	819.35	821.98	1.24	0.108	1.859	-0.959	0.0050
5	4NN_error	4 NN row standard	error	6	820.08	822.71	1.97	0.075	2.678	-0.539	0.0076
6	5NN_lag	5 NN row standard	lag	6	820.30	822.93	2.19	0.067	2.989	-0.465	0.0085
7	6NN_err	6 NN row standard	error	6	820.49	823.12	2.38	0.061	3.287	-0.713	0.0095
8	3NN_lag	3 NN row standard	lag	6	820.76	823.39	2.65	0.053	3.762	-0.370	0.0111
9	4NN_lag	4 NN row standard	lag	6	822.19	824.82	4.08	0.026	7.691	-0.369	0.0250
10	7NN_err	7 NN row standard	error	6	822.23	824.86	4.12	0.026	7.846	-0.643	0.0256
11	6NN_lag	6 NN row standard	lag	6	822.49	825.12	4.38	0.022	8.935	-0.437	0.0297
12	Dist_thre_72km_Dur	dist threshold = 73 km, row	Durbin	9	819.02	825.23	4.49	0.021	9.449	-1.597	0.0011
13	5NN_Dur	5 NN row standard	Durbin	9	819.16	825.37	4.63	0.020	10.135	-0.750	0.0009
14	8NN_lag	8 NN row standard	lag	6	823.17	825.80	5.06	0.016	12.554	-0.437	0.0443
15	7NN_lag	7 NN row standard	lag	6	824.23	826.86	6.12	0.009	21.328	-0.360	0.0840
16	Dist_thre_72km_lag	dist threshold = 73 km, row	lag	6	824.80	827.43	6.69	0.007	28.361	-0.419	0.1201
17	6NN_Dur	6 NN row standard	Durbin	9	821.63	827.84	7.10	0.006	34.846	-0.804	0.0033
18	8NN_Dur	8 NN row standard	Durbin	9	821.72	827.93	7.19	0.005	36.450	-0.961	0.0037
19	4NN_Dur	4 NN row standard	Durbin	9	823.61	829.82	9.08	0.002	93.780	-0.553	0.0058
20	7NN_Dur	7 NN row standard	Durbin	9	824.56	830.77	10.03	0.001	150.799	-0.676	0.0166
21	3NN_Dur	3 NN row standard	Durbin	9	824.89	831.10	10.36	0.001	177.851	-0.466	0.0054

The AIC score of the top spatial autoregressive model (5NN_err) is 818.11, which is considerably smaller than that of the top OLS model (E) with AIC = 825.213. Thus it appears that the spatial autoregressive models are a significant improvement over the OLS models.

Although the estimated spatial parameters (lamda/rho) appear large in comparison to the usual positive spatial parameters, they are not incorrect. According to Schabenberger and Gotway (2005, p. 336) using a row-standardised weights matrix forces an upper limit of one for rho/lamda, but there is no lower limit.

Table 5-11 provides a comparison of the parameter estimates of the best spatial autoregressive model (5NN_err) and the best OLS model (E).

Table 5-11. Comparison of parameters from model E and model 5NN_err

Model type	Variables	Estimate	Std. Error	z value	Pr(>|z|)
Error – 5 NN	Intercept	78.335	4.096	19.126	< 2.2e-16 ***
OLS	Intercept	76.540	6.056	12.639	< 2.0e-16 ***
Error – 5 NN	Slope	-1.686	0.260	-6.482	9.1e-11 ***
OLS	Slope	-1.672	0.390	-4.280	4.7e-05 ***
Error – 5 NN	OpDecFst	3.632	1.500	2.420	0.0155 *
OLS	OpDecFst	5.063	1.998	2.535	0.0130 *
Error – 5 NN	Dist2Wat	-3.257	1.039	-3.135	0.0017 **
OLS	Dist2Wat	-2.945	1.568	-1.879	0.0636 .
Error – 5 NN	Lamda	-0.706	n/a	n/a	0.0025 **

It can be seen that the parameter estimates do not change significantly between models, but the significance of all variables increases. Distance to water increases from $p = 0.06$ to $p = 0.002$, and slope from 5e-5 to 9e-11. Maps of the predicted values and residuals of model 5NN_err show improvement over the OLS model, E. For comparison, maps of the observed SLL100, SLL100 predicted from model E, SLL100 predicted from model 5NN_err, and the residuals of model 5NN_err are presented in Figure 5-6.
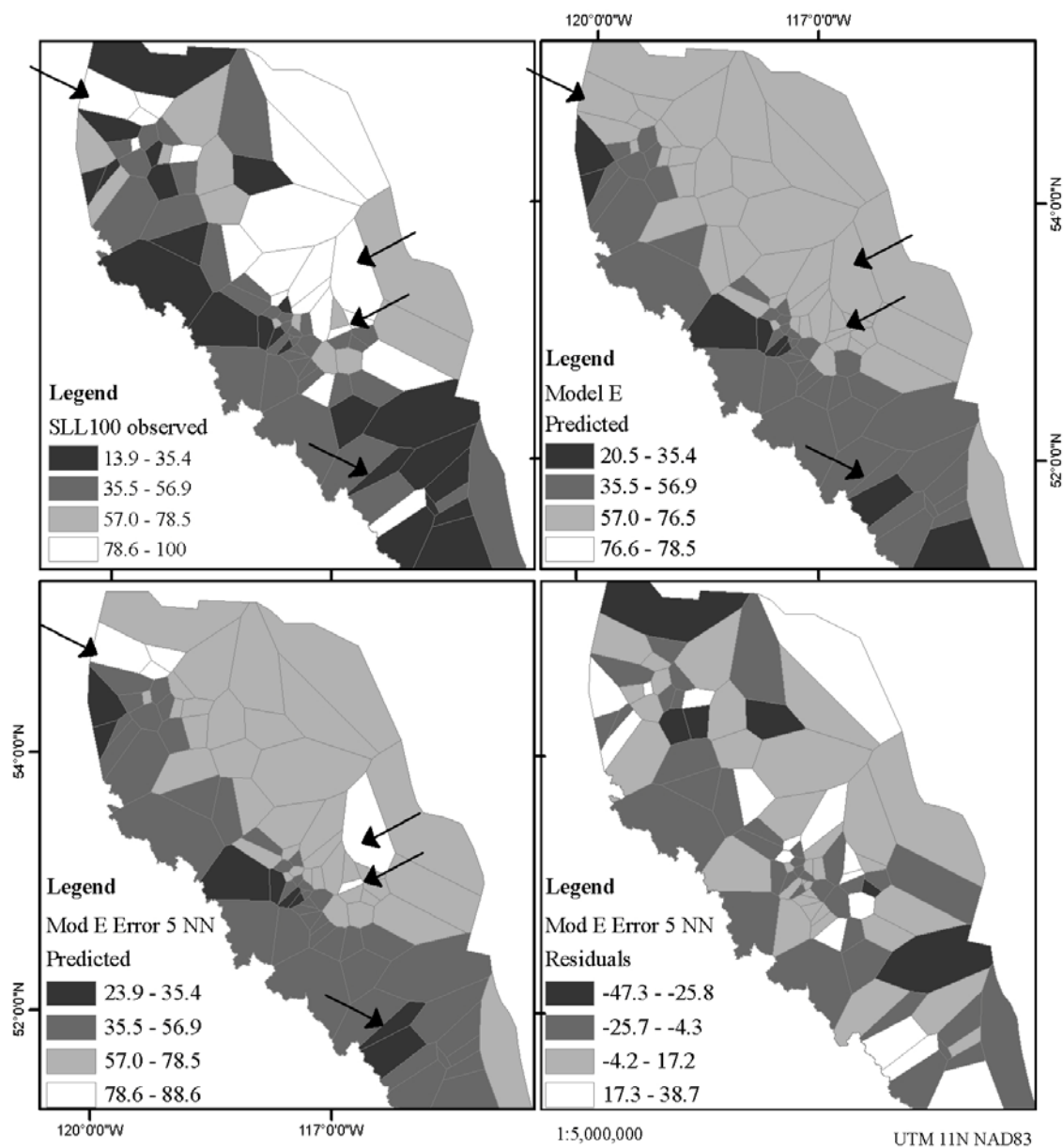
Figure 5-6. A comparison of observed SLL100, model E -predicted SLL100, model 5NN_err - predicted SLL100, and the residuals from Model 5NN_err

The residuals of 5NN_err have decreased slightly from [-48.0 to 43.9] for the

OLS model, to [-47.3 to 38.7]. The arrows in the figure point to a few observation units

where the spatial autoregressive model more accurately predicts SLL100. All predicted

intervals are based on the original equal interval ranges of the observed SLL100.

Finally, the residuals are examined for normality in the diagnostics plots below. It appears the residuals are approximately normally distributed, although there is some divergence in the upper tail.
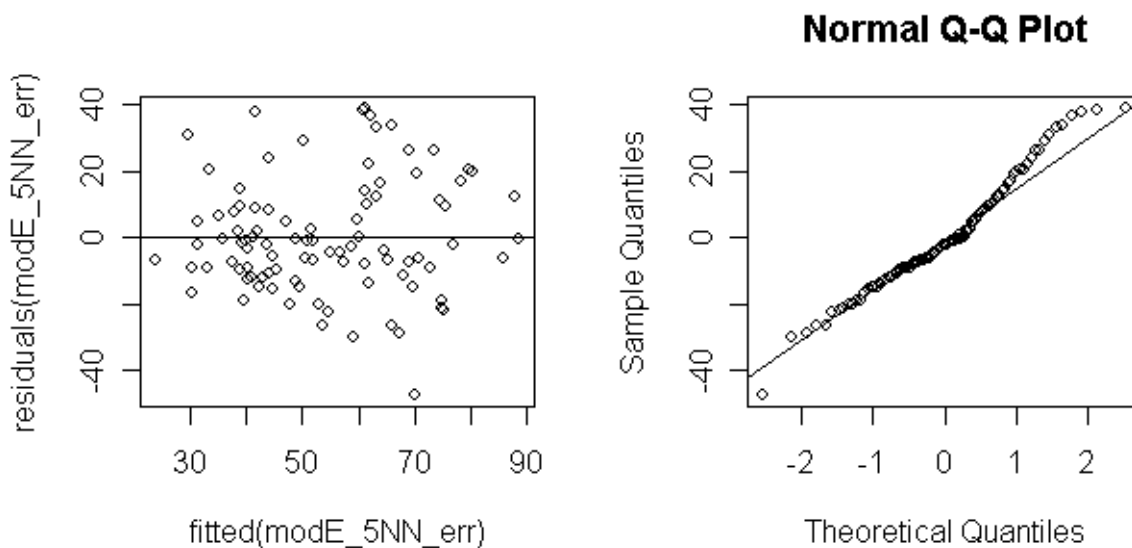
Figure 5-7. Diagnostics plots of residuals from model 5NN_err

5.2 Results for study area B

5.2.1 OLS linear models

Using the same procedures as previously, the following OLS linear models were developed and then ranked using AIC_c scores. Twenty models were ranked, but only the top sixteen are shown here in Table 5-12. The top three models are most likely the best models with $\Delta_i < 2$ and evidence ratios < 3.

Table 5-12. Ranked OLS models for study area B

Rank	Model	Environmental Variables	k	AICc	Δ_i	w_i	Evidence ratio
1	E	Slope + Northeast	4	340.03	0.00	0.294	1.000
2	F	Slope + Northeast + OpMixFst	5	340.22	0.19	0.268	1.097
3	H	Slope + DecFst	4	341.03	1.00	0.179	1.648
4	A	Slope	3	342.28	2.25	0.095	3.087
5	J	Slope + OpDecFst	4	342.36	2.33	0.092	3.209
6	K	Elev + Northeast + MaxX	5	345.26	5.23	0.021	13.689
7	I	MaxX + Northeast + OpDecFst + RegAll	6	347.15	7.12	0.008	35.171
8	C	Northeast + Herbs + OpMixFst + CldFst	6	347.45	7.42	0.007	40.838
9	D	Flat + Northeast + OpFst + log(RegFst+1)	6	347.97	7.94	0.005	52.872
10	G	Northeast + Herbs + OpMixFst + CldFst + log(WetFst+1)	7	348.19	8.16	0.005	59.064
11	L	MaxX_km + Northeast + Herbs + CldFst	6	348.35	8.32	0.005	63.960
12	Q	North + OpDecFst	3	348.52	8.48	0.004	69.458
13	O	North + OpDecFst + RegAll	5	348.61	8.58	0.004	73.128
14	M	Northeast + Dist2Wat + OpDecFst + RegAll	6	348.83	8.80	0.004	81.619
15	R	MaxX + Northeast + Dist2Town + Herbs + CldFst	7	348.94	8.90	0.003	85.821
16	B	MaxY + North + OpFst	5	350.89	10.86	0.001	227.649

The most significant variable again seems to be slope which appears in the top five models, but is absent in the following models. The top two models are distinguished from the other three by the inclusion of northeast aspect and appear to be slightly more supported than the other three top models. An examination of diagnostics plots to assess normality and heteroskedasticity of the residuals of the two top models (E and F) indicated that model F was the most normal and least heteroskedastistic. Due to these desirable characteristics model F was chosen for further analysis. The fit and parameters of model F are shown in Table 5-13 and diagnostics in Table 5-14.

Table 5-13. Model F parameter estimates and fit

Variable	Coefficient	Std.Error	t-Statistic	Pr(>|t|)	
Intercept	86.023	10.800	7.965	2.27E-09	***
Slope	-2.210	0.564	-3.919	0.0004	***
Northeast	-86.852	36.501	-2.379	0.0229	*
OpMixFst	2.166	1.436	1.508	0.1404	
Signif. codes: 0 '***' 0.001 '**' 0.01 '*' 0.05 '.' 0.1 ' ' 1					

F-statistic	12.991	**Prob(F-statistic)**		7.35E-06
Number of observations	39	**Degrees of Freedom**		35
Number of variables	4	**R-squared**		0.527
AIC	338.398	**Adjusted R-squared**		0.486
Mean dependent variable	56.045	**Log likelihood**		-164.199
S.D. dependent variable	23.700	**Sum of squared residuals**		10364.400
Sigma-square	296.126	**Sigma-square ML**		265.754
S.E. of regression	17.208	**S.E. of regression ML**		16.302

Slope has a negative coefficient and is by far the most significant parameter in the model. Northeast aspect is also fairly significant with a negative coefficient. Open mixed forest (like open deciduous forest in model E) has a positive coefficient. This model has a good fit with an adjusted $R^2 = 0.486$.

Table 5-14. Diagnostics of Model F

Regression Diagnostics			
Multicollinearity condition number			8.597951
Test of normality of errors			
Test	df	value	*p*-value
Jarque-Bera	2	0.5147571	0.773076
Diagnostics for Heteroskedasticity			
Random Coefficients			
Test	df	value	*p*-value
Breusch-Pagan test	3	2.4112	0.4915
Koenker-Bassett test	3	2.1366	0.5445
Specification Robust Test			
Test	df	value	*p*-value
White	9	6.246471	0.7150195
Correlation Matrix			
	Intercept	Slope	OpDecFst	Dist2Wat
Intercept	1	-0.846	-0.664	-0.435
Slope	-0.846	1.000	0.593	0.084
OpDecFst	-0.664	0.593	1	-0.135
Dist2Wat	-0.435	0.084	-0.135	1.000
Variance Inflation Factors			
Intercept	Slope	OpDecFst	Dist2Wat
1	1.609143	1.627481	1.063232

It can be seen from Table 5-14 that the multicollinearity condition number is less than 10, and the variance inflation factors are all less than 2. The tests for heteroskedasticity and normality are not significant indicating that the residuals can be assumed to be normally distributed and homoskedastic. This is confirmed by the diagnostics plots below.
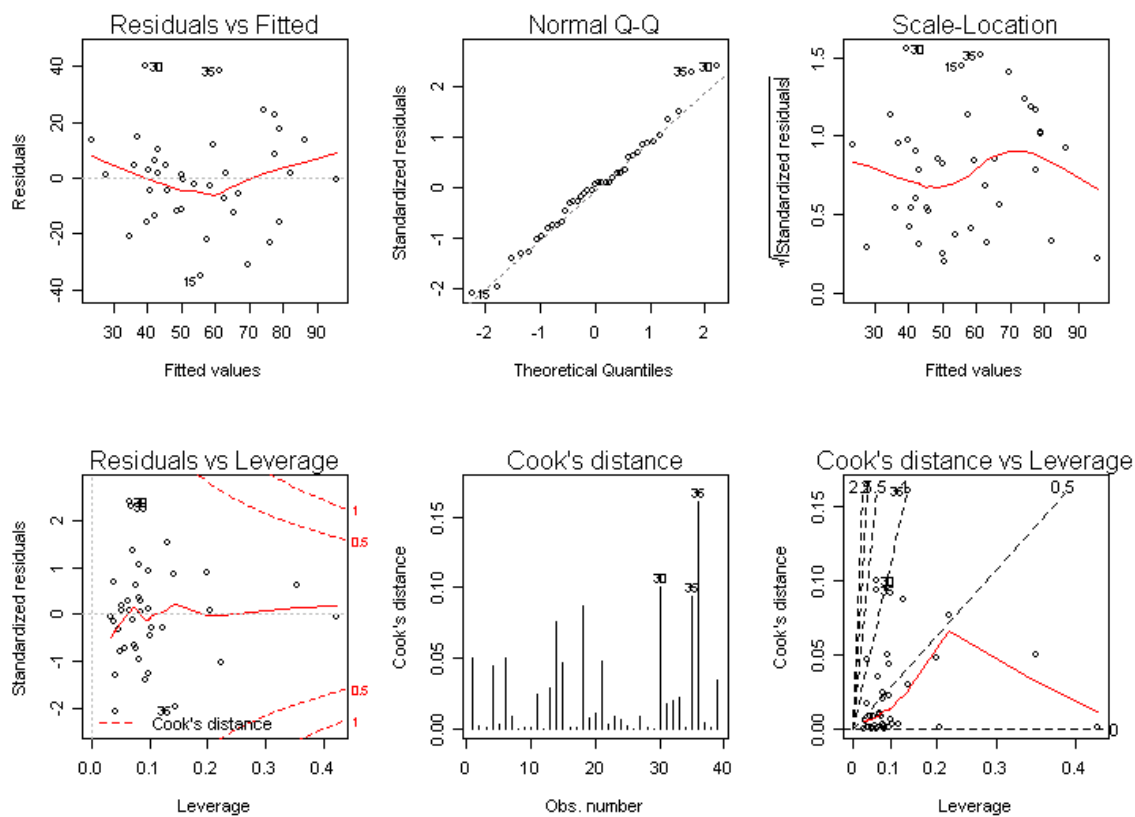
Figure 5-8. Diagnostics plots of Model F

Observation 36 has a larger Cook's distance than the other observations; however it is well below 1, the usual threshold for concern (Golberg & Cho, 2004). The explanatory variables of model F and the dependent variable, SLL100, are mapped in Figure 5-9.
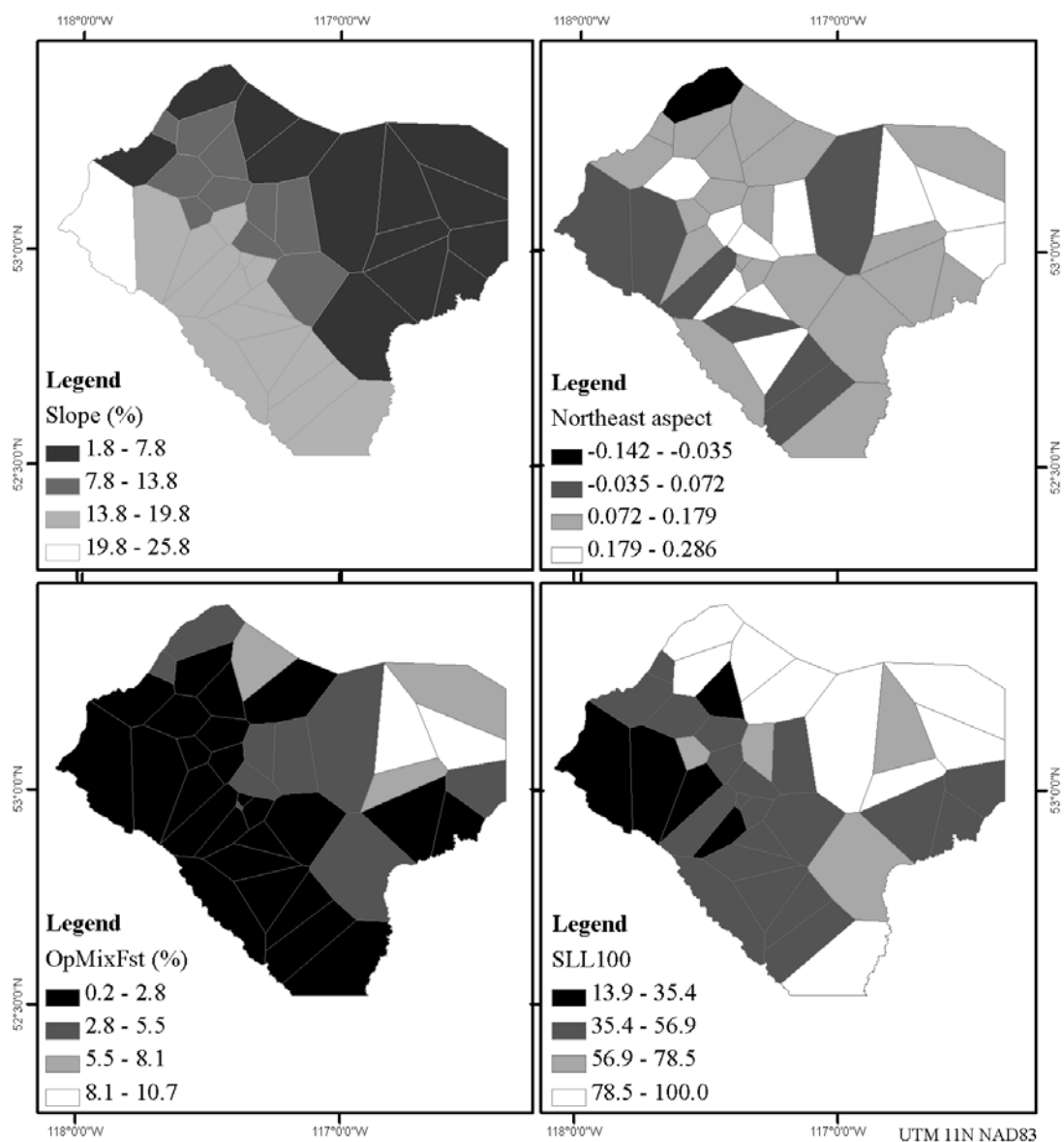
Figure 5-9. Spatial distribution of slope, open mixed forest (OpMixFst), northeast aspect (Northeast) and SLL100

From Figure 5-9, it is clear study area B has spatial clustering like the larger study area. One to ten nearest neighbours were used to test all the variables for spatial dependence. The most significant results are shown in Table 5-15. Only northeast aspect did not have significant positive dependence.

Table 5-15. Results of Moran's *I* tests for slope, open mixed forest, distance to water and SLL in study area B

Variable	Neighbourhood	Test	Observed Moran's I (I_{obs})	Pr ($I_{obs} > I$)
SLL100	7 NN – row standardised	Randomisation	0.222452851	2.229e-06
Slope	7 NN – row standardised	Randomisation	0.586308293	< 2.2e-16
Open mixed forest	10 NN – row standardised	Randomisation	0.315870076	2.925e-11
Neastness	10 NN – row standardised	Randomisation	-0.01858225	0.4411

Figure 5-10 maps the distribution of the residuals and predicted values of model F. The predicted values match the spatial pattern of the observed values of SLL100; however, the residuals tend to show patterns of both clustering and heterogeneity.
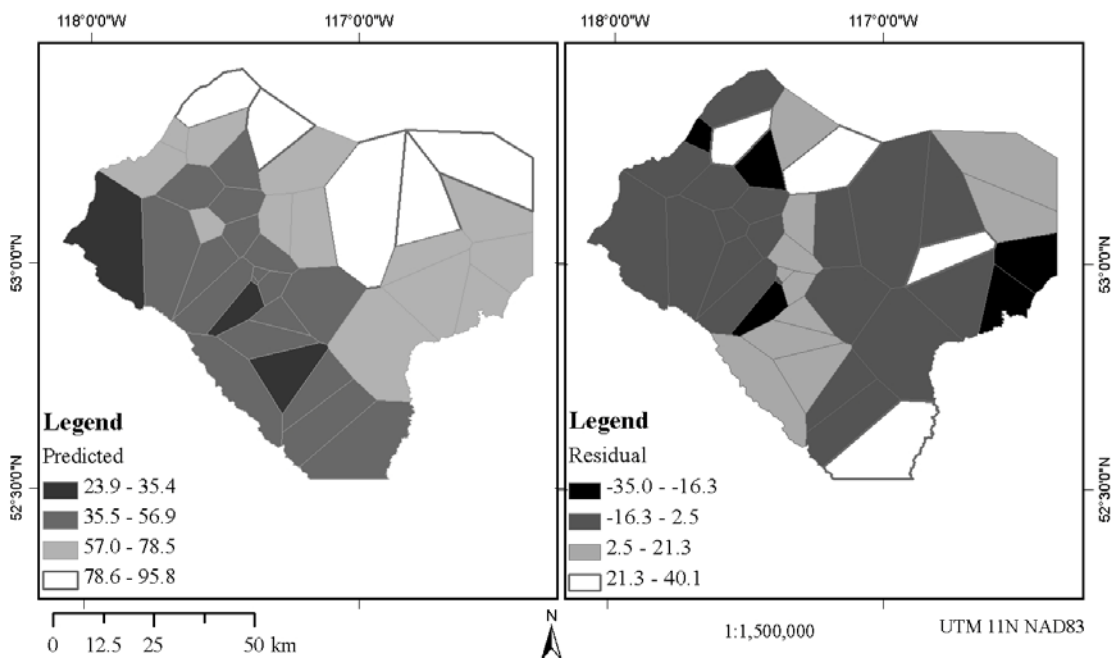
Figure 5-10. Predicted values and residuals of Model F

5.2.2 Spatial dependence tests

The residuals of model F were tested using the same spatial neighbourhoods as used in study area A. In addition, least cost distance neighbourhoods were tested since a cost surface was available for this area. Least cost distances were used to select nearest neighbours and define distance thresholds. Very few of these neighbourhoods were able to detect significant dependence. This is could be due to a conflicting pattern of both positive and negative spatial dependence.

Significant negative spatial dependence was detected using the second largest nearest neighbour distance of 16.684 km, shown in Figure 5-11. Nearest neighbourhoods and distance threshold neighbourhoods based on least cost distances computed from the cost surface did not find any significant spatial dependence. The residuals of model F were also tested for spatial dependence using the two overlap proportions (#1 and #2). Results were mildly significant for # 1. The Moran's *I* test results are summarised in the table below.

Table 5-16. Moran's *I* tests for distance threshold neighbours and overlap neighbours, study area B

Neighbourhood	Test	Observed Moran's I (I_{obs})	Pr ($I_{obs} > I$)
Distance threshold = 17 km	Normal	-0.20	0.94
	Exact		0.97
	Saddle		0.97
Overlap # 1	Normal	-0.05	0.77
	Exact		0.79
	Saddle		0.79

The distance threshold and overlap neighbourhoods are shown in Figure 5-11.
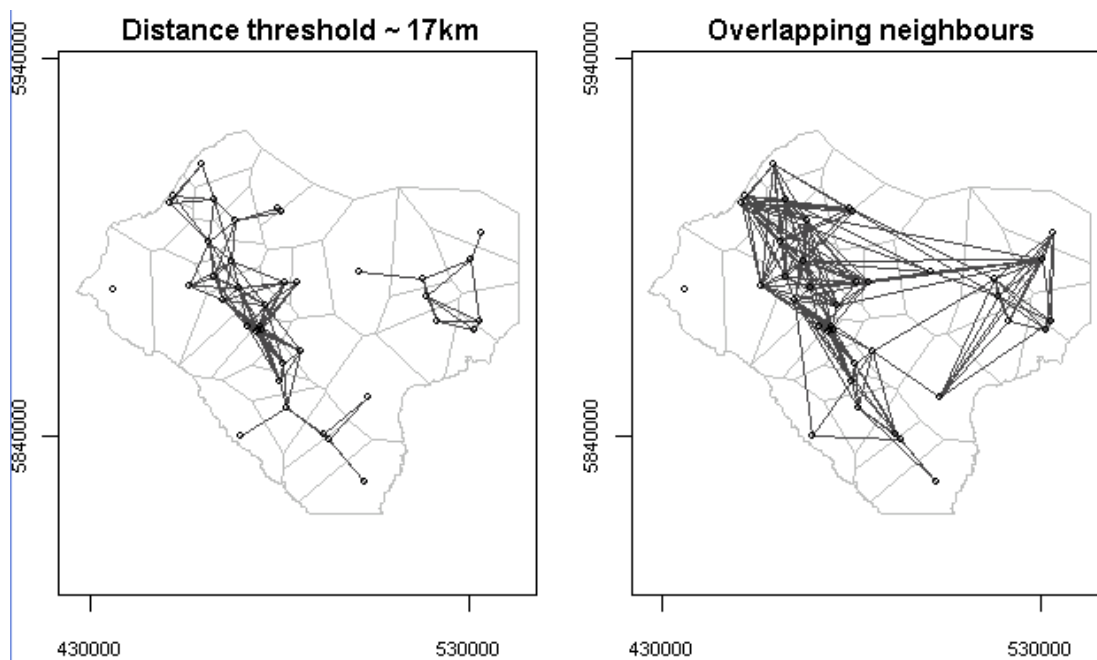
Figure 5-11. Distance threshold and Overlapping neighbours

The relationship between the distance threshold neighbourhood and residuals is explored further in Figure 5-12 which superimposes the neighbourhood over the residuals. This neighbourhood appears to capture the main line of heterogeneity in a north-south direction.
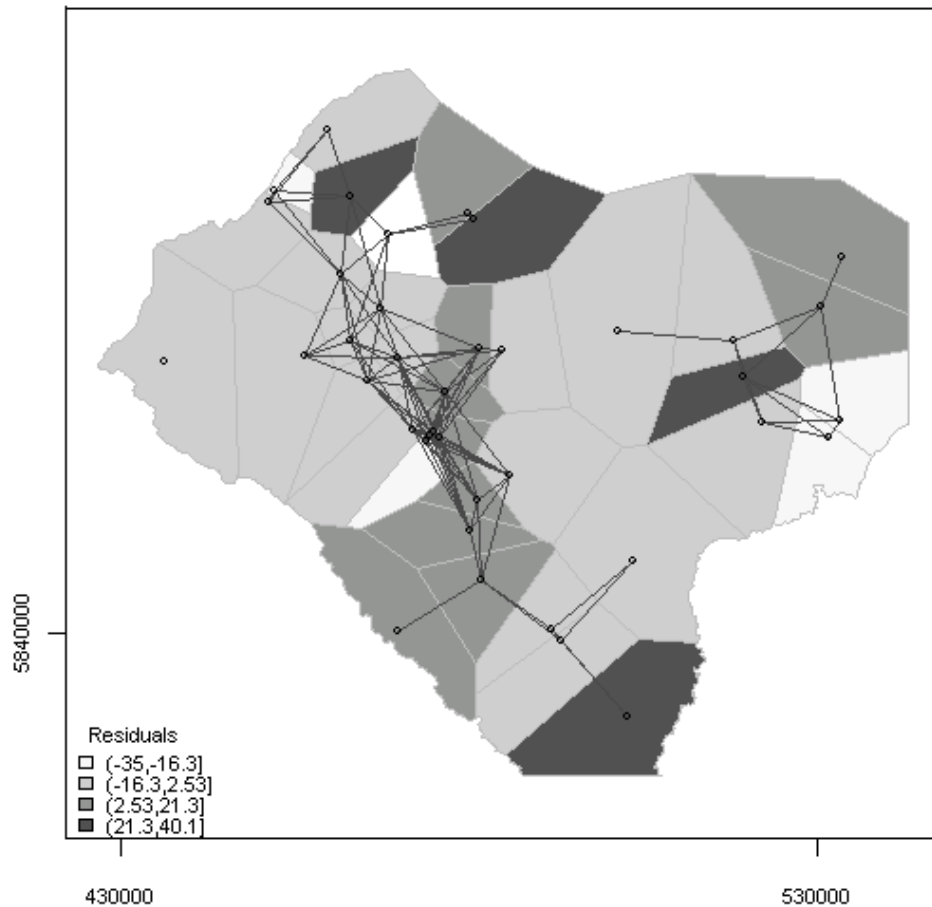
Figure 5-12. Residuals of model F and the distance threshold neighbourhood.

Using the family neighbourhood to test for spatial dependence, positive spatial dependence was found. The family neighbourhood unfortunately had seventeen bears without family relations due to incomplete data. If this dataset were complete, it is hypothesized that stronger spatial dependence would have been detected. The results are shown in Table 5-17.

Table 5-17. Moran's *I* tests for family neighbourhood weights

Neighbourhood	Test	Observed Moran's I (I_{obs})	Pr ($I_{obs} > I$)
Family neighbours - row standardised	Normal Exact Saddle	0.166	0.173 0.060 0.060
Family neighbours - variance stabilised	Normal Exact Saddle	0.166	0.151 0.048 0.046

The family-based neighbourhood is shown Figure 5-13. It is clear that it does not follow

a conventional spatial pattern.
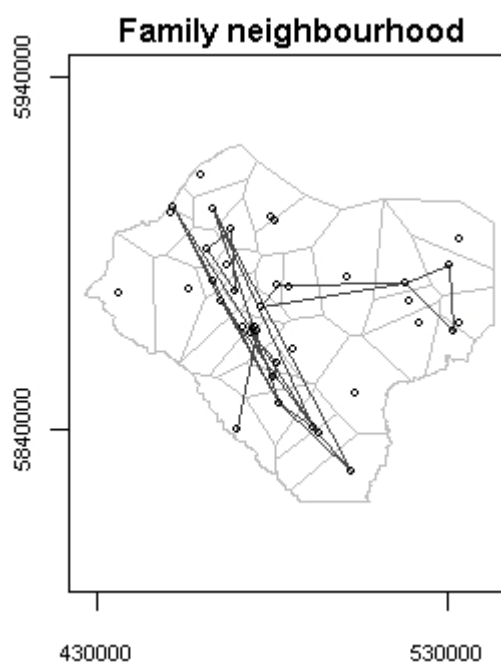
Figure 5-13. Spatial neighbourhood based on family kinship

5.2.3 Spatial autoregressive models

Using the distance threshold neighbourhood, the overlap neighbourhoods # 1 and # 2, and

the family neighbourhood, error, lag and Durbin models were developed and ranked

using AIC as before. The ranked models are shown in Table 5-18.

Table 5-18. Ranked spatial autoregressive models for study area B

Model	Type	Neighbourhood	k	AICc	Δ$_i$	w$_i$	Evidence ratio	Rho/ Lamda	p -value
Dist_thre_17km_err	error	Distance thresh = 16.7 km	6	336.36	0.000	0.433	1.000	λ = -0.737	0.010
Dist_thre_17km _lag	lag	Distance thresh = 16.7 km	6	337.04	0.680	0.308	1.405	ρ = -0.509	0.014
Ovlap1_lag	lag	Overlap # 1	6	338.77	2.410	0.130	3.337	ρ = -0.563	0.039
Ovlap2_lag	lag	Overlap # 2	6	339.19	2.830	0.105	4.116	ρ = -0.577	0.050
Dist_thre_17km Dur	Durbin	Distance thresh = 16.7 km	9	342.96	6.602	0.016	27.138	ρ = -0.574	0.008
Fam_Dur	Durbin	Family & weighted	9	346.53	10.172	0.003	161.733	ρ = 0.288	0.039
Ovlap2_Dur	Durbin	Overlap % 2	9	346.85	10.492	0.002	189.796	ρ = -0.579	0.059
Fam_Dur	Durbin	Family - binary	9	347.20	10.842	0.002	226.093	ρ = 0.262	0.060
Ovlap1_Dur	Durbin	Overlap % 1	9	347.60	11.242	0.002	276.151	ρ = -0.561	0.066

The top three models provide the best fit to the data. The error and lag models based on a distance threshold of ~ 17 km are very similar. The next most significant model is a lag model with the overlap # 1 neighbourhood. All of these models (except those based on the family neighbourhoods) have negative spatial parameters. Again negative spatial dependence is the dominant spatial pattern. It is interesting to note that the spatial parameters of the family neighbourhood models were positive. These models, however, have large Akaike differences and very evidence ratios, indicating that they are very poor models given the data.

Only the first two spatial autoregressive models (Dist_thre_17km_err and Dist_thre_17km_lag) provide a slight improvement in the AIC_c score for model F. AIC_c = 338.4 for model F and AIC_c = 336.36 and 337.04 for Dist_thre_17km_err and Dist_thre_17km_lag respectively. A comparison of the estimated parameters of the OLS model and the best spatial error and spatial lag model is given in Table 5-19.

Table 5-19. Comparison of the parameters of Model F and the best error and lag models

Model	Variable	Estimate	Std. Error	z - value	Pr(>|z|)	
OLS	Intercept	86.023	10.800	7.965	2.27E-09	***
Error – Dist thresh	Intercept	78.402	7.308	10.729	< 2.20E-16	***
Lag – Dist thresh	Intercept	118.778	15.252	7.788	6.88E-15	***
OLS	Slope	-2.210	0.564	-3.919	0.0004	***
Error – Dist thresh	Slope	-1.748	0.373	-4.689	2.74E-06	***
Lag – Dist thresh	Slope	-2.938	0.572	-5.133	2.86E-07	***
OLS – Dist thresh	OpMixFst	2.166	1.436	1.508	0.1404	
Error – Dist thresh	OpMixFst	2.859	0.928	3.080	0.0021	**
Lag – Dist thresh	OpMixFst	3.017	1.244	2.425	0.0153	*
OLS – Dist thresh	Northeast	-86.852	36.501	-2.379	0.0229	*
Error – Dist thresh	Northeast	-85.903	29.521	-2.910	0.0036	**
Lag – Dist thresh	Northeast	-87.414	31.282	-2.794	0.0052	**
Error – Dist thresh	Lambda	-0.737			0.0098	**
Lag – Dist thresh	Rho	-0.509			0.0144	*

In all cases, the error and lag models increase the significance of the explanatory variables, while the parameter values themselves do not change significantly. A visual comparison of the observed SLL100, the residuals of model F, and the predicted and residual values from model Dist_thre_17km_err can be seen in Figure 5-14. It appears that the error model more accurately predicts the observed SLL100 and the residuals are more randomly distributed in space in comparison to model F. The range of the residuals

also decreased from [-35.0 to 40.1] for model F to [-26.1 to 33.7] for

Dist_thre_17km_err.
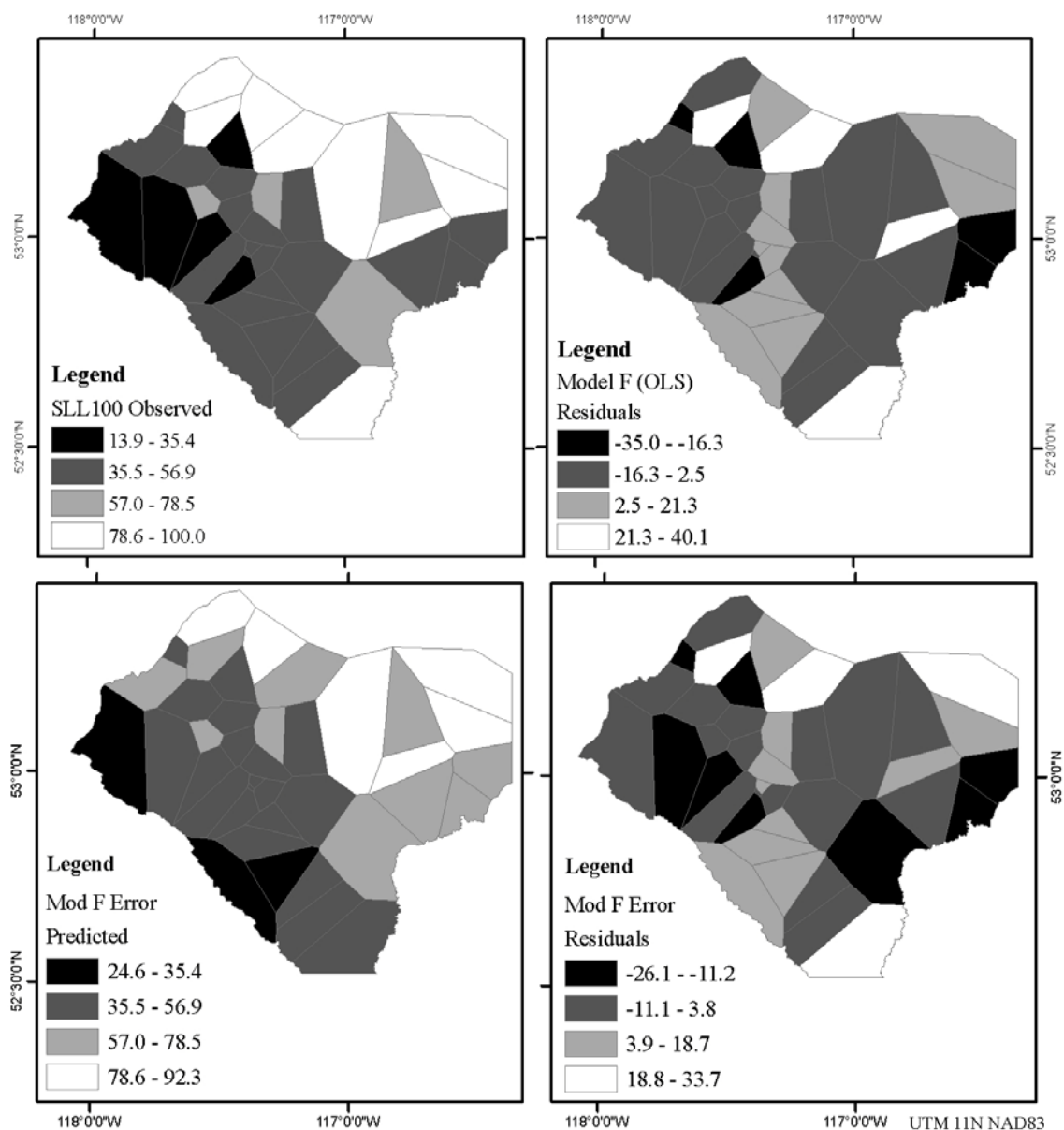
Figure 5-14. Comparison of observed SLL100, predicted SLL100 and residuals using model F and model Dist_thre_17km_err

Finally, a plot of residuals versus fitted values for the distance threshold neighbours and a

Q-Q plot reveal that the residuals are very close to normally distributed.
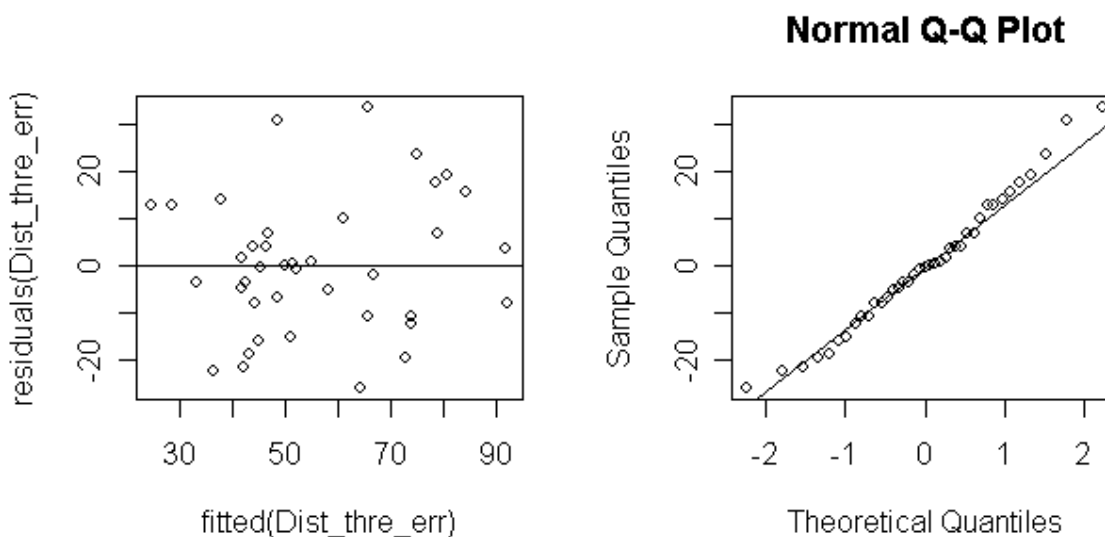
Figure 5-15. Diagnostics plots of residuals from model Dist_thre_17km_err

5.3 Discussion

5.3.1 Environmental variables

Slope was shown to be by far the most significant explanatory variable of the top models

for both the whole study area (A) and the subset area (B) (see Table 5-3, Table 5-4, Table

5-12, Table 5-13). In the OLS models, slope had a negative coefficient of – 1.7 for study

area A, and – 2.2 for study area B, and $p = 5e-5$ and $p = 4e-4$, respectively. The

significance of slope increased dramatically in the spatial autoregressive models while

the coefficient estimates remained similar (Table 5-11, Table 5-19).

Since slope is highly correlated with several other variables (see Table 5-2), it is

not likely to be driving body length directly. Slope is highly positively correlated with

elevation, herbaceous and shrubby vegetation, and distance away from roads and wells. It is negatively correlated with closed canopy, wetlands and regenerating forest. Therefore, while high elevation and steeply sloped areas are further away from disturbance features such as roads, wells and regenerating lands, i.e. clearcuts, the bears are smaller. Thus, it is more likely that reduced availability of high quality foods in these areas causes smaller body length, rather than stress.

It has been shown by Munro et al. (2006) that grizzly bears at higher elevations in the west-central Rockies eat nearly 2.5 times fewer ungulates than bears in the foothills. This is due to a much lower density of ungulates at the higher elevations. The eating of meat is well known to be associated with larger body size in grizzly bears (Schwartz, et al., 2003). Grizzly bears living at high elevations have to compensate by eating roots which are more prevalent in the alpine, subalpine and shrub habitats (Munro et al., 2006). However, the mountains have a lower abundance of food than the foothills due to their later green-up periods and earlier frosts in Fall (Munro et al,. 2006). Insects tend to occur in wet and regenerating forests (Munro et al., 2006), which are found at a greater abundance in the lower elevations as shown in this study. Nearly all food sources have a shorter period of availability in the mountains, including fruits, ungulates and insects (Munro et al., 2006).

SLL100 was also found to have a positive correlation with open deciduous forest and open mixed forest in study area A and B. These two variables are highly correlated with each other ($r = 0.9$), hence it can be assumed that the presence of one vegetation type indicates the presence of the other. In the OLS models, open deciduous forest has a positive coefficient estimate of 5.1 and $p = 0.01$, and open mixed forest, 2.2 and $p = 0.1$.

The significance of both variables increases in the spatial autoregressive models. These

forests offer bears fruits, another important component in their diets (Munro et al. 2006).

Distance to water was in the final OLS model for study area A with a coefficient

estimate of – 2.9 and $p = 0.06$. This coefficient became more significant in the spatial

autoregressive model, such that its probability decreased to 0.002. A negative correlation

indicates that the further grizzly bears are from major water sources such as rivers and

waterbodies, the smaller their body size. A larger distance could imply that these grizzly

bears are living in less desirable xeric habitats which have decreased vegetation

abundance and ungulate availability. It was shown by Munro et al. (2006) that most

ungulate kills by grizzlies were made in wet forests.

For the smaller study area, B, northeast aspect, was the third explanatory variable

in model F. It had a large negative coefficient (~86) with $p = 0.02$ in the OLS model. The

significance of this variable increased by a factor of 10 in the spatial autoregressive

model. Since northeast slopes are associated with xeric conditions (Strong, 1992), this

again could relate to the reduced availability of open, mixed forests and wet forests, and

insects, fruit and ungulates inhabiting these areas.

5.3.2 Spatial dependence tests

An examination of spatial dependence in SLL100 using Moran's *I* revealed strong

positive spatial dependence. The probability of the observed Moran's *I* was < 3e–7 for

several nearest neighbour weight matrices. This made further exploration of spatial

dependence in the residuals of OLS models necessary. It was important to determine

whether the environmental variables included within the OLS models could account for the spatial dependence in the dependent variable.

The residuals of the best model, E, for study area A, were found to have significant negative spatial dependence using a variety of neighbourhoods. Thus, the explanatory variables accounted for the positive dependence, thereby revealing negative dependence. Using three and five nearest neighbours (Figure 5-4 and Table 5-7) the probability of Moran's I was less than 0.05. The distance threshold neighbourhood of 73 km also found significant negative spatial dependence with $p \sim 0.95$ (see Table 5-8 and Figure 5-5). The scales of these three neighbourhoods were similar as shown in Table 5-9. Neighbourhood distances ranged from 0.3 km to 66 km, 73 km and 92 km for the three NN, distance threshold and five NN neighbourhoods respectively. These neighbourhoods seem to distinguish three distinct population groups which are separated by Highway 16 and Highway 11 (Figure 5-4). The median scale of these neighbourhoods also corresponds to the distance threshold neighbourhood of study area B, with a distance threshold of 17 km.

The spatial weight matrices based on the proportion of overlap were not found to be significant, nor the family weights. Overlap neighbourhoods may not have been significant for two reasons. 1) Those bears that were close to each other but not overlapping, were not considered as neighbours. 2) The method of home range overlap was not computed in the most appropriate manner. Due to the biases in home range area caused by KDE estimation, it may have been better to compute a weighted proportion of overlap based on the home range utilisation grids.

The family neighbourhood was unable to detect anything in study area A due to the fact that the database was largely incomplete.

In study area B, significant negative spatial dependence ($p \sim 0.95$) was revealed by the neighbourhood of observations within 17 km of each other. The overlap neighbour weights # 1 and # 2 also found weak negative spatial dependence with $p \sim 0.78$ and $p \sim 0.65$ respectively. Least cost distance neighbours also did not find spatial dependence. Positive spatial dependence was detected for study area B using the family neighbourhood. Moran's I was observed to be 0.17 with a significance of $p = 0.04$ using the variance-stabilised version of the weight matrix and the exact and Saddlepoint tests.

The negative spatial autocorrelation found in both study areas, is difficult to explain without further investigation. It is possible that it is caused by some form of competitive process between bears which causes differential access to food, or one or more missing variables that is/are naturally heterogeneous.

5.3.3 Spatial autoregressive models

Promising spatial weight matrices (described in the previous section) were used to develop spatial error, lag and Durbin autoregressive models. It was found that several of the spatial autoregressive models provided a significant improvement in the AIC scores over the original OLS models (Table 5-3 and Table 5-10, and Table 5-12 and Table 5-18). Also, environmental parameters increased in significance in all cases (Table 5-11 and Table 5-19). This is to be expected as negative spatial dependence tends to cause the variance to be overestimated in OLS models (Anselin & Bera, 1998). The estimated spatial parameters, ρ and λ, were negative in all of the models except models using the

family neighbourhood. However, the family neighbourhood models were very weakly supported according to their Akaike weights. It was found that the top spatial models improved the actual predicted values, reduced the range of the residuals and resulted in a random spatial distribution of the residuals.

Spatial error models were found to dominate the top models of study area A (Table 5-10), while spatial lag models were most common in the top models of study area B (Table 5-18). At this stage it is difficult to know why a particular spatial model is the best as little is currently known about the spatial processes that may be operating.

5.4 Summary

This chapter presented the major findings of this research. Grizzly bear home ranges were delineated using kernel density estimation and used to compute environmental variables for each bear (Chapter 4). Using these variables, OLS regression models were developed to relate grizzly bear straight-line length to the environmental variables. Slope, open mixed forest, open deciduous forest, distance to water, and northeast aspect were found to be significant variables.

A variety of spatial neighbourhood weight matrices were developed and used to test the residuals of the OLS models for spatial dependence. Significant negative spatial dependence was found in the residuals of the OLS models. In study area A, three NN, five NN, and distance threshold neighbours (within 73 km) were best able to detect spatial dependence. In study area B, significant spatial dependence was detected using a distance threshold neighbourhood of 17 km.

Spatial error, lag and Durbin autoregressive models were developed using the significant spatial neighbourhoods. These models were reviewed in terms of the significance of the estimated spatial parameters, the significance of the environmental parameter estimates and the AIC scores. It was found that the top spatial autoregressive models had significant negative spatial parameters, and that there were several improvements over the OLS models. The AIC scores decreased from the OLS models, the range of the residuals decreased and spatial dependence was removed from the residuals.

Five nearest neighbours and neighbours within a distance threshold of 73 km were best able to characterise the spatial dependence in the data and improve the regression models for the whole study area. These neighbourhoods seem to capture three grizzly bear population units which are known to be genetically distinct. For the smaller subset area, a distance threshold of 17 km provided the best neighbourhood for modelling negative spatial dependence and improving regression models.

Chapter Six: Conclusions

This chapter summarises the main findings as they relate to the objectives presented in chapter one. It also documents contributions to knowledge, and provides suggestions for future research.

6.1 Summary of findings

6.1.1 Spatial dependence in straight-line length

The hypothesis that positive spatial dependence exists within the straight-line length dataset was tested using Moran's *I* and found to be highly significant using a variety of spatial neighbourhoods. Using thirteen nearest neighbours, the maximum spatial dependence of $I = 0.16$ was observed with the one-tailed probability $= 1.6e\text{-}7$.

6.1.2 Relationship between transformed straight-line length and environmental variables

Straight-line length (SLL) measures the skeletal length of grizzly bears. The natural logarithm of SLL has a positive linear correlation with the natural logarithm of total body mass (Cattet et al. 2002). SLL was chosen as the variable of interest since increased body size is associated with increased reproductive success and population density (Hilderbrand et al., 1999). In this study SLL100 was transformed to a value between 0 and 1 in order to remove statistical differences between reproductive groups and allow easier interpretation of low values as poor and higher values as good. The transformed

SLL - SLL100 - was found to be negatively correlated with slope, positively correlated with the percentage of open deciduous forests and negatively correlated with the distance to water for the whole study area (A). For the smaller study area, B, SLL100 was found to be negatively correlated with slope, positively correlated with the percentage of open mixed forest and negatively correlated with northeast aspect.

Slope was by far the most significant variable in all models in both study areas, yet slope is not likely to influence body size directly. Rather, it is highly correlated with increased elevation and, therefore, decreased food availability. The Subalpine and Alpine Subregions become productive later and frosts tend to occur earlier in the Fall than in the foothills. Munro et al. (2006) also documented that bears in the foothills consumed more than two times more ungulates than those at higher elevations. It is well established that the consumption of meat is related to the body size of grizzly bears (Hildebrand et al., 1999; Schwartz et al., 2003), and, thus, a reduction in meat availability at higher elevations should result in smaller body sizes. Furthermore, regenerating, wet, open, and mixed forests were negatively correlated with slope and elevation and are known to provide insects and fruits (Munro et al., 2006) which are good sources of food for grizzly bears.

Distance to water and slopes facing northeast may also measure the availability and quality of food. Areas further away from rivers and waterbodies, as well as slopes with a northeast aspect, are drier and therefore less likely to have areas of open, mixed and wet forests.

6.1.3 Testing for spatial dependence in the OLS residuals and spatial neighbourhoods

Choice of spatial neighbourhood configuration was found to determine the ability of

Moran's *I* tests to detect significant spatial dependence. Many of the neighbourhoods

used in this study (proportion overlap, family neighbourhood for area A, least cost

distance neighbourhoods for area B) were unable to identify spatial dependence in the

residuals of the OLS models. Significant negative spatial dependence was detected for

area A using nearest neighbours and distance threshold neighbourhoods. Negative spatial

dependence was also found in study area B using distance threshold neighbours. In area

B significant positive spatial dependence was found using the family neighbourhood.

However, this neighbourhood had seventeen isolated observations and, thus, these results

should be viewed with caution.

It was surprising to find negative spatial dependence in the residuals of the OLS

models when strong positive spatial dependence had been identified in the dependent

variable. However, this surprising result is not completely implausible. Griffith (2006)

discusses the presence of hidden negative autocorrelation despite test results of

significance positive autocorrelation. In reality, most spatial patterns exhibit positive and

negative autocorrelation at a local scale, but positive spatial dependence usually

dominates using global statistics (Griffith, 2006). This interesting result warrants further

investigation to uncover the causes of this pattern. At this point the following possible

explanations are offered:

1)   Landscapes are heterogeneous entities consisting of a mosaic of patches at a

variety of scales (Forman, 1995). Natural and human disturbances such as

fires and clear cutting create new patches and increase heterogeneity in the landscape (White & Picket, 1985). Thus, negative spatial dependence could reflect the natural patchiness/heterogeneity of one or more missing variables in the model.

2)   It is possible that some bears are better at preying on ungulates than other bears, thus making their overall body length and size bigger than average.

3)   Perhaps an appropriate description or representation of the spatial process has not yet been discovered. Many of the approaches used here are largely naïve, and those that were more logical such as family neighbourhoods and least cost neighbours, had insufficient data to test conclusively.

4)   The data may have been over-smoothed in the estimation of home ranges and the averaging of health variables therefore resulted in an overly smoothed signal that is difficult to identify.

5)   The dataset has too few observations, making it vulnerable to spurious test results. It may not be possible to detect the overall pattern of the dataset with these small sample sizes and the unusual elongated arrangement of observations in a northwest – southeast direction.

It is of interest that the family neighbourhood applied to study area B was the only neighbourhood to show significant positive spatial dependence. It was expected that genetic relations could generate similarity in related bears, i.e., large parents produce large offspring. It was also interesting to note that this neighbourhood did not exhibit a clear spatial pattern that resembled other spatial configurations tested here.

6.1.4 Spatial autoregressive models

Due to the detection of significant spatial dependence in the residuals, it was deemed

necessary to develop spatial autoregressive models and compare these to the OLS

models. It was found that the spatial autoregressive models provided a substantial

improvement over the OLS models when the appropriate spatial weight matrix and form

of autoregressive model (error, lag or Durbin) were used. In this study, three and five

nearest neighbours and the distance neighbourhood (73 km) produced the best results

study area A, while the top model for study area B was based on the distance threshold

neighbourhood (17 km). For study area A, the AIC score decreased dramatically from

the OLS models. For both study areas the autocorrelation in the residuals was removed,

the range of the residuals decreased and the significance of the environmental parameters

increased. This was to be expected as negative spatial dependence tends to cause the

variance of estimates to be over-estimated in OLS models (Schabenberger & Gotway,

2005). In this study the estimated spatial parameters, ρ (lag dependence) and λ (error

dependence), were negative in all models, except those models using the family

neighbourhood. This result corresponded to the Moran's *I* tests using the family

neighbourhood. It should be noted that the family models were not well supported by the

data according to the Akaike weights and evidence ratios.

In study area A spatial error models were the top models according to AIC scores,

Akaike weights and evidence ratios. However, for the smaller area, B, spatial lag models

best reflected the data. It is difficult to understand why a particular form of the spatial

model is superior to another since the spatial processes that may be operating are not well understood at this stage.

It can be concluded that significant negative spatial dependence was present in the data and the incorporation of an appropriate spatial weights matrix within regression models improved the explanatory power of those models.

6.1.5 Evaluation of spatial weights matrices

For study area A, Moran's *I* tests revealed the most significant *p*-values for three NN, five NN and the distance threshold neighbourhood of 73 km. These neighbourhoods also led to the best spatial autoregressive models in terms of the AIC scores. The scale of these three neighbourhoods was very similar and separate three spatial groups of observations. These groups in fact correspond to the FRI population units shown in Figure 4.1 which are considered to be genetically distinctive (Stenhouse, 2007).

All of the other tested neighbourhoods were unsuccessful for the larger area. No significant spatial dependence was identified when neighbourhood weights were derived from the proportion of home range overlap. There are two possible explanations for this. Bears that were close to each other but did not have any core home range overlap were not considered to be neighbours, despite the fact that they may have been living adjacent to each other. A second cause could be that the proportion of core home range overlap was not computed in a suitable manner. Due to bias in home range assessment resulting from the method employed for this work, i.e., kernel density estimation, it may have been

better to compute the weighted proportion of overlap based on the home range density grids generated from the KDE process.

The family neighbourhood did not reveal spatial dependence in study area A. This was most likely due to the fact that over 50 % of the observations had no neighbours due to a lack of data. Similarly, the network neighbours were unable to detect spatial dependence.

In study area B, significant negative spatial dependence was only revealed by the neighbourhood of observations within 17 km of each other. Interestingly, significant positive spatial dependence was detected for this area using the family neighbourhood. This corresponds with our expectation of the size of offspring being partially determined by the size of the parents.

6.2 Contributions to knowledge

This research demonstrated that spatial dependence should be considered when developing regression models that relate grizzly bear health to environmental variables in the Alberta Rocky Mountains and foothills. This may be applicable to other wildlife studies which sample individuals from the same population and study area. This research showed that although the parameter estimates themselves did not vary substantially between the OLS and spatial autoregressive models, the significance of these parameters was greatly affected. This suggests that inferences from OLS models could be flawed. In particular, a variable selection approach such as backward deletion may delete the incorrect variables based on the significance of parameters in OLS models. To improve

our understanding of which variables affect grizzly bear health, it is essential that important variables are correctly identified.

Another important finding is that the selection of an appropriate spatial weight matrix is essential for detecting spatial dependence that may be present in the data. It is necessary to test a variety of neighbourhoods and weights since theories regarding the nature of spatial dependence may be naive, or inaccurately formulated and measured. Instead of finding positive spatial dependence as was expected, negative dependence was detected. This indicates that our understanding of the key spatial processes and patterns in this context may be misinformed. The non-spatial neighbourhood, based on kinship, was the only neighbourhood to detect positive spatial dependence. This suggests that a substantive theory can improve our ability to derive spatial neighbourhoods and that it is necessary to think beyond simple configurations of space.

6.3 Future research

The following suggestions are made for further research in health-environment regression modelling.

Explore alternative means of home range delineation

The delineation of an appropriate home range is crucial since the home range determines what features are considered for analysis. If the home ranges are over-estimated, the data will be overly smoothed, and if they are under-estimated, important factors may be excluded. There are many other new methods available for home range estimation such as local convex hull and Brownian-bridge models which may be more

suitable for this study. Steiniger et al. (2010), Laver and Kelly (2008) and Powell (2000) can be referenced for a review of these methods.

Explore other means of defining centroids

This research used the point of maximum utilisation of the home range utilization grids to compute nearest neighbours, distance neighbours and network neighbours. Other centroids such as the centre of gravity should be investigated to see what effect this would have on neighbourhood configurations and the detection of spatial dependence.

Explore the use of other health variables such as Body Condition Index

There are several other measures of health, or some combination of these, that could be explored for use as the dependent variable in regression models. In chapter four, body condition index (BCI) was identified as a potentially useful measure of health which warrants further investigation

Alternative methods for computing the proportion of home range overlap as a measure of covariance between nearby observations

The method used in this research to compute the proportion of overlap between home ranges was based on a simple intersection of the core home range polygons. However, due to biases that are likely present in the estimated home ranges, this may not reflect the true overlap. It is suggested that the density grids generated from the KDE estimation process be used to estimate home range overlap as a weighted proportion.

Neighbourhoods based on family relationships

The family relationship neighbourhood warrants further investigation given its suggestion of positive dependence in the data. As more DNA studies are completed by the FRI and the family trees of the grizzly bears become more complete, it will be possible to test for spatial dependence using this neighbourhood more reliably.

Local Indicators of Spatial Association

Maps of the OLS residuals suggested that there were clusters of both positive and negative spatial dependence. Global measures of spatial dependence, such as Moran's *I,* only measure the average spatial dependence in the dataset, and hence local variations may be hidden (Anselin, 1995). It is therefore recommended that local indicators of spatial association (LISA) be investigated as an alternative means for testing and exploring spatial dependence within the dataset (Anselin, 1995).

Study the effects of environmental change on health

Several datasets of environmental change over the past decade have been created by the FRI. This offers the possibility of matching the available GPS and health data with the specific environmental conditions at the time that they were acquired. In this research it was decided to take the average of the health data and merge annual GPS datasets together to mitigate the effects of the temporal mismatch between the GPS datasets and the health measurements. This may have over-smoothed the data thereby reducing the overall fit of the model and hiding spatial patterns. Other approaches, which take greater advantage of the environmental change data that is now available, should be investigated. This would be an interesting area of research that allows more accurate quantification of the effects of changing environmental conditions on grizzly bear health.

Investigate the causes of observed spatial dependence

Finally, the motivation for modelling spatial dependence is not only to improve regression models, but also to identify and hopefully explain the causes of spatial dependence. This can reveal interesting ecological or behavioural processes which may provide useful information for management decisions. For example, the observed negative spatial dependence may have been caused by the heterogeneity of the landscape, which is exacerbated by human activities such as gas extraction, clearcutting and the construction of access roads. In the future these activities could be managed to reduce unnaturally patchy and fragmented landscapes which degrade habitat quality.

References

Achuff, P. L. (1984). Cardinal Divide Area; Resource Description and Comparison with other Rocky Mountain Areas *Natural Areas Technical Report*. Alberta.

Akaike, H. (1973). Information theory as an extension of the maximum likelihood principle. In B. N. Petrov & F. Csaki (Eds.), *Second International Symposium on Information Theory*. Budapest: Academiai Kiado.

Anselin, L. (1984). Specification tests on the structure of interaction in spatial econometric models. *Regional Science Association, 54*, 165 - 182.

Anselin, L. (1990). What is special about spatial data? Alternative perspectives on spatial data analysis. In D. A. Griffith (Ed.), *Spatial Statistics, Past, Present and Future* (pp. 63 - 77): Ann Arbor, ML: Institute of Mathematical Geography.

Anselin, L. (1995). Local Indicators of Spatial Association - LISA. *Geographical Analysis, 27*(2), 93 - 115.

Anselin, L., & Bera, A. (1998). *Spatial Dependence in Linear Regression Models with an Introduction to Spatial Econometrics*. New York: Marcel Dekker.

Arthur, S. M., & Schwartz, C. C. (1999). Effects of sample size on accuracy and precision of brown bear home range models. *Ursus, 11*, 139-148.

Austin, M. (2007). Species distribution models and ecological theory: A critical assessment and some possible new approaches. *Ecological Modeling, 200*(1), 19.

Bekoff, M., & Mech, L. D. (1984). Simulation analyses of space use: home range estimates, variability and sample size. *Behavior Research Methods, Instruments and Computers, 16*, 32 - 37.

Belant, J. L., & Follmann, E. H. (2002). Sampling considerations for American black and brown bear home range and habitat use. *Ursus, 13*, 299-315.

Benn, B., & Herrero, S. (2002). Grizzly Bear Mortality and Human Access in Banff and Yoho National Parks, 1971-98. *Ursus, 13*, 213-221.

Blanchard, B. M. & Knight, R. R. (1991). Movements of yellowstone grizzly bears. *Biological Conservation, 58* (1)*, 41 - 67

Brown, D. E. (1985). *The grizzly in the southwest.* Norman: University of Oklahoma Press.

Brunsdon, C., Fotheringham, A. S., & Charlton, M. E. (1996). Geographically Weighted Regression: A Method for Exploring Spatial Nonstationarity. *Geographical Analysis, 28*, 281-198.

Burnham, K. P., & Anderson, D. R. (1998). *Model selection and inference: a practical information-theoretic approach*. New York: Springer.

Burrough, P. A., & McDonnell, R. A. (1998). *Principals of Geographic Information Systems*: Oxford University Press.

Burt, W. H. (1943). Territoriality and home range concepts as applied to mammals. *Journal of Mammalogy, 24*(3), 346-352.

Calhoun, J. B., & Casby, J. U. (1958). Calculation of home range and density of small mammals. *U.S. Public Health Monograph, 55*, 24 pp.

Cattet, M., Vijayan, J.D. & Janz, D. (2007). Chapter 6: Wildlife Health. In G. B. Stenhouse & K. Graham (Eds.), *Foothills Research Institute Grizzly Bear Program 2007 Annual Report* (pp. 144-157). Hinton, Alberta: Foothills Research Institute.

Cattet, M., Caulkett, N. A., Obbard, M. E., & Stenhouse, G. B. (2002). A body-condition index for ursids. *Canadian Journal of Zoology, 80*, 1156-1161.

Cliff, A. D., & Ord, J. K. (1973). *Spatial Autocorrelation*. London: Pion.

Cliff, A. D., & Ord, J. K. (1981). *Spatial Processes Models and Applications*. London: Pion.

Cordy, C. B., & Griffith, D. A. (1993). Efficiency of least squares estimators in the presence of spatial autocorrelation. *Communications in Statistics - Simulation and Computation, 22*(4), 1161 - 1179.

Craighead, J. J., & Mitchell, J. A. (1982). Wild mammals of North America. In J. A. Chapman & G. A. Feldhamer (Eds.), *Wild mammals of North America*. Baltimore: John Hopkins University Press.

Cressie, N. A. C. (1993). *Statistics for Spatial Data*. New York: Wiley.

Doreian, P. (Ed.). (1981). *Estimating Linear Models with Spatially Distributed Data* (Vol. 9). San Francisco: Jossey - Boss.

Elsasser, T. H., Klasing, K.C., Filipov, N. & Thompson, F. (2000). The Metabolic Consequences of Stress: Targets for Stress and Priorities of Nutrient Use. In G. P. Moberg & J.A. Mench (Eds.), *Biology of Animal Stress: Basic Principles and Implications for Animal Welfare*. New York, U.S.A.: CABI Publishing.

Faraway, J. J. (2002). *Practical regression and anova using R*.

Forman, R. (1995). Some general principals of landscape and regional ecology. *Landscape Ecology, 10*(3), 133 - 142.

Fortin, M. J., & Dale, M. R. T. (2005). *Spatial Analysis: A Guide for Ecologists*. Cambridge N.Y.: Cambridge University Press.

Gabriel, K. R., & Sokal, R. R. (1969). A new statistical approach to geographic variation analysis. *Systematic Ecology, 18*, 259–270.

Geary, R. C. (1954). The Contiguity Ration and Statistical Mapping. *The Incorporated Statistician, 5*(3), 115 - 145.

Getis, A., & Ord, J. K. (1992). The analysis of spatial association by use of distance statistics. *Geographical Analysis, 24*, 189–206.

Golberg, M. A., & Cho, H. A. (2004). *Introduction to Regression Analysis*. Southampton, Boston: WIT Press.

Government of Alberta. (2009). *Five-year grizzly bear population study complete*.

Government of Canada. (2002, 2009-11-06). Mammals (terrestrial) Bear, Grizzly. *Wildlife Species Search.* Retrieved 2010-01-20, 2010, from http://www.cosepac.gc.ca/eng/sct1/searchdetail_e.cfm

Government of Canada. (2009). About COSEWIC, 2010, from http://www.cosewic.gc.ca/eng/sct6/index_e.cfm

Griffith, D. A. (2006). Hidden Negative Spatial Autocorrelation. *Journal of Geographical Systems, 8(4)*, 335-355.

Griffith, D. A. (Ed.). (1996). *Introduction: The Need for Spatial Statistics*. Boca Raton: CRC Press.

Griffith, D. A., & Layne, L. (1999). *A casebook for spatial statistical data analysis*. New York, Oxford: Oxford University Press.

Haining, R. P. (2003). *Spatial Data Analysis : Theory and Practice*. Cambridge: Cambridge University Press.

Harris, S., Cresswell, W. J., Forde, P. G., Trewhella, W. J., Woollard, T., & Wray, S. (1990). Home-range analysis using radio-tracking data - a review of problems and techniques particularly as applied to the study of mammals. *Mammal Review, 20*((2/3), 97-123.

Hepple, L. W. (1976). A maximum-likelihood model for econometric estimation with spatial series. In I. Masser (Ed.), *Theory and practice in regional science.* (pp. 90 - 104). London: Pion.

Hildebrand, G. V., Schwartz, C. C., Robbins, C. T., Jacoby, M. E., Hanley, T. A., Arthur, S. M., et al. (1999). The importance of meat, particularly salmon, to body size, population productivity, and conservation of North American brown bears. *The Canadian Journal of Zoology, 77*, 132 - 138.

Hilderbrand, G., Schwartz, C., Robbins, C., Jacoby, M., Hanley, T., Arthur, S., et al. (1999). Importance of meat, particularly salmon, to body size, poulation productivity, and conservation in North American brown bears. *Canadian Journal of Zoology, 77*, 132 - 138.

Hjelle, Ø., & Daehlen, M. (2006). *Triangulations and applications*. Berlin; New York: Springer-Verlag.

Horner, M. A., & Powell, R. A. (1990). Internal structure of home ranges of black bears and analyses of home range overlap. *Journal of Mammalogy, 71*, 402-410.

IUCN Standards and Petitions Subcommittee. (2010). Guidelines for Using the IUCN Red List Categories and Criteria Version 8.0. Prepared by the Standards and Petitions Subcommittee in March 2010.

Janz, D., Cattet, M., Viijan, M., & Stenhouse, G. (2006). Chapter 5: Animal Health. In G. Stenhouse & K. Graham (Eds.), *Foothills Research Program 2006 Annual Report* (pp. 87). Hinton, Alberta.

Kaluzny, S. P., Vega, S. C., Cardoso, T. P., & Shelly, A. A. (1998). *S+ Spatial Stats User's Manual for Windows and Linux*. New York: Springer.

Laskin, D., McDermid, G., Pape, A., Wunderle, A., & Klassen, J. (2006). Chapter 2: Remote sensing and habitat map production 2006. In G. Stenhouse & K. Graham (Eds.), *Foothills Model Forest Grizzly Bear Research Program 2006* (pp. 87). Hinton, Alberta.

Laver, P. (2005). Kernel Home Range Estimatino for ArcGIS, using VBA and ArcObjects. User Manual (Beta v.2 - 7): Department of Fisheries and Wildlife Services, Virginia Tech.

Laver, P., & Kelly, M. J. (2008). A critical review of home range studies. *Journal of Wildlife Management, 72*(1), 290 - 298.

Linke, J., McDermid, G. J., Laskin, D. N., McLane, A. J., Pape, A. D., Cranston, J., et al. (2009). A disturbance-inventory framework for flexible and reliable landscape monitoring. *Photogrammetric Engineering and Remote Sensing, 75*(8), 981 - 995.

Linke, J., McDermid, G. J., Pape, A. D., McLane, A. J., Laskin, D. N., & Hall-Beyer, M. (2009). The influence of patch delineation mismatches on multi-temporal landscape pattern analysis. *Landscape Ecology, 24*(2), 157 - 170.

Linke, J., McLane, A., Laskin, D., & Cranston, J. (2008). Chapter 2: Annual Changes in landcover, vegetation, and landscape structure in BMAs 3 and 4, 1998 - 2005. In

G. Stenhouse & K. Graham (Eds.), *Foothills Research Institute Grizzly Bear Program 2007 Annual Report* (pp. 204). Hinton, Alberta.

Loftin, C., & Ward, S. K. (1983). A Spatial Autocorrelation Model of the Effects of Population Density on Fertility. *American Sociological Review, 48*(1), 121 - 128.

Mace, G. M., Collar, N. J., Gaston, K. J., Hilton-Taylor, C., Akcakaya, H. R., Leader-Williams, N., et al. (2008). Quantification of Extinction Risk: IUCN's System for Classifying Threatened Species. *Conservation Biology, 22*(6), 1424-1442.

Mattson, D., J., & Merrill, T. (2002). Extirpations of Grizzly Bears in the Contiguous United States. *Conservation Biology, 16*(4), 1123-1136.

McDermid, G., Collingwood, A., Cranston, J., He, Y., Hird, J., Franklin, S., et al. (2008). Chapter 4: Remote Sensing Mapping and Research Update. In G. B. Stenhouse & K. Graham (Eds.), *Foothills Research Institute Grizzly Bear Program 2008 Annual Report* (pp. 204). Hinton, Alberta.

McDermid, G., Collingwood, A., Cranston, J., He, Y., Hird, J., Franklin, S., et al. (2009). Chapter 4: Remote Sensing Mapping and Research Update. In G. B. Stenhouse & K. Graham (Eds.), *Foothills Research Institute Grizzly Bear Program 2008 Annual Report* (pp. 204). Hinton, Alberta.

McDermid, G. J., Linke, J., Pape, A. D., Laskin, D. N., McLane, A. J., & Franklin, S. E. (2008). Object-based approaches to change analysis and thematic map update: challenges and limitations. *Canadian Journal or Remote Sensing, 34*(5), 462 - 466.

McLellan, B. N. (1985). Use availability analysis and timber selection by grizzly bears. In G. Contreras & K. Evans (Eds.), *Proceedings of the grizzly habitat symposium,*

Missoula, Montana (pp. 163 - 166). Ogden, UT: U.S. Forest Service General Technical Report.

McLellan, B. N. (1998). Maintaining Viability of Brown Bears along the Southern Fringe of Their Distribution. *Ursus, 10*, 607-611.

McLellan, B. N., & Hovey, F. W. (2001). Natal dispersal of grizzly bears. *Canadian Journal of Zoology, 79*(5), 838–844.

Messner, S. F., & Anselin, L. (2004). Spatial Analyses of Homicide with Areal Data. In M. F. Goodchild & D. G. Janelle (Eds.), *Spatially Integrated Social Science* (pp. 127 - 144). Oxford: Oxford University Press.

Moberg, G. P., & Mench, J. A. (Eds.). (2000). *Biology of Animal Stress: Basic Principles and Implications for Animal Welfare*. New York, U.S.A.: CABI Publishing.

Mohr, C. O. (1947). Table of Equivalent Populations of North American Small Mammals. *American Midland Naturalist, 37*(1), 223 - 249.

Montgomery, D. C., & Peck, E. A. (1982). *Introduction to linear regression analysis*. New York: Wiley.

Moran, P. A. P. (1950). Notes on Continuous Stochastic Phenomena. *Biometrika, 37*(1/2), 17-33.

Munro, R. H. M., Nielsen, S. E., Price, M. H., Stenhouse, G. B., & Boyce, M. S. (2006). Seasonal and diel patterns of grizzly bear diet and activity in West-Central Alberta. *Journal of Mammalogy, 87*(6), 1112–1121.

Nagy, J. A., & Haroldson, M. A. (1990). *Comparisons of some home range and population parameters among four grizzly bear populations in Canada*. Paper presented at the International Conference on Bear Research and Management.

Nathan, R., Getz, W. M., Revilla, E., Holyoak, M., Kadmon, R., Saltz, D., et al. (2008).
A movement ecology paradigm for unifying organismal movement research.
PNAS. *PNAS, 105*(49), 19052-19059.

Natural Regions Committee. (2006). Natural regions and subregions of Alberta. In D. J.
Downing & W. W. Pettapiece (Eds.).

Nielsen, S. E., Boyce, M. S., Gordon, B. S., & Munro, R. H. M. (2002). Modeling
Grizzly Bear Habitats in the Yellowhead Ecosystem of Alberta: Taking
Autocorrelation Seriously. *Ursus, 13*, 45-56.

Nielsen, S. E., Stenhouse, G. B., & Boyce, M. S. (2006). A habitat-based framework for
grizzly bear conservation in Alberta. *Biological Conservation, 130*, 217-229.

Odland, J. (1988). *Spatial Autocorrelation*. Newbury Park: Sage Publications.

Okabe, A., Boots, B., & Sugihara, K. (1992). *Spatial Tesselations: Concepts and
Applications of Voronoi Diagrams*. New York: Wiley.

Ord, K. (1975). Estimation methods for models of spatial interaction. *Journal of
American Statistical Association, 70*, 120- 126.

Paquet, P., & Hackman, A. (1995). *Large carnivore conservation in the Rocky
Mountains*. Toronto, On.: World Wildlife Fund.

Powell, R. A. (2000). Animal home ranges and territories and home range estimators. In
L. Boitani & T. K. Fuller (Eds.), *Research techniques in animal ecology:
controversies and consequences* (pp. 65 - 110). New York, New York, USA:
Columbia University Press.

Proctor, M. F., Servheen, C., Miller, S. D., Kasworm, W. F., & Wakkinen, W. L. (2004). A comparative analysis of management options for brizzly bear conservation in the U.S.-Canada trans-border area. *Ursus, 15*(2), 145-160.

Ross, P. I. (2002). Update COSEWIC status report on the grizzly bear Ursus arctos in Canada. Committee on the Status of Endangered Wildlife in Canada.

Schabenberger, O., & Gotway, C. A. (2005). *Statistical Methods for Spatial Data Analysis*: Chapman & Hall/CRC.

Schwartz, C. C., Miller, S. D., & Haroldson, M. A. (2003). Grizzly Bear, Ursus arctos. In G. A. Feldhamer, B. C. Thompson & J. A. Chapman (Eds.), *Wild Mammals of North America. Biology, Management, and Conservation. Second Edition*. Baltimore and London: The John Hopkins University Press.

Schwartz, C. C., Miller, S. D., & Haroldson, M. A. (2003). Shrinking distribution of the Grizzly Bear during post-glacial, historic and present time. [Image] In G. A. Feldhamer, B. C. Thompson & J. A. Chapman (Eds.), *Wild Mammals of North America. Biology, Management, and Conservation. Second Edition*. Baltimore and London: The John Hopkins University Press.

Seaman, D. E., Griffith, B., & Powell, R. A. (1998). KERNELHR: a program for estimating animal home ranges. *Wildlife Society Bulletin, 26*(1), 95-100.

Seaman, D. E., Millspaugh, J. J., Kernohan, B. J., Brundige, G. C., Raedeke, K. J., & Gitzen, R. A. (1999). Effects of sample size on kernel home range estimates. *Journal of Wildlife Management, 63*, 739-747.

Seaman, D. E., & Powell, R. A. (1990). *Identifying patterns and intensity of home range use*. Paper presented at the International Conference on Bear Research and Management.

Seaman, D. E., & Powell, R. A. (1996). An evaluation of the accuracy of kernel density estimators for home range analysis. *Ecology, 77*, 2075 - 2085.

Silverman, B. W. (1986). *Density estimation for statistics and data analysis.* London: Chapman and Hall.

Statistics Canada. (2009, 2009-09-22). Alberta: Population urban and rural, by province and territory. Retrieved 2010-07-11, 2010, from http://www40.statcan.ca/l01/cst01/demo62j-eng.htm

Steiniger, S., Timmins, T. L., & Hunter, A. J. S. (2010). *Implementation and Comparison of Home Range Estimators for Grizzly Bears in Alberta, Canada, based on GPS data.* Paper presented at the GIScience, Zurich, Switzerland.

Stenhouse, G. B. (2007). Chapter 9: Delivery of New Products and Development of Training Programs. In G. Stenhouse & K. Graham (Eds.), *Foothills Research Institute Grizzly Bear Program 2007 Annual Report.* (pp. 204). Hinton, Alberta.

Stenhouse, G. B., & Munro, R. (2000). Foothills Model Forest Grizzly Bear Research Project 1999 Annual Report. (pp. 107).

Stenhouse, G. B., & Munro, R. (2001). Foothills Model Forest Grizzly Bear Research Program 2000 Annual Report (pp. 87).

Stenhouse, G. B., Boulanger, J., Lee, J. L., Graham, K., Duval, J., & Cranston, J. (2005). Grizzly Bear Associations along the Eastern Slopes of Alberta. *Ursus, 16*(1), 31 - 40.

Stephens, D. W., Brown, J. S., & Ydenberg, R. C. (2007). *Foraging: behaviour and ecology*. Chicago: University of Chicago Press.

Stetzer, F. (1982). Specifying weights in spatial forecasting models: the results of some experiments. *Environment and Planning A, 14*, 571 - 584.

Storer, T. I., & Trevis, L. P. J. (1955). *Califronia grizzly*. Berkley: University of California Press.

Strong, W. L. (1992). *Ecoregions and Ecodistricts of Alberta*. Edmonton.

Sui, D. Z. (2004). Tobler's First Law of Geography: A Big Idea for a Small World? *Annals of the Association of American Geographers, 94*(2), 269-277.

The Calgary Herald. (2010). Alberta government will recognize grizzly bear as a 'threatened' animal. *Calgary Herald*. Retrieved from http://www.calgaryherald.com/technology/Alberta+government+will+recognize+grizzly+bear+threatened+animal/3108349/story.html#ixzz0tQID6gm7

Tiefesldorf, M. (2002). The Saddlepoint Approximation of Moran's I's and Local Morna's I's reference distributions and their numerical evaluation. *Geographical Analysis, 34*, 20.

Tobler, W. (1970). A computer movie simulating urban growth in the Detroit region. *Economic Geography, 46(2)*, 234 - 240.

Toussaint, G. T. (1980). The relative neighbourhood graph of a finite planar set. *Pattern recognition, 12*, 261–268.

Turchin, P. (1998). *Quantitative analysis of movement: Measuring and modeling population redistribution in animals and plants*. Sunderland, MA: Sinauer Associates Inc.

Underhill, L. & Bradfield, D. (1996). *IntroSTAT* Second Edition. Kenwyn: Juta & Co, Ltd.

Weaver, J. L., Paquet, P. C., & Ruggiero, L. F. (1996). Resilience and Conservation of Large Carnivores in the Rocky Mountains. *Conservation Biology, 10*(4), 964-976.

White, G. C., & Garrot, R. A. (1990). *Analysis of wildlife radio-tracking data*. New York: Academic Press.

White, P. S., & Picket, S. T. (1985). Natural Disturbance and Patch Dynamics: An Introduction. In S. T. Picket & P. S. White (Eds.), *The ecology of natural disturbance and patch dynamics* (pp. 3 - 9). San Diego, CA: Academic Press.

Worton, B. J. (1989). Kernel methods for estimating the utilization distribution in home-range studies. *Ecology, 70*(1), 164-168.

Worton, B. J. (1995). Using Monte Carlo simulation to evaluate kernel-based home range estimates. *Journal of Wildlife Management, 59*(4), 794 - 801.

Zadeh, L. (1965). Fuzzy Sets. *Information and Control, 8*(3), 338-353.